2016

Investigating The Function Of Aintegumenta-Like6 (AIL6) In Arabidopsis Flower Development

Han Han
University of South Carolina

INVESTIGATING THE FUNCTION OF *AINTEGUMENTA-LIKE6 (AIL6)* IN ARABIDOPSIS FLOWER DEVELOPMENT

by

Han Han

Bachelor of Science
Capital Normal University, 2010

Submitted in Partial Fulfillment of the Requirements

For the Degree of Doctor of Philosophy in

Biological Sciences

College of Arts and Sciences

University of South Carolina

2016

Accepted by:

Beth A. Krizek, Major Professor

Erin L. Connolly, Committee Member

Lewis H. Bowman, Committee Member

Richard L. Goodwin, Committee Member

Zhengqing Fu, Committee Member

Cheryl L. Addy, Vice Provost and Dean of The Graduate School

DEDICATION

To my mama and baba,

ACKNOWLEDGEMENTS

First, I would like to thank my advisor, Dr. Beth Krizek, for her great mentorship. I am grateful to her immediate help and valuable feedback I got over these years. Her effort in improving my independent research ability, writing and public speaking skills benefits me in a life-time.

Second, I would like to thank my committee members, Dr. Erin Connolly, Dr. Johannes Stratmann, Dr. Lewis Bowman, Dr. Richard Goodwin and Dr. Zhengqing Fu for the helpful advice and suggestions throughout the years. Especially, I want to thank Dr. Erin Connolly for inspiring and supporting me to pursue higher education in plant molecular biology in the beginning.

I would like to thank our funding sources, National Science Foundation (NSF), and SPARC for supporting our research. I thank Syngenta for the ALC switch plasmids (pJH0022 and pACN), and Dr. Jeff Twiss for use of the Leica TCS SP8X confocal microscope.

I would also like to thank my previous labmates: Janaki Mudunkothge, Andrew Kierstead and Olivia Haley for their helpful discussions and their invaluable friendship. I also got lots of help from friends in Biology Department: Anshika, Claire, Min, C.J, Huan, and Jian.

Lastly, I would like to thank my family friend Dr. Y. Wang for his support over the past ten years. Greatest and sincere thank to my mama, baba, and dearest XD for standing behind and supporting me.

ABSTRACT

AINTEGUMENTA (*ANT*) and *AINTEGUMENTA-LIKE6* (*AIL6*) encode related transcription factors with partially overlapping roles in floral organ development in the model plant *Arabidopsis thaliana*. *ANT* and *AIL6* do not make equivalent contributions to these processes. Loss of *ANT* function by itself results in smaller flowers, demonstrating that the role of *ANT* in organ size control cannot be provided by *AIL6.* Loss of *AIL6* function on its own has no phenotypic consequences indicating that all of its roles in flower development can be provided by *ANT* or some other genes. To further probe the function of AIL6 in flower development, we investigated the molecular basis for the distinct functions of ANT and AIL6 and began to characterize the AIL6 protein. To determine whether the functional differences between *ANT* and *AIL6* are a consequence of differences in gene expression and/or protein activity, we made transgenic plants in which a genomic copy of *AIL6* was expressed under the control of the *ANT* promoter (i.e. *ANT:gAIL6*). *ANT:gAIL6* can rescue the floral organ size defects of *ant* mutants when *AIL6* is expressed at similar levels as *ANT* in wild type. Thus, the functional differences between *ANT* and *AIL6* result primarily from gene expression differences. However, *ANT:gAIL6 ant* lines that express *AIL6* at higher levels display additional phenotypes including reduced numbers of floral organs, mosaic floral organs, subtending filaments or bracts, and bigger petals. The severity of these phenotypes correlates with overall *AIL6* mRNA levels. Such phenotypes were not observed in previously characterized transgenic lines in which the coding region of *AIL6* (*cAIL6*) was expressed under the constitutive

35S promoter. In some *35S:cAIL6* lines, larger flowers are produced, similar to transgenic plants that overexpress *ANT*. To further investigate the basis for these phenotypic differences in *AIL6* overexpression lines, we made two different inducible *AIL6* transgenic lines. Induction of AIL6 activity in both of these lines resulted in distinct floral phenotypes depending on the developmental stage of the flower at the time of treatment. Induction of high AIL6 activity in older flowers resulted in larger floral organs while induction of high AIL6 activity in younger flowers resulted in the production of petaloid sepals and in some cases other mosaic floral organs. Furthermore, we show that the distinct phenotypes observed in different *AIL6* overexpression lines are likely explained by differences in both the levels and spatial/temporal accumulation of *AIL6* mRNA. Initial investigations into AIL6 protein activity show that AIL6 can activate transcription in yeast through a promoter containing ANT consensus binding sites, suggesting that AIL6 has similar DNA binding specificities as ANT. Using chromatin immunoprecipitation assays, we identified floral organ identity genes as potential targets of AIL6 regulation. Our results contribute to our understanding of flower development and identify potential genetic tools to engineer flowers with altered floral organ identity and size.

TABLE OF CONTENTS

LIST OF TABLES

LIST OF FIGURES

CHAPTER 1

INTRODUCTION

Arabidopsis thaliana is a popular model plant that belongs to the Brassicaceae family (Figure 1.1). Arabidopsis can complete its entire lifecycle in six weeks and their flowers naturally self-pollinate. It was the first plant to have its genome sequenced and is a popular tool for understanding the molecular biology of many plant traits. The development of higher plants is divided into two phases: embryonic and post-embryonic. In animals, organs are produced during embryogenesis, whereas most plant organs are generated post-embryonically. During embryogenesis in plants, two small groups of stems cells are positioned at each of the two ends of the apical-basal axis: the shoot apical meristem (SAM) and the root apical meristem. During post-embryonic development, the SAM at the top of the plant gives rise to the aerial plant body including stems, leaves and flowers, whereas the root apical meristem at the basal end generates roots.

The SAM is a dome-like structure that generates lateral organs (e.g. leaves and flowers) around its periphery, while maintaining a pool of undifferentiated cells in its center. The SAM can be divided into three specialized zones: the central zone, the peripheral zone and the rib zone (Figure 1.2A). In the central zone, a small population of pluripotent stem cells divides infrequently. In the peripheral zone, cells divide more rapidly and their descendants become incorporated in lateral primordia. Cells within the rib zone give rise to stem tissues. The organizing center, a niche required for the induction and maintenance of stem cells, lies within the central zone and is defined based

on the expression domain of a key regulator of meristem activity, the *WUSCHEL (WUS)* gene (Mayer et al., 1998). The balance of cell numbers among these zones must be carefully maintained for continuous meristem function. Loss of too many stem cells results in meristem termination while too much cell division in the central zone results in overproliferation of the meristem (fasciation).

WUS works with several *CLAVATA (CLV)* genes in a feedback loop to maintain stem cell number within the meristem (Figure 1.2B). The *CLV* genes act in opposition to *WUS* to promote the loss of stem cell from the meristem. *WUS*, transcribed in the organizing center, specifies and maintains stem cell identity in overlying cells. WUS protein, a homeodomain transcription factor, migrates into the central zone, where it directly actives *CLV3* (Yadav et al., 2011). CLV3 is processed into a secreted signaling peptide that binds to the extracellular domain of the leucine-rich receptor kinase CLAVATA1 (CLV1), triggering an intracellular signaling cascade that in turn represses *WUS* transcription from the upper layers of the central zone and restricts it to the organizing center (Brand et al., 2000; Clark et al., 1997; Fletcher et al., 1999; Kondo et al., 2006; Ogawa et al., 2008). *wus* mutants fail to properly maintain meristems, resulting in premature termination of the SAM and production of flowers that lacked most central organs (stamens and carpels). Overexpression of *CLV3* mimics the *wus* loss of function phenotype (Brand et al., 2000). Conversely, mutations in *CLV* genes fail to restrict *WUS* expression in Arabidopsis and thus result in fascinated meristems. The WUS/CLV feedback loop is not the only pathway known to play a role in stem-cell maintenance and fate. For example, the KNOTTED1-LIKE HOMEOBOX (KNOX) family transcription

factor STM functions in a parallel and complementary fashion to the WUS/CLV pathway and prevents stem cells from differentiating (Lenhard et al., 2002).

The arrangement of lateral organs on the stem is called phyllotaxis. In wild type Arabidopsis, leaves and flowers arise at an angle of 137.5 degrees relative to the previous one giving rise to a spiral phyllotaxis. Lateral organ initiation occurs at sites in the periphery of the SAM corresponding to maxima of the plant phytohormone auxin (Benková et al., 2003; Heisler et al., 2005; Reinhardt et al., 2000; Reinhardt et al., 2003). These maxima are generated by both local auxin biosynthesis and directional transport of auxin within the shoot apex [reviewed in (Vernoux et al., 2010)]. Auxin, produced by young leaves, moves into the shoot apex and undergoes polar transport that is mediated primarily by the auxin effluxer *PINFORMED1 (PIN1)* (Gälweiler et al., 1998; Wiśniewska et al., 2006). Once a primordium is initiated, it acts as an auxin sinks, depleting the surrounding region of auxin. Auxin levels are thus highest in the region furthest from existing primordia and a new primordium is initiated at this position. As lateral organ primordia mature and become more distant from the SAM, they switch from being auxin sinks to being sources of auxin. Thus cyclical patterns of auxin buildup and depletion underlie the spiral phyllotaxis of lateral organ initiation in Arabidopsis.

In Arabidopsis, the shoot apical meristem (SAM) progresses through a vegetative phase where leaf primordia initiate on its flanks and form rosette leaves (Figure 1.1). The vegetative phase is characterized by two subphases, a juvenile phase and an adult phase. The juvenile phase is defined by the development of small leaves that lack trichomes on the abaxial epidermis. During the adult phase, the SAM produces large leaves with trichomes present on both abaxial and adaxial epidermis and acquires reproductive

competence. The juvenile-to-adult phase transition is also termed the vegetative phase change.

After producing a certain number of leaves, plants switch to a reproductive developmental phase (Figure 1.1). The SAM, now also called the inflorescence meristem (IM), first produces two to three cauline leaves and associated axillary inflorescences (also called branches) in the early inflorescence phase, and then produces individual flowers in the flower formation phase. An inflorescence is a stem with flowers. The timing of the switch from vegetative development to reproductive development is critical for reproductive success. Environmental cues such as temperature, photoperiod and nutrient availability activate multiple signaling pathways that converge to regulate the expression of floral integrators that promote flowering. Later, these floral integrators activate the expression of floral meristem identity genes that promote flower formation from the IM.

The two most important floral meristem identity genes are *APETALA1 (AP1)* and *LEAFY (LFY)* (Irish and Sussex, 1990; Weigel et al., 1992). Mutations in these genes result in replacement of early flowers with inflorescences (*lfy*) or flowers with inflorescence features (*ap1*). In other words, flowers lose their identity as flowers and instead take on properties of an inflorescence. *lfy ap1* double mutants show a more complete replacement of flowers by inflorescences than either single mutant. The switch from the production of inflorescences to flowers is also promoted by two partially redundant AP2/ERF (APETALA2/Ethylene Response Factor) transcription factors: AINTEGUMENTA (ANT) and AINTEGUMENTA-LIKE 6 (AIL6). *ant ail6* double mutants, like *lfy*, show a delay in the formation of the first flower (Yamaguchi et al.,

2016). The timing of flower formation is tightly regulated by control of *LFY* expression. The auxin response factor MONOPTEROS (MP) and ANT/AIL6 act in parallel pathways to activate *LFY* expression to promote the switch to flower formation (Yamaguchi et al., 2016).

Similar to leaf primordia, flower primordia called floral meristems (FMs) arise from the peripheral regions of the SAM at auxin maxima (Benková et al., 2003). Mutations in the auxin effluxer *PIN1* result in a pin-like inflorescences in which flower primordia are not initiated but the meristem continues to grow. This phenotype is also observed in *mp* single mutants as well as *ant ail6 lfy* triple mutants (Przemeck et al., 1996; Yamaguchi et al., 2013). Application of auxin paste to *pin1* shoot apices results in flower initiation at the corresponding site where auxin was applied demonstrating that auxin accumulation is both necessary and sufficient for flower initiation (Reinhardt et al., 2000; Reinhardt et al., 2003). MP directly activates the expression of *ANT*, *AIL6* and *LFY* to promote the continuous flower primordia initiation.

The floral meristem identity genes *LFY* and *AP1* also act later within flower primordia to activate the expression of genes that specify floral organ identity. These genes are called floral homeotic genes or floral organ identity genes. In Arabidopsis, four kinds of floral organs (sepals, petals, stamens and carpels) arise in precise positions within four concentric rings called whorls. From the outside to the inside, four sepals arise in the outermost first whorl, four petals arise in the second whorl, six stamens arise in the third whorl and two fused carpels are present in the forth whorl. For sepals, the position adjacent to the SAM is called the adaxial position and the side furthest from the SAM is the abaxial position (Figure 1.3). The other two sides are called the lateral

positions. Arabidopsis flower development has been characterized into a series of stages (1-14) based on morphological parameters (Smyth et al., 1990). Stage 1 of flower development is characterized by the development of a bulge on the flank of the IM. Stage 3 of flower development corresponds to the period in which sepal primordia are first visible within the flower primordium and stage 6 is when all four types of floral organ primordia have been initiated (Figure 1.3).

Four classes of floral homeotic genes (A, B, C, E), that are active in different whorls, act in different combinations to specify floral organ identity [reviewed in (Krizek and Fletcher, 2005)] (Figure 1.4). Mutations in the class A, B or C genes result in homeotic transformations in floral organ identity in two adjacent whorls of the flower, while loss of all class E genes results in flowers that consist only of leaf-like organs. For example, loss-of-function alleles of the A-class gene *AP2* result in homeotic transformations of sepals to carpels and petals to stamens (Jofuku et al., 1994). *AP1* and *AP2* are A-class genes that are active in first and second whorls. The B-class genes *AP3* and *PI (PISTILLATA)* function in the second and third whorls. The C-class gene *AGAMOUS* (*AG*) functions in the third and forth whorls. The E-class genes, the *SEPALLATA* genes, *(SEP1/SEP2/SEP3/SEP4)* are expressed in all four whorls. The combination of class AE genes specify sepals in the first whorl, class ABE genes specify petals in the second whorl, class BCE genes specify stamens in the third whorl, and class CE genes specify carpels in the center. By manipulating the spatial activity domains of the floral homeotic genes, it is possible to completely transform one organ into another. For example, misexpression of the two class B genes throughout the entire flower

primordia results in flowers with two outer whorls of petals (ABE functions) and two inner whorls of stamens (BCE functions) (Krizek and Meyerowitz, 1996).

AP1, AP3, PI, AG and SEP1-4 are members of the MADS domain transcription factor family, while AP2 is the founding member of the plant specific AP2/ERF family (Riechmann and Meyerowitz, 1998). Biochemical studies have shown that AP1 and AG form homodimers while AP3 and PI form a heterodimer, all of which can bind DNA (Riechmann et al., 1996). Furthermore, SEP proteins also interact with AP1, AP3, PI and AG to form higher order complexes (Honma and Goto, 2001). Distinct tetrameric MADS domain proteins complexes, consisting of SEP proteins with specific combinations of the floral organ identity factors, regulate different target genes to specify distinct floral organ identities in different whorls (i.e. the quartet model) (Smaczniak et al., 2012; Theissen and Saedler, 2001).

While the molecular mechanisms specifying floral organ identity are well-studied, little is known about other aspects of flower development, such as the processes that control floral organ numbers, floral organ sizes, and the positioning of floral organ initiation.

Genes involved in maintaining or terminating of floral meristem cells, such as *STM*, *WUS*, *CLV1*, *CLV2*, *CLV3* and *AG*, can affect the numbers of floral organs produced by FMs. Much like stem cells in the SAM, stem cells within the FM are initially maintained by WUS/CLV signaling. However, while the SAM is indeterminate, the FM is determinate and all of its stem cells are consuming during floral organ initiation. In stage 3 floral buds, the class C gene *AG* is induced by LFY and WUS in the center of flower (Lenhard et al., 2001; Lohmann et al., 2001). In stage 6 flowers, AG

represses *WUS* and turns off floral stem cell activity. The floral meristem of *ag* flowers fails to terminate in the production of the fourth whorl organs. Instead, *ag* flowers are indeterminate and continue to produce new cells that are incorporated into many extra whorls of sepals and petals (Yanofsky et al., 1990).

Increased or reduced numbers of floral organs often reflect the secondary consequence of disruption to the balance between the dampening and promotion of proliferation of the undifferentiated stem cells. In mutants of three *CLV* genes, there is an increase in the number of all four floral organ types, particularly the inner whorls of stamens and carpels (Clark et al., 1997; Fletcher et al., 1999). In contrast, mutations in *STM* and *WUS* generate flowers with reduced numbers of organs especially in the inner whorls (Endrizzi et al., 1996; Mayer et al., 1998). Other genes affecting these key regulators of floral stem cells also show defects in floral organ numbers. For example, mutations in the bZIP transcription factor *PERIANTHIA (PAN)* frequently demonstrate five-fold symmetry in their outer three floral whorls rather than the normal bilateral symmetry seen in the wild type (Chuang et al., 1999). *PAN* affects floral stem cell activities through direct activation of *AG* (Das et al., 2009; Maier et al., 2009).

Flower development requires the formation of correct boundaries that separate adjacent whorls and adjacent floral organs within a whorl. Boundaries correspond to regions with reduced rates of cell division (Zadnikova and Simon, 2014). Failure to establish organ boundaries results in fused floral organs. *CUP-SHAPED COTYLEDON1 (CUC1), CUC2* and *CUC3* are all expressed in boundaries between floral organ primordia; double mutant combinations of the three *CUC* genes produce flowers that exhibit fusions between adjacent floral organs (Aida et al., 1997; Hibara et al., 2006).

CUCs prevent the inter-sepal boundary from differentiating into sepal tissue. The tri-helix transcription factor PETAL LOSS (PTL) acts in concert with *CUC1* and *CUC2* in the formation of sepal boundaries but in a different pathway (Brewer et al., 2004). PTL suppresses growth in the inter-sepal zone and is required to establish auxin maxima at the presumptive petal initiation sites (Lampugnani et al., 2013). Another gene, *RABITT EARS (RBE)*, encoding a zinc finger transcriptional repressor, is specifically expressed in petal primordia and is required for proper petal development and inter-sepal boundary maintenance. The *rbe* mutants result in aberrant or elimination of petals and fused sepals (Krizek et al., 2006; Takeda et al., 2004). RBE negatively regulates *microRNA164s* expression and microRNA164s in turn fine-tunes *CUC1* and *CUC2* expression in organ boundaries (Huang et al., 2012). The aforementioned transcriptional network involving *CUCs*, *PTL* and *RBE* reveals the presence of strong feedback control and interdependency between the establishment of boundaries and organ development.

The correct regulation of organ size is a fundamental developmental process, the failure of which can compromise organ function and organismal integrity. Final organ sizes mainly result from the combined effects of cell proliferation and cell expansion in plants. In plants, the initial growth of lateral organ primordia is primarily due to increases in cell division and later growth is primarily due to cell expansion. Mutants that change the rate and/or duration of either the cell proliferation or cell expansion phases can be responsible for alterations in floral organ size. Several factors like the transcription factor *AUXIN-REGULATED GENE INVOLVED IN ORGAN SIZE (ARGOS)* (Hu et al., 2003), the AP2 transcription factor *ANT* (Elliott et al., 1996; Klucher et al., 1996) and the single C2H2 zinc finger transcription factor *JAGGED* (*JAG)* (Dinneny et al., 2004; Ohno et al.,

2004) promote cell proliferation and organ growth while other factors like the E3 ligase *BIG BROTHER (BB)* (Disch et al., 2006) and the putative ubiquitin receptor *DA1* (Li et al., 2008) limit organ sizes by limiting cell proliferation. Other genes promote or limit cell expansion, such as *EXPANSIN10 (EXP10)* (Cho and Cosgrove, 2000), the cytochrome P450 *ROTUNDIFOLIA3 (ROT3)* (Kim et al., 1999; Kim et al., 1998), *ANGUSTIFOLIA (AN)* (Tsuge et al., 1996) and *BIGPETALp* (Szécsi et al., 2006). Furthermore organisms can make bigger organs by increasing ploidy (e.g. (Sonoda et al., 2009)). In many organ size mutants, there is partial compensation between cell number and cell size. For example, the small petals in *rbe* mutants have overall fewer cells but those cells are bigger in size (Huang and Irish, 2015). In animals, several key pathways of organ size control has been identified, such as the Hippo pathway and the target of rapamycin pathway [reviewed in (Crickmore and Mann, 2008; Hwang et al., 2008)]. However, homologs to the Hippo pathway are not found in plants and plant organ sizes are mainly regulated by plant specific factors.

Besides their roles in the switch to flower formation and the initiation of flower primordia, the two AP2/ERF transcription factors ANT and AIL6 play additional roles in some less well-understood aspects of floral organ initiation and development. Mutations in *ANT* result in flowers with smaller organs (Figure 1.5) while ectopic expression of *ANT* results in larger flowers (Krizek, 1999). Mutations in *AIL6* have no phenotypic consequences but *ant ail6* double mutants display more severe floral organ defects than *ant* (Krizek, 2009) This indicates that *ANT* and *AIL6* have partially redundant functions although *AIL6* cannot provide all of the same functions as *ANT*. This may be due to the fact that *ANT* mRNA is detected at higher levels and in a broader spatial pattern than

AIL6 mRNA during floral organ development (Figure 1.6). We investigated the molecular basis for the distinct functions of *ANT* and *AIL6* by expressing a genomic copy of *AIL6* under the control of the *ANT* promoter and determined whether this transgene could complement the *ant* mutant phenotype (Chapter 2).

ant ail6 double mutant flowers consist of small sepals, filamentous organs, stamen-like organs, undefined organs and unfused carpel valves, which arise in random positions within flower primordia and in fewer number than in wild type (Figure 1.5). Thus *ANT* and *AIL6* have partially overlapping roles in regulating floral organ number, positioning, identity and growth.(Krizek, 2009) The loss of petal and stamen identities and partial loss of carpel identity in *ant ail6* appears to be a consequence of reduced expression of the floral organ identity genes *AP3* and *AG*. This suggests that *AP3* and *AG* might be targets of ANT and AIL6 regulation. Experiments to test this hypothesis are described in Chapter 3.

Members of the AP2/ERF transcription factor family contain one or two copies of the AP2/ERF repeat which is a DNA-binding domain of approximately 60 amino acids (Jofuku et al., 1994; Hao et al., 1998). The AP2 subfamily of the AP2/ERF family has two AP2 repeats and consists of 15 of the total 146 AP2/ERF proteins (Riechmann et al., 2000). The ANT clade of the AP2 subfamily named the *AIL/PLETHORA (AIL/PLT)* group contains eight genes: *ANT*, *AIL1*, *AIL5*, *AIL6*, *AIL7*, *PLT1*, *PLT2* and *BABY BOOM* (*BBM*) (Nole-Wilson et al., 2005). As a group, AIL proteins share 70% amino acid identity within two AP2 repeats and the intervening linker, but little similarity outside of this region. While AIL6 and AIL7 share high sequence similarity throughout their

sequences, they have different expression patterns in flowers (Figure 1.6) and *ail6 ail7* double mutate have no obvious phenotype (Krizek, 2009).

DNA binding and transcriptional activation functions have been described for ANT, but very little is known about AIL6 protein. ANT can bind to and activate transcription through the following DNA sequence: 5'-ttgGTGCACATATCCCGATGCTTaca-3' (referred to as binding site 15 or BS 15) (Krizek, 2003; Nole-Wilson and Krizek, 2000). Experiments to examine whether AIL6 can activate transcription through BS 15 are described in Chapter 3.

AIL6 also plays important functions in some other plant development processes. It acts redundantly with *AIL5* and *AIL7* in regulating phyllotaxis in the shoot by promoting auxin biosynthesis in the center of the SAM as well as the spacing and arrangement of lateral root primordia partially through function downstream of auxin responsive factors ARF7 and ARF19 (Hofhuis et al., 2013; Pinon et al., 2013; Prasad et al., 2011). Also, *AIL6* acts redundantly with *ANT* and *AIL7* to maintain the shoot apical meristem and with *PLT1*, *PLT2* and *BBM* to maintain root apical meristem (Galinha et al., 2007; Mudunkothge and Krizek, 2012). *plt1 plt2 ail6* triple mutants are rootless and *plt1 plt2 ail6 bbm* quadruple mutants completely lack roots and hypocotyls (Galinha et al., 2007). Last but not the least, *AIL5*, *AIL6*, and *AIL7* redundantly control the intermediate steps leading to de novo shoot regeneration by regulating *PLT1* and *PLT2* and shoot-promoting factors like *CUC2* to allow shoot regeneration (Kareem et al., 2015).

The evolution of *AIL* genes can be traced back into the moss *Physcomitrella patens* in land plants (Aoyama et al., 2012). Four orthologs of AIL/PLT proteins are reported to determine stem cell identity in the non-vascular plant moss *Physcomitrella*

patens. *AIL5/PLT5*-like genes was proposed to be the common ancestor of the eudicot and monocot *AIL* gene family lineages (Prasad et al., 2011). After the diverge of monocots and eudicots, *AIL* gene sequences formed separate subclades (Floyd and Bowman, 2007; Kim et al., 2006). *AIL* genes appeared to be important regulators for various plant development processes, including plant stem cell maintenance, growth and auxin signaling responses.

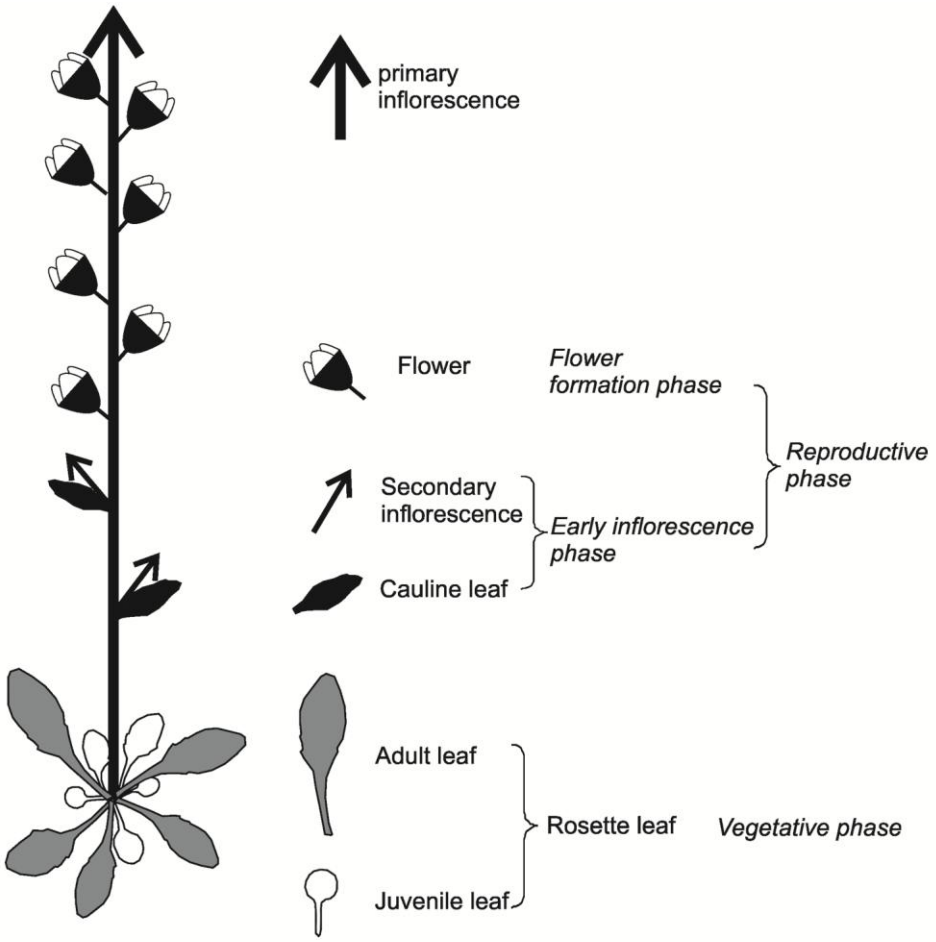

Figure 1.1 A schematic representation of an *Arabidopsis thaliana* plant. During the vegetative phase, the plant produces juvenile leaves and adult leaves. The rosette leaves refer to both juvenile leaves and adult leaves. During reproductive phase, the plant generates cauline leaves subtending secondary inflorescences in the early inflorescence phase and individual flowers during the flower formation phase.

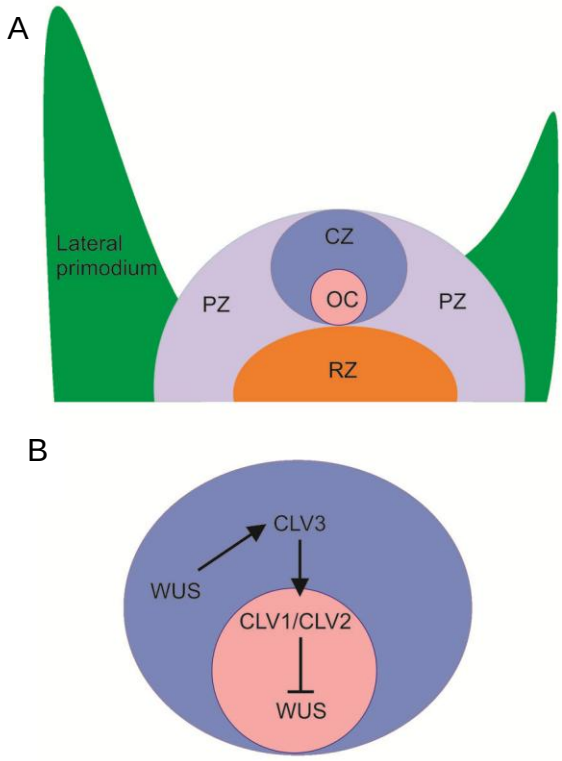

Figure 1.2 Shoot apical meristem (A) Schematic representation of tissue organization within the shoot apical meristem. Abbreviations: CZ, central zone; OC, organizing center; PZ, peripheral zone; RZ, rib zone; Lateral primordia are leaves during vegetative development and flowers during reproductive development. (B) Schematic representation of WUS/CLV signaling within the shoot apical meristem. *WUS*, transcribed in the organizing center (pink), specifies and maintains stem cell identity in overlying cells. WUS protein migrates into the central zone (blue), where it directly actives *CLV3*. CLV3 is processed into a secreted signaling peptide that binds to the extracellular domain of the leucine-rich receptor kinase CLV1, triggering an intracellular signaling cascade that in turn represses *WUS* transcription from the upper layers of the central zone and restricts it to the organizing center. Arrows indicate positive regulatory interactions and bars indicate negative regulatory interactions.

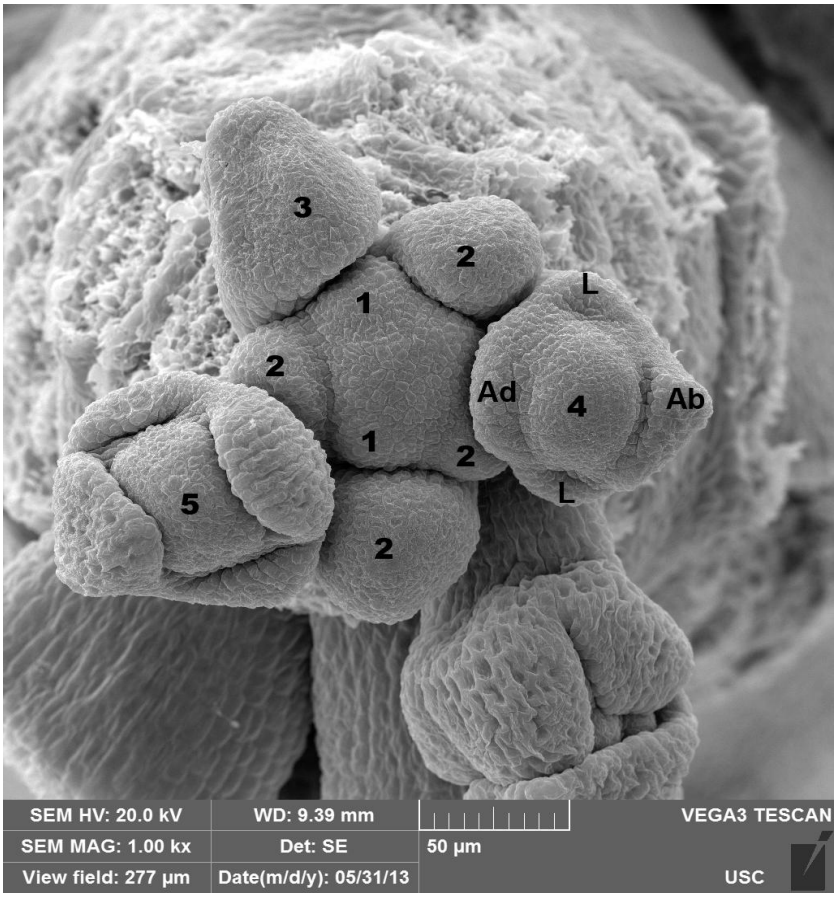

Figure 1.3 A scanning electronic micrograph of the primary inflorescence of Arabidopsis. This is a top down view of the inflorescence apex of a 26-day-old plant after the older flower buds have been removed. The stage of each bud is indicated. The abaxial (Ab), adaxial (Ad), and lateral (L) sepals on the stage 4 bud are indicated. Bar=50µm.

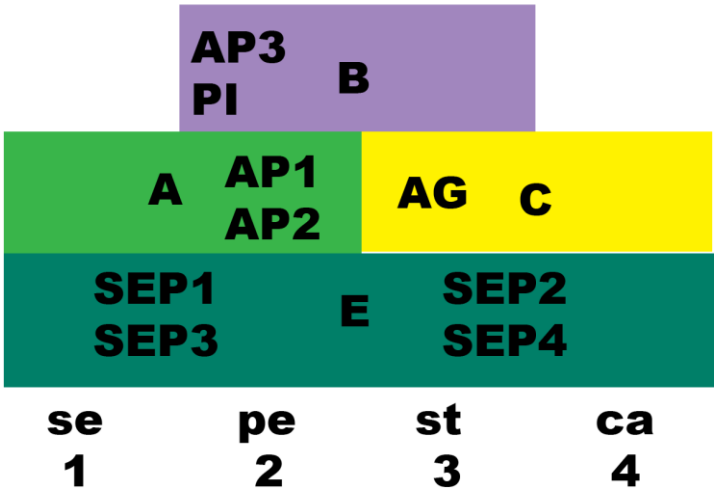

Figure 1.4 The classic ABCE model for floral organ identity (Reviewed in Krizek, B.A. and Fletcher, J.C., 2005). Abbreviations: se, sepals; pe, petals; st, stamens; ca, carpels.

Figure 1.5 L*er* (left), *ant-4* (middle), and *ant-4 ail6-2* (right) flowers. Photograph by B. Krizek. Used with permission.

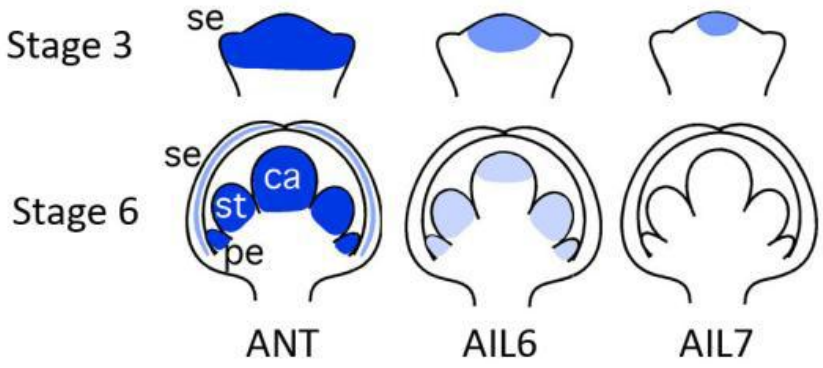

Figure 1.6 *ANT, AIL6,* and *AIL7* mRNA expression in stage 3 and stage 6 flowers. (Krizek, 2015a) Reproduced with permission.

CHAPTER 2

AINTEGUMENTA-LIKE6 CAN FUNCTIONALLY REPLACE *AINTEGUMENTA* BUT ALTERS ARABIDOPSIS FLOWER DEVELOPMENT WHEN MISEXPRESSED AT HIGH LEVELS[1]

INTRODUCTION

Two members of the Arabidopsis AINTEGUMENTA-LIKE (AIL) transcription factor family, AINTEGUMENTA (ANT) and AINTEGUMENTA-LIKE 6 (AIL6) play partially overlapping roles in several aspects of flower development (Krizek, 2009, 2011; Yamaguchi et al., 2016; Yamaguchi et al., 2013). ANT and AIL6 promote the switch to flower formation by upregulation of *LEAFY* (*LFY*), which encodes a transcription factor that specifies floral meristem identity (Weigel et al., 1992). ANT, AIL6 and LFY then promote flower primordia initiation at the sites of auxin maxima within the periphery of the inflorescence meristem.(Benková et al., 2003; Heisler et al., 2005; Reinhardt et al., 2000; Yamaguchi et al., 2013) Auxin accumulation in these cells activates MONOPTEROS (MP), an AUXIN RESPONSE FACTOR (ARF), which induces expression of *LFY*, *ANT* and *AIL6* to bring about primordia initiation and outgrowth (Yamaguchi et al., 2013). In addition, LFY provides these primordia with a floral fate while ANT and AIL6 promote growth of the floral primordia

[1]Han, H. and B.A. Krizek. Submitted to *Plant Molecular Biology*, 13/07/2016

(Elliott et al., 1996; Klucher et al., 1996; Krizek, 1999; Krizek, 2009; Krizek and Eaddy, 2012; Schultz and Haughn, 1993; Weigel et al., 1992; Weigel and Nilsson, 1995).

After establishment of a flower primordium, *ANT* and *AIL6* regulate the initiation and development of floral organs within the flower. In wild-type flowers, floral organ primordia arise at precise positions within four concentric whorls. These primordia subsequently adopt fates as sepals, petals, stamens or carpels based on the activities of distinct combinations of floral organ identity genes (also known as floral homeotic genes), as summarized in the ABCE model [reviewed in(Krizek and Fletcher, 2005)]. Loss of both *ANT* and *AIL6* functions together result in flowers with small sepals, filamentous organs, stamen-like organs, undefined organs and unfused carpel valves (Krizek, 2009). These organs do not arise in characteristic positions within the flower or in distinct whorls (Krizek, 2009). Thus *ANT* and *AIL6* contribute to floral organ positioning within the flower, the establishment of floral organ identity, floral organ growth, and carpel patterning.

ANT and AIL6 do not make equivalent contributions to these processes. Loss of *ANT* function by itself results in smaller flowers (Elliott et al., 1996; Klucher et al., 1996), demonstrating that the role of *ANT* in organ size control cannot be provided by *AIL6.* Loss of *AIL6* function on its own has no phenotypic consequences indicating that all of its roles in flower development can be provided by *ANT* or some other gene (Krizek, 2009). Some of the functional differences between *ANT* and *AIL6* may arise from differences in gene expression, as *ANT* mRNA is present at higher levels and in a broader domain than *AIL6* mRNA in young flowers, and *ANT* mRNA persists much longer in developing floral organs (Elliott et al., 1996; Nole-Wilson et al., 2005). We

investigated whether gene expression differences underlie the functional differences between *ANT* and *AIL6* by expressing a genomic copy of *AIL6* under the control of the *ANT* promoter. The *ANT:gAIL6* transgene largely rescues the organ size defects of *ant* mutants, indicating that *AIL6* can promote growth of floral organs when expressed in the same domains and at the same levels as *ANT*.

ANT:gAIL6 ant lines expressing *AIL6* at higher levels show changes in flower development that include the production of fewer floral organs and mosaic floral organs such as petaloid sepals. In addition, these flowers show defects in the initiation and growth of floral organ primordia. The severity of these phenotypes is correlated with *AIL6* mRNA levels. Similar phenotypes are observed in *ANT:gAIL6* lines in a wild-type background and in transgenic lines in which *AIL6* is misexpressed using an ethanol inducible system (i.e. *35S:AlcR/AlcA:gAIL6*). Such phenotypes are not observed in *35S:ANT* plants suggesting that AIL6 can regulate genes that are not targets of ANT regulation. *35S:AlcR/AlcA:gAIL6* plants as well as transgenic plants expressing a steroid inducible genomic copy of *AIL6* under the control of the *35S* promoter (i.e. *35S:gAIL6-GR*) produce larger flowers, similar to *35S:ANT* plants (Krizek, 1999; Mizukami and Fischer, 2000). *35S:gAIL6-GR* flowers produce some petaloid sepals but do not produce other mosaic organs observed in *35S:AlcR/AlcA:gAIL6* flowers. We compare the phenotypes described here with earlier *AIL6* misexpression experiments; it is likely that the somewhat distinct phenotypes of these lines are a consequence of differences in the levels and patterns of AIL6 expression.

MATERIALS AND METHODS

Plant materials and growth conditions

The *ant-4* allele was described previously (Baker et al., 1997; Nole-Wilson et al., 2005). *ant-4* was PCR genotyped as described previously (Krizek, 2009). Plants were grown on a soil mixture of Metro-Mix 360:perlite:vermiculite (5:1:1) in 16hr days (100-150 $\mu mol \cdot m^{-2} \cdot s^{-1}$) at 20-22°C.

Plasmid construction and plant transformation

A genomic copy of *AIL6* corresponding to most of the coding region and 919bp of 3' sequence was obtained by digestion of BAC F12B17 with *Kpn*I and *BamH*I and ligation into BJ36. The first 141bp of the *AIL6* coding region were added to this genomic fragment by PCR amplification with AIL6-27 (5'-ATACGGTACCATGATGGCTCCGATGACGAACTGGTTAACGTTTTCTCTGTCACCAATGGAGATGTTGAGGTCATCTGA-3') and AIL6-44 (5'-ACACGAGCATGTACTGTTGAG-3') and digestion with *Kpn*I to create *gAIL6*/BJ36. A 6.2kb *ANT* promoter sequence was subcloned from pBluescript into the *Sal*I site of *gAIL6*/BJ36. *ANT:gAIL6* was subcloned into the NotI site of pART27 and transformed into *Agrobacterium tumefaciens* strain ASE by electroporation. L*er* and *ant-4* plants were transformed with this *Agrobacterium* strain by vacuum infiltration (Bechtold et al., 1993). Transformants were selected for kanamycin resistance. Plants homozygous for the transgene were used for phenotypic characterization.

For the ethanol inducible constructs, *AlcR* was subcloned from pJH0022 into BJ97 using *Eco*RI and *Hind*III. The *35S* promoter was subsequently subcloned from pJH0022 into the *Eco*RI site of *AlcR*/BJ97. *35S:AlcR* was subcloned from BJ97 into the *Not*I site of pMLBart. *AlcA* was first subcloned from pACN into the HindIII site of pBluescript and subsequently subcloned into the *Pst*I and *Sal*I sites of *gAIL6*/BJ36. *AlcA:gAIL6* was subcloned into the *Not*I site of pART27. *35S:AlcR*/pMLBart and *AlcA:gAIL6*/pART27 and were transformed into Agrobacterium strain ASE by electroporation. Transformants were selected for either basta (pMLBart) or kanamycin (pART27) resistance. *35S:AlcR* transgenic line 95 was crossed with *AlcA:gAIL6* line 49. Plants homozygous for both transgenes were used for phenotypic characterization.

For the *35S:gAIL6-GR* construct, 919bp of *AIL6* 3' sequence was subcloned into the *Xba*I site of pART7, which contains a *35S* promoter. A genomic copy of *AIL6* lacking the stop codon was subcloned into *AIL6* 3'/pART27 using *Sma*I and *BamH*I. The ligand binding domain of the glucocorticoid receptor (GR) was added to the *BamH*I site of *gAIL6-3'*/pART7. *35S:gAIL6-GR-3'* was subcloned from pART7 into pART27 using *Not*I and transformed into *Agrobacterium tumefaciens* strain ASE by electroporation. L*er* plants were transformed with this *Agrobacterium* strain by vacuum infiltration (Bechtold et al., 1993). Transformants were selected for kanamycin resistance. Plants homozygous for the transgene were used for phenotypic characterization.

AIL6m:gAIL6-VENUS was constructed by first cloning a 919bp fragment of *AIL6* 3' sequence into the XbaI site of 9Ala-VENUS/BJ36. This *AIL6* 3' sequence was PCR amplified with AIL6-46 (5'-AATATCTAGAAACCAATCATATAAGTTGATTGAG-3') and AIL6-47 (5'-AAGATCTAGACCTCGGCTAGGAAATATGTTT-3'). A genomic

copy of *AIL6* was created in pGEM3Z and subcloned into the *Sma*I/*Bam*HI sites of 9Ala-VENUS-3'/BJ36. 591 bp of *AIL6* 5' sequence was subcloned into the *Sma*I site of *gAIL6-VENUS-3'*/BJ36 to create *AIL6m:gAIL6-VENUS*/BJ36. *AIL6m:gAIL6-VENUS* was subcloned into the *Not*I site of pART27 and transformed into the *Agrobacterium* strain ASE by electroporation. L*er* plants were transformed with this *Agrobacterium* strain by vacuum infiltration (Bechtold et al., 1993). Transformants were selected for kanamycin resistance. Individual lines were crossed into the *ant-4/+ ail6-2* background. *AIL6m:gAIL6-VENUS* line 5 complements *ail6-2* such that *AIL6m:gAIL6-VENUS-3' ant-4 ail6-2* flowers resemble *ant-4* flowers. Plants from *AIL6m:gAIL6-VENUS* line 5 in the *ail6-2* background were used for confocal microscopy.

Petal size and petal cell size measurements

Petal measurements were performed on at least 12 petals from at least 6 different plants. These flowers corresponded to those at at positions 1-10 on an inflorescence for *35S:cAIL6* and *35S:gAIL6*. For the inducible lines (*35S:AlcR/AlcA:gAIL6* and *35S:gAIL6-GR*), these flowers corresponded to stage 14 flowers at later positions on the inflorescence. Petal measurements were performed as described previously (Trost et al., 2014). Petal area, length and width were determined using Image J software or a program written in MATLAB.

For petal size measurement, individual flowers were cleared in chloral hydrate (8g chloral hydrate, 11ml water, 1ml glycerol) and imaged with differential interference contrast (DIC) optics on an Olympus BX60 microscope.

Scanning electron microscopy

Tissue for SEM was fixed, dehydrated, dissected and coated as previously described (Krizek, 1999). For viewing ovules, carpels were sliced with a razor blade immediately before fixation. SEM analyses were performed on an FEI Quanta 200 ESEM or a Tescan Vega3 SBU Variable Pressure SEM.

RNA isolation and RT-qPCR

RNA was extracted from inflorescences using TRIzol (Life Technologies) and treated with Turbo DNase (Life Technologies). In some cases, the RNA was further purified on an RNeasy column (Qiagen) and DNased while on the column. First-strand cDNA synthesis was performed using qScript cDNA Supermix (Quanta BioSciences). qPCR reactions were performed on a BioRad CFX96 using PerfeCTa SYBR Green FastMix for iQ (Quanta BioSciences) and AIL6 primers described previously (Krizek and Eaddy, 2012). Data analyses were carried out as described previously (Krizek and Eaddy, 2012). Two to three biological replicates were used for each experiment. For the absolute quantification RT-qPCR experiment comparing *ANT* and *AIL6* mRNA expression in L*er*, standard calibration curves were generated using a known amount of plasmids containing either *ANT* or *AIL6* cDNA quantitated on a Qubit fluorometer.

In situ hybridization

Inflorescences were fixed, embedded, sectioned, hybridized and washed as described previously except that a hybridization temperature of 53^{o}C was used with the long *AIL6* probe (see below) (Krizek, 1999). The digoxigenin-labeled *AP3* antisense

RNA probes was synthesized as described previously (Jack et al., 1992). For the *PI* probe, a *Xho*I/*Nco*I fragment of *PI* cDNA was subcloned into the *Sma*I site of pGEM3Z vector. PI/pGEM3Z was linearized with *BamH*I and transcribed with T7 RNA polymerase. Two different *AIL6* antisense RNA probes were used. The experiments shown in Figure 2.14 and Figure 2.9 used a previously described *AIL6* probe (Nole-Wilson et al., 2005). The experiments in Figure 2.3, Figure 2.5, Figure 2.13 and Figure 2.18 used a long *AIL6* probe in which nucleotides 497 to1691 of the *AIL6* cDNA were PCR amplified with AIL6-FW (5'-TCGGAAGGACTCATCTTGCT-3') and AIL6-RV (5'-CCCTGAACGTTGGAGTTGTT-3') using Phusion DNA polymerase and cloned into the *Sma*I site of pGEM3Z. Long *AIL6*/pGEM3Z was linearized with *Hind*III and transcribed with T7 RNA polymerase.

Ethanol and dex induction of transgenes

35S:AlcR/AlcA:gAIL6 plants were treated with mock (H_2O) or ethanol vapor by placing 2mls of water or 2mls of 100% ethanol in 2ml centrifuge tubes in half of the pots in a tray. The tray was covered with a plastic dome. 14-16 day old plants were treated once for eight hours while 29-30 day old plants were treated three times (every other day) for four hours each day. Inflorescences of 23-26 day old *35S:gAIL6-GR* plants were treated two or three times by pipetting a mock (0.1% ethanol and 0.015% Silwet) or dex (10μM dexamethasone and 0.015% Silwet) solution every other day to the inflorescences.

Confocal Microscopy

Flowers were dissected from live inflorescence using a 26-gauge needle. Inflorescences were transferred to a coverslip onto which a 24 well adhesive silicone isolator (Grace Bio-Labs) had been placed and filled with approximately 10µl of 0.8% agarose/0.5x MS salts. Confocal image stacks were acquired using a Leica TCS SP8X confocal microscope with a 40x water-immersion lens. A 514nm laser line was used to excite VENUS and a 640nm laser line was used to excite chlorophyll. Fluorescence was detected with a 520-560nm (VENUS) or a 650nm long pass filter (chlorophyll). Gain settings of 250 (VENUS) and 30 (chlorophyll) were held constant. For the inflorescence apex Z-stacks were collected using an average of four optical slices every 2µm for a total of 20µm. For individual stage three flowers, Z-stacks were collected using an average of four optical slices every 2µm for a total of 10µm. Zoom was set on one for inflorescence meristem pictures and 1.75 for stage 3 flower primordium pictures.

RESULTS

Expression of *AIL6* under the *ANT* promoter rescues the floral organ size defects of *ant*

To investigate whether the functional differences between *ANT* and *AIL6* arise from differences in their expression patterns and/or distinct protein activities, we expressed a genomic copy of *AIL6* under the control of the *ANT* promoter in the *ant-4* background. The *ANT* promoter used in this construct complements *ant-4* when fused to the *ANT* coding sequence (Krizek, 2009). We generated 13 *ANT:gAIL6 ant* transgenic

lines that fell into four phenotypic classes referred to as C1 (lines 19,61,69,70,74,83,89), C2 (lines 17,18), C3 (lines 68,77) and C4 (lines 53,62). Phenotypic and molecular characterizations were performed on one representative homozygous line of each class: line 69 (C1-69), line 18 (C2-18), line 68 (C3-68) and line 62 (C4-62) (Figure 2.1A-F). All four of these lines largely rescue the floral organ size defects of *ant-4* as shown for petals (Figure 2.1G) and stamen anthers (Figure 2.2A-F). However, the flowers of these lines differed in other aspects including floral organ number, the presence of mosaic organs, and the presence of subtending filaments or bracts (Figure 2.1A-F; Table 2.1). C1-69 flowers had a wild-type appearance, although they produced a few petaloid sepals, slightly smaller petals and fewer stamens than L*er* and had similar numbers of flowers with fused floral organs as *ant-4* (Figure 2.1C, G; Table 2.1). In C2-18, early-arising flowers have a wild-type appearance but later-arising flowers produce some petaloid sepals, have fewer petals compared with *ant-4*, have reduced numbers of stamens compared with L*er*, and are often subtended by very short filaments (Figure 2.1D; Table 2.1). The number of mosaic first whorl organs is greatly increased in C3-68. These flowers also show reduced numbers of floral organs in whorls 2-4 and are often subtended by filaments (Figure 2.1E; Table 2.1). Reductions in floral organ number are even more severe in C4-62 (Figure 2.1F; Table 2.1). First whorl sepals are often replaced by filaments or petals, the carpels exhibit reductions in valve tissue, and bracts frequently subtend the flowers. Second whorl organs are almost completely lost in C4-62 and it is sometimes difficult to distinguish first and second whorl organs.

For two of the four classes (C1 and C3), we observed variation in the ability of the *ANT:gAIL6* transgene to rescue the female sterility defects of *ant* mutants. While the

two C2 lines produced seeds and neither of the two C4 lines produced seeds, we observed that two of seven C1 lines and one of two C3 lines produced seeds. None of the fertile *ANT:gAIL6 ant* lines set as many seeds as wild type. To investigate whether the defects in seed production might be a consequence of the inability of *ANT:gAIL6* to rescue *ant* ovule defects, we examined ovules in two C1 lines: C1-69 which produces seeds and C1-61 which does not produce seeds. The ovules of *ANT:gAIL6 ant* C1-69 are smaller than those of wild type but the integuments fully enclose the nucellus (Figure 2.2G-I). Thus, C1-69 largely complements the *ant* loss of integument phenotype. In *ANT:gAIL6 ant* C1-61, integument growth is partially rescued, but the nucellus is not fully enclosed by the integuments (Figure 2.2J). Therefore, the inability of C1-61 to produce seeds is associated with reduced integument growth compared with C1-69. Furthermore, we found that *AIL6* mRNA levels are lower in *ANT:gAIL6 ant* C1-61 ovules as compared with C1-69 ovules (Figure 2.3A-C). Thus, differences in seed set in these two lines are correlated with the extent of integument growth and *AIL6* mRNA levels in developing ovules.

In addition to producing fewer seeds than wild type, *ANT:gAIL6 ant* C1-69, C2-18, C3-68 and C4-62 produce seeds that vary in size and seed coat color (Figure 2.4A-F). *ANT:gAIL6 ant* C1-69 seeds are light yellow/light green in color while the color ranged from light green to light brown for *ANT:gAIL6 ant* C2-18, C3-68, and C4-62. Variation in seed size and color was reported previously for transgenic lines in which the coding region of *AIL6* was expressed under the control of the *35S* promoter (i.e. *35S:cAIL6*) (Krizek and Eaddy, 2012). Thus, high levels of *AIL6* can interfere with seed development.

ANT:gAIL6 ant phenotypes are correlated with *AIL6* mRNA levels

To investigate whether the different *ANT:gAIL6 ant* phenotypic classes might be a consequence of different *AIL6* mRNA levels, we performed RT-qPCR on RNA from *ANT:gAIL6 ant* C1-69, C2-18, C3-68, and C4-62 inflorescences. *AIL6* mRNA levels were approximately 9, 13, 17 and 21 fold higher in *ANT:gAIL6 ant* C1-69, C2-18, C3-68, and C4-62, respectively compared to wild type (Figure 2.5A). Thus, the severities of the additional *ANT:gAIL6 ant* phenotypes are correlated with *AIL6* mRNA levels. In addition, there is a dosage effect of the transgene; flowers from *ANT:gAIL6 ant* C4-62 plants hemizygous for the transgene have a less severe phenotype than flowers from plants homozygous for the transgene (Figure 2.6A-C).

We next investigated which *ANT:gAIL6 ant* line produced *AIL6* mRNA levels that were most similar to the levels of *ANT* mRNA in L*er* inflorescences. An absolute RT-qPCR experiment showed that wild-type inflorescences contain approximately 8-fold more copies of *ANT* mRNA than *AIL6* mRNA. Thus, C1-69, which has 9-fold higher levels of *AIL6* mRNA compared with wild type, most closely approximates normal *ANT* mRNA copy numbers. The additional phenotypes resulting from higher *AIL6* expression levels in C2-18, C3-68 and C4-62, can be considered a result of overexpression of *AIL6* above normal levels of *ANT* mRNA. To confirm that *AIL6* mRNA accumulated in a spatial and temporal pattern in *ANT:gAIL6* C1-69 flowers similar to that of *ANT* mRNA in wild-type flowers, we performed in situ hybridization. The *AIL6* mRNA expression pattern in *ANT:gAIL6 ant* C1-69 closely matches that of *ANT* mRNA expression in wild-type flowers (Elliott et al., 1996) (Figure 2.5B-E,I-K). *AIL6* mRNA is expressed at higher

levels in incipient and young floral primordia in *ANT:gAIL6 ant* as compared with wild type (Figure 2.5F,G,I,J). In stage 4 flowers, *AIL6* mRNA is mainly present in the floral meristem of wild-type flowers but accumulates to high levels in both the floral meristem and sepal primordia of *ANT:gAIL6* ant C1-69 (Figure 2.5F,I). *AIL6* mRNA is detected at high levels in stage 7 *ANT:gAIL6 ant* flowers, while *AIL6* mRNA is not detected much after stage 6 in wild-type flowers (Figure 2.5G,J) (Nole-Wilson et al., 2005). *AIL6* mRNA was not expressed in wild-type ovules but was detected in developing ovule primordia of older *ANT:gAIL6 ant* flowers (Figure 2.5H,K).

ANT:gAIL6 lines in a wild-type background display alterations in flower development similar to those observed in the *ant* background

To further investigate the consequences of overexpressing *AIL6*, we transformed wild-type plants with the *ANT:gAIL6* transgene. Generation of these transgenic plants allowed us to investigate whether the *ANT:gAIL6* transgene conferred the same phenotypes in a background containing *ANT* activity. Of the 15 lines obtained, three lines (lines 2, 13, 14) have a wild-type appearance (Figure 2.7A,B). The remaining 12 lines showed phenotypic variations similar to those observed in the *ant-4* background, and we characterized these lines as weak (six lines), strong (four lines) or severe (two lines) and performed floral organ counts on one line from each class: line 2 (wild type), line 12 (weak), line 4 (strong) and line 16 (severe) (Figure 2.7A-E; Table 2.2). Based on these floral organ counts, line 12 (weak) most resembles *ANT:gAIL6 ant* C1-69, line 4 (strong) most resembles *ANT:gAIL6 ant* C3-68 and line 16 (severe) most resembles *ANT:gAIL6 ant* C4-62 (Tables 2.1, 2.2).

Flowers from the weak line 12 produce a small number of petaloid sepals in the first whorl (Figure 2.7C; Table 2.2). In the strong line 4, flowers frequently contained petaloid sepals and subtending filaments, and had reduced numbers of petals and stamens (Figures. 2.7D, 8A, 8B; Table 2.2). We observed that petaloid sepals were more often present in the adaxial position, followed by the abaxial position as compared with the lateral positions (Table 2.3). In addition, first whorl organs showed increasing petal identity in the first whorl as the plants aged (Table 2.4). Thus in later-arising flowers, these organs were characterized as sepaloid petals rather than petaloid sepals. In the severe line 16, flowers contained various mosaic organs and reduced numbers of floral organs (Figures 2.7E, 8E, 8G; Table 2.2). The positioning of floral organs is severely disrupted in line 16; we characterized organs as being present in the outer whorl, stamen whorl or inner whorl for organ counts (Table 2.2). *ANT:gAIL6* line 16 flowers do not make a normal gynoecium. Instead, the organs that arise in the center of the flower have reduced or absent carpel valve tissue, in some cases stigmatic tissue is present on top of a thin cylinder (Figure 2.8F). In other cases, stamenoid carpels or filaments are present in the center of the flower (Figure 2.7E; Table 2.2). Only rarely are any seeds obtained from line 16 homozygous plants. Line 16 flowers are often subtended by filaments or bracts, with early-arising flowers more likely to be subtended by a filament and later-arising flowers more likely to be subtended by a bract (Table 2.4; Figure 2.7E, 8G). These bracts have a combination of sepal-like and leaf-like cells (Figure 2.8H). There is often further growth in the bract axil resulting in the formation of additional leaf-like outgrowths (Figure 2.8I). For both line 4 and line 16, the phenotypic defects become more severe

with developmental age (Table 2.4). Older flowers show reduced numbers of sepals, petals and stamens and increasing numbers of mosaic organs.

We examined early flower development in *ANT:gAIL6* lines 4 and 16. The outer whorl organs of lines 4 and 16 are often narrower than those of wild type and do not fully enclose the floral bud by the time of stamen primordia initiation (Figure 2.8C, J-L). While four whorls can be distinguished in line 4 flowers (Figure 2.8D), only three whorls are visible in line 16 (Figure 2.8J, K). In addition, many floral organs in line 16 show altered morphology with filament-like structures present in the outer whorl and altered development of the innermost carpel primordia (Figure 2.8K, L). Many fewer floral organ primordia are initiated in line 16 (Figure 2.8J). While flower initiation from the inflorescence meristem is similar to wild type in line 4, in line 16 plants, the inflorescence meristem gets progressively smaller and is consumed in flower initiation (Figure 2.8M-P).

We used RT-qPCR to investigate whether the severity of the *ANT:gAIL6* flower phenotypes are correlated with *AIL6* mRNA levels. *AIL6* mRNA levels were approximately 2.5, 7, 20 and 43 fold higher in lines 2 (wild type), 12 (weak), 4 (strong) and 16 (severe), respectively, compared to wild type (Figure 2.7F). Thus, as described previously for *ANT:gAIL6* lines in the *ant* background, the severity of the *ANT:gAIL6* phenotypes in a wild-type background is correlated with *AIL6* mRNA levels. It also appears to be independent of *ANT* activity. We confirmed that *AIL6* mRNA in *ANT:gAIL6* lines 4 and 16 was expressed in a spatial pattern similar to that of *ANT* in wild type (Figure 2.9A-F). In addition, we found that *AIL6* mRNA is present in the filaments and bracts that subtend *ANT:gAIL6* line 4 and 16 flowers (Figure 2.9C, E, F).

The *ANT* promoter is initially active in the cryptic bracts that do not grow out in wild-type (Long and Barton, 2000). Thus our results suggest that *AIL6* expression in these cells is sufficient to promote outgrowth of these organs.

The class B floral homeotic genes *AP3* and *PI* are misexpressed in *ANT:gAIL6* flowers

The partial transformation of first whorl sepals to petals in *ANT:gAIL6* flowers suggests that the class B genes *AP3* and *PI* are misexpressed in some first whorl cells. In wild-type flowers, these genes are expressed in second and third whorl cells where they contribute to the specification of petal and stamen identities, respectively (Figure 2.10A, C, E, G). In *ANT:gAIL6* lines 4 and 16, we detected both *AP3* and *PI* mRNA in the first whorl primordia of stage 3 flowers (Figure 2.10B, F; Figure 2.11A-D). The expansion of *AP3* and *PI* expression into the first whorl is correlated with high level expression of *AIL6* in the first whorl of *ANT:gAIL6* flowers, as conferred by the *ANT* promoter. *AP3* and *PI* expression was maintained in first whorl organs of *ANT:gAIL6* line 16 at later stages of development (Figure 2.10D, H). We did not observe *AP3* or *PI* mRNA expression in the center whorl, although stamenoid carpels are occasionally present here in lines 4 and 16 (Table 2.2). *AP3* and *PI* were not expressed in the filaments and bracts subtending *ANT:gAIL6* flowers (Figure 2.10B).

ANT:gAIL6 misexpression phenotypes are distinct from previously published *AIL6* misexpression phenotypes

Previously we published a description of transgenic plants in which the coding region of *AIL6* was expressed under the control of the constitutive *35S* promoter from cauliflower mosaic virus (i.e. *35S:cAIL6*) (Krizek and Eaddy, 2012). These plants produced flowers with changes in floral organ size and morphology that were correlated with *AIL6* mRNA levels. *35S:cAIL6* line 22, which expressed *AIL6* at approximately 55-fold higher levels than wild type, produced flowers with dramatic alterations in floral organ morphology and defects in cellular differentiation (Figure 2.12B). In contrast, *35S:cAIL6* line 31 which expressed *AIL6* at approximately 30-fold higher levels than wild type produced larger floral organs with relatively normal morphologies (Figure 2.12C). The increased floral organ size of *35S:cAIL6* line 31 is shown for petals (Table 2.5). Increases in petal size are also observed for *ANT:gAIL6 ant* C4-62 (Figure 1G) and *ANT:gAIL6* line 16 (Table 2.5), indicating that high levels of *AIL6* misexpression in the *ANT* expression domain can also alter floral organ size.

Previously, we had also generated *35S:gAIL6* lines in which the genomic region of *AIL6* was expressed under the control of the *35S* promoter (Yamaguchi et al., 2016). *35S:gAIL6* lines have flower phenotypes similar to wild type and *AIL6* mRNA expression levels 2-3 fold higher than wild type (Figure 2.12D; Table 2.5). We were only able to generate six *35S:gAIL6* lines; this may be due to harmful consequences of expressing high levels of *AIL6* mRNA in embryos.

Differences in the flower phenotypes of *35S:gAIL6*, *35S:cAIL6* and *ANT:gAIL6* are likely a consequence of differences in *AIL6* mRNA levels and distribution (Figure

2.13; Supplementary Table 2.4). *AIL6* mRNA is present in a similar spatial and temporal domain in L*er* and *35S:gAIL6* line 6 (Figure 2.13A-D). This, together with the fact that *AIL6* mRNA levels are only 2.5 fold higher in *35S:gAIL6* line 6 compared with wild type, likely explains the absence of a flower phenotype (Yamaguchi et al., 2016). *AIL6* is misexpressed in some floral organs of stage 4 and older flowers of *35S:cAIL6* lines 31 and 22 (Figure 2.13E-G) (Krizek and Eaddy, 2012) while in *ANT:gAIL6* line 16, *AIL6* mRNA accumulates to high levels throughout young flowers (stage 1-4) (Figure 2.13H). To further probe the basis for the different *AIL6* misexpression phenotypes, we made two types of *AIL6* inducible lines under the control of the *35S* promoter: an ethanol inducible transgene (*35S:AlcR/AlcA:gAIL6*) and a steroid-inducible transgene (*35S:gAIL6-GR*).

Misexpression of *AIL6* using an ethanol inducible system results in mosaic organs, reductions in floral organ number and alterations in petal size

In the ethanol-inducible system (Roslan et al., 2001), the transcription factor AlcR is expressed constitutively under the control of the *35S* promoter while a genomic copy of *AIL6* is under the control of the *AlcA* promoter, which is bound by AlcR only in the presence of ethanol (i.e. *35S:AlcR/AlcA:gAIL6*). We examined *AIL6* mRNA levels in *35S:AlcR/AlcA:gAIL6* plants at eight, 12 and 24 hours after the start of a single eight hour ethanol treatment. *AIL6* mRNA levels were induced 144 fold at the end of the ethanol treatment compared with untreated plants (Figure 2.14A). *AIL6* mRNA levels dropped over time after removal of the ethanol (Figure 2.14A). We also examined the spatial distribution of *AIL6* mRNA using in situ hybridization. In water treated *35S:AlcR/AlcA:gAIL6* inflorescences, *AIL6* mRNA accumulated in a similar pattern as

that described previously for wild-type inflorescences (Figure 2.14B). In ethanol treated *35S:AlcR/AlcA:gAIL6* inflorescence *AIL6* mRNA accumulated to high levels in almost all tissues (Figure 2.14C). However, we did not observe *AIL6* mRNA in stage 1 and 2 flowers in ethanol-treated plants (Figure 2.14C).

35S:AlcR/AlcA:gAIL6 plants treated with a single eight hour ethanol treatment at 14-16 days of age produced flowers that displayed alterations in floral organ development from approximately 13 to 16 days after ethanol treatment (Table 2.6). They produce fewer floral organs and a variety of mosaic organs (Figure 2.14D-F). These phenotypes are similar to those observed in *ANT:gAIL6* flowers. No phenotypes were observed in mock or ethanol-treated L*er* flowers, in mock or ethanol-treated flowers from transgenic lines containing either *35S:AlcR* or *AlcA:gAIL6*, or in mock-treated plants containing both transgenes (i.e. *35S:AlcR/AlcA:gAIL6*) (Figure 2.15A-D). In ethanol-treated *35S:AlcR/AlcA:gAIL6* flowers, the most dramatic reductions in floral organ number were observed in flowers that matured 15 days after the ethanol treatment; these flowers contained 9.6 organs while water-treated *35S:AlcR/AlcA:gAIL6* flowers contained 15.5 floral organs (Table 2.6). A variety of mosaic organs were present in these flowers including petaloid sepals, stamenoid sepals and stamenoid petals (Figure 2.14E, F). In addition, ethanol-treated *35S:AlcR/AlcA:gAIL6* flowers display altered patterns of floral organ initiation. In stage 3 wild-type and mock treated *35S:AlcR/AlcA:gAIL6* flowers, the abaxial sepal primordium arises first followed by the two lateral sepals and then the adaxial sepal primordia (Figure 2.14H). In *35S:AlcR/AlcA:gAIL6* stage 3 flowers, lateral sepal primordia are visible earlier than the abaxial sepal primordia (Figure 2.14I). In addition, the sepal primordia in the ethanol-treated flowers do not grow as fast as in the

untreated flowers, and they do not fully enclose the developing flower. Thus organ primordia in the inner whorl are visible (Figure 2.14J). We also often observed a "reduced" flower that was very small with very few floral organs (Figure 2.14G, K; Table 2.6). Such flowers could be observed on the inflorescence meristem at approximately six days after the ethanol treatment and reached maturity at 15-16 days after the ethanol treatment (Figure 2.14K; Table 2.6).

While a single ethanol treatment to 14-16 day old *35S:AlcR/AlcA:gAIL6* plants produces flowers with phenotypes similar to *ANT:gAIL6*, we did not observe increases in petal size. Since this phenotype might be dependent on *AIL6* mRNA levels, developmental stage of the flower and/or age of the plant, we tried different ethanol treatment regimes. Exposure of older *35S:AlcR/AlcA:gAIL6* plants (29-30 days old) to 3 four hour ethanol treatments resulted in larger petals from approximately 6-10 days post treatment (Figure 2.14L, M; Table 2.5). At later days after the treatments, these plants also produced mosaic floral organs and exhibited reductions in floral organ number. Thus *35S:AlcR/AlcA:gAIL6* flowers can recapitulate all of the phenotypes observed in *ANT:gAIL6* plants. Since distinct phenotypes are observed at different times after *AIL6* induction, the developmental stage of the flower at the time of treatment likely plays a role in determining the consequences on flower development. Furthermore, since different ethanol treatment regimes were required for the production of larger petals as compared with mosaic organs, overall *AIL6* levels, the length of time of high AIL6 activity, and/or the developmental age of the plant may also help to determine the nature of the phenotype.

35S:gAIL6-GR lines produce larger flowers and some petaloid sepals

In *35S:gAIL6-GR*, a genomic copy of *AIL6* was fused in frame with the ligand-binding domain of the glucocorticoid receptor (GR). Upon treatment with the steroid dexamethasone (dex), AIL6-GR protein can enter the nucleus to regulate gene expression. Dex treatment of *35S:gAIL6-GR* plants results in the production of larger flowers from approximately 9-13 days post treatment as shown for two lines (lines 7 and 30) (Figure 2.16C, E). We also observed the production of some petaloid sepals in the first whorl of dex-treated *35S:gAIL6-GR* flowers approximately 14-20 days after the first dex treatment (Figure 2.16D, F; Table 2.7). Neither of these phenotypes was observed in dex treated L*er* flowers (Figure 2.16A, B). The larger flower phenotype of *35S:gAIL6-GR* flowers closely resembles that of *35S:ANT* and dex-treated *35S:ANT-GR* (Krizek, 1999; Yamaguchi et al., 2016). Petal epidermal cells were of similar size in mock and dex-treated *35S:gAIL6-GR* flowers suggesting that the increase in organ size is largely due to the presence of more cells (Figure 2.17A-D).

AIL6 mRNA levels were approximately 100 fold higher in *35S:gAIL6-GR* lines 7 and 30 compared with L*er* (Figure 2.18A). In situ hybridization shows higher levels and a broader accumulation pattern of *AIL6* mRNA in *35S:gAIL6-GR* lines 7 and 30 compared with L*er* (Figure 2.18B-G), although *AIL6* mRNA levels were low in stage 1 flowers of *35S:gAIL6-GR* (Figure 9C, D).

DISCUSSION

AIL6 can functionally replace *ANT*

The ability of *AIL6* to complement *ant* when expressed under the control of the *ANT* promoter suggests that the functional differences between *ANT* and *AIL6* are largely a consequence of the different expression patterns of these genes. This is likely due to both the lower overall expression of *AIL6* as compared with *ANT* as well as to differences in the spatial and temporal expression patterns of the genes. *ANT* mRNA is detected in a broader pattern and persists longer in developing floral organs as compared with *AIL6* (Elliott et al., 1996; Nole-Wilson et al., 2005). The ability of *AIL6* to functionally replace *ANT* indicates that AIL6 likely regulates many of the same target genes as ANT when expressed at *ANT* levels in these cells. Specifically, the ability of *AIL6* to rescue the floral organ size defects of *ant* indicates that AIL6 can regulate genes that promote floral organ growth. The ability to regulate common targets is consistent with the high sequence similarity of ANT and AIL6 within the AP2 repeat regions, particularly at positions previously shown to be important for DNA binding by ANT (Krizek, 2003; Nole-Wilson et al., 2005). Thus, these proteins may have similar intrinsic DNA-binding specificities.

We find that the phenotypes in *ANT:gAIL6 ant* plants are correlated with varying levels of *AIL6* mRNA. While expression of *AIL6* at levels comparable to *ANT* in wild-type inflorescences rescues *ant* flowers back to wild-type, higher *AIL6* mRNA levels result in altered patterning within the flower primordium including defects in floral organ positioning and growth and altered spatial expression of the floral homeotic genes. Such phenotypes have not observed in plants misexpressing *ANT*. *35S:ANT* flowers produce

larger flower organs but do not show defects in floral organ initiation or identity (Krizek, 1999; Mizukami and Fischer, 2000). Thus, in cells with high levels of AIL6 protein, additional targets appear to be regulated by AIL6 that are not regulated by ANT, suggesting some functional differences within these two proteins. It is not known whether such genes are regulated by AIL6 under physiological conditions.

AIL6 misexpression phenotypes depends on the developmental stage of the flower

We observe somewhat different flower phenotypes with different *AIL6* misexpression constructs. This is at least partially a consequence of the developmental stage of the flower at the time of *AIL6* overexpression as described here for two different inducible *AIL6* lines. The earliest phenotype observed in both ethanol-treated *35S:AlcR/AlcaA:gAIL6* and dex-treated *35S:gAIL6-GR* was the production of larger flowers which occurred approximately 6-10 days after the first ethanol treatment in *35S:AlcR/AlcaA:gAIL6* plants and 9-13 days after the first dex treatment in *35S:gAIL6-GR* plants. Other phenotypes, including the production of mosaic organs and reductions in floral organ number, were recorded later (13-16 days after ethanol treatment and 14-20 days after dex treatment), meaning that the flower primordia were younger at the time of AIL6 induction. This suggests that there is a window during flower primordium development in which *AIL6* overexpression can affect floral organ initiation and identity specification. After this window has passed, *AIL6* overexpression can affect floral organ growth but not floral organ identity.

We note phenotypic differences between the two types of inducible *AIL6* lines (Table 2.8). *35S:gAIL6-GR* flowers show only modest effects on floral organ number and

the only mosaic floral organs produced are petaloid sepals. In contrast, *35S:AlcR/AlcA:gAIL6* flowers show dramatic reductions in floral organ number and produce a variety of mosaic floral organs. The basis for these differences is not clear. Both induction systems result in high levels of *AIL6* mRNA accumulation and a broad spatial pattern of *AIL6* expression. However, the relative levels and duration of nuclear localized AIL6 protein may vary in the two systems. The levels and persistence of nuclear localized GR fusion proteins can vary depending on the number and spacing of the dex treatments (Ito et al., 2007). Thus, it is possible that a different course of dex treatments might affect the *35S:gAIL6-GR* phenotype and result in the production of more mosaic floral organs.

Concentration dependent effects of AIL6 activity

Phenotypic differences of *ANT:gAIL6* lines in both the *ant-4* and L*er* backgrounds are correlated with steady-state *AIL6* mRNA levels and dosage of the transgene. This suggests a concentration dependent effect of AIL6 activity on gene expression. Different levels of AIL6 activity could result in different levels of activation of a particular set of target genes, with distinct floral phenotypes dependent on the absolute level of target gene activation. This seems the most likely explanation of the different classes of *ANT:gAIL6* phenotypes, which are somewhat similar but vary in severity. Another possibility is that different levels of AIL6 activity regulate distinct target genes with a particular phenotype resulting from the regulation of a unique set of target genes. This could occur via distinct DNA-binding affinities for cis-acting regulatory elements and via combinatorial control with other transcription regulators. For example, target genes

containing high affinity cis-acting elements could be activated in cells with low levels of AIL6 while target genes containing low affinity cis-acting elements would only be activated in cells with high levels of AIL6. Alternatively, some AIL6 protein-protein interactions may only occur when AIL6 protein levels are high. It is also possible that the phenotypes associated with high *AIL6* mRNA levels are a result of the sequestering of transcriptional co-activators or co-repressors thus limiting the activation or repression of other genes that are unrelated to the biological function of AIL6 (i.e. squelching) (Ptashne, 1988).

Whether concentration-dependent regulatory effects of *AIL6* occur in wild-type flowers is not known. We have observed dosage effects of *AIL6* in both the *ant-4* and *ant-4 ail7-1* backgrounds, suggesting that absolute levels of AIL6 are important in certain contexts (Krizek, 2015a). Graded distributions of AIL proteins including AIL6 have been observed in the root with highest levels in the root apical meristem defining stem cell identity and lower levels required for cellular differentiation (Galinha et al., 2007). Using an AIL6-VENUS protein fusion, which complements *AIL6* function as assayed in the *ant-4 ail6-2* background, we have observed gradients of AIL6 protein within young flower primordia (Figure 2.19). Interestingly, the AIL6 protein distribution differs from *AIL6* mRNA distribution in stage three flowers. While *AIL6* mRNA is detected at higher levels in the floral meristem dome as compared with sepal primordia (Nole-Wilson et al., 2005), higher AIL6 protein is observed in the periphery of stage three and four flowers. The significance, if any, of the AIL6 protein gradient in flower patterning or floral organ development is not known. Identification of AIL6 regulatory targets and their spatial

pattern of activation in relation to AIL6 levels may help to reveal whether such gradients contribute to flower development.

Table 2.1 Floral organ counts for L*er*, *ant-4* and *ANT:gAIL6 ant-4* lines C1-69, C2-18, C3-68, C4-62 (flowers 1-30 counted).

	L*er*	***ant-4***	**C1-69**	**C2-18**	**C3-68**	**C4-62**
Whorl 1:						
Se	4.00	4.01	3.97	3.11	1.62	0.78
Pe/Se			0.03	0.88	1.52	0.54
Se/Pe					0.54	0.30
Filament				0.02	0.58	1.57
Pe					0.22	1.11
Pe-St mosaic					0.04	0.33
St; St-like					0.03	0.19
Se-St mosaic						0.01
total	**4.00**	**4.01**	**4.00**	**4.01**	**4.55**	**4.83**
Whorl 2:						
Pe	4.00	3.77	3.90	2.75	1.23	0.33
Se/Pe					0.02	0.01
Filament			0.01	0.01	0.02	0.03
Pe-St mosaic					0.01	0.01
total	**4.00**	**3.77**	**3.91**	**2.76**	**1.28**	**0.38**
Whorl 3:						
St	5.77	4.77	5.36	4.89	4.14	2.86
St-like			0.01	0.07	0.17	0.05
Filament			0.01	0.03	0.03	
Ca/St, St/Ca				0.12	0.02	
total	**5.77**	**4.77**	**5.38**	**5.11**	**4.36**	**2.91**
Whorl 4:						
Ca	2.0	2.00	2.00	1.95	1.58	0.30
St/Ca					0.19	0.07
thin cylinder					0.01	0.11
St-like						0.02
Filament						0.48
total	**2.0**	**2.00**	**2.00**	**1.95**	**1.78**	**0.98**
Total all whorls	**15.77**	**14.55**	**15.29**	**13.83**	**11.97**	**9.10**
% of flowers with subtending filament	0.00	0.0	0.0	68.0	83.3	20.0
% of flowers with subtending bract	0.00	0.0	0.0	0.0	7.50	77.3
% of flowers with organ fusion (Se, St)	0.76	8.3	8.3	39.3	25.8	5.3

Abbreviations: Se, sepal; Pe/Se, petaloid sepal; Se/Pe, sepaloid petal; Pe, petal; Pe-St mosaic, petal-stamen mosaic organ; St, stamen; Se-St mosaic, sepal-stamen mosaic organ; Ca/St, carpelloid stamen; St/Ca, stamenoid carpel; Ca, carpel

Table 2.2 Floral organ counts for L*er* and *ANT:gAIL6* lines 2, 12, 4 and 16 (flowers 1-30 counted).

	L*er*	***ANT:gAIL6* line 2**	***ANT:gAIL6* line 12**	***ANT:gAIL6* line 4**		***ANT:gAIL6* line 16**
Whorl 1:					**Outer Whorl:**	
Se	4.00	4.00	3.99	1.94	Se	0.36
Pe/Se			0.02	1.21	Pe/Se	0.34
Se/Pe				0.73	Se/Pe	0.49
Filament				0.02	Filament	1.82
Pe				0.16	Pe	0.74
St/Pe				0.01	Pe-St mosaic	0.36
total	**4.00**	**4.00**	**4.01**	**4.07**	St/Fil	0.25
					St	0.61
Whorl 2:					Se-Pe-St mosaic	0.27
Pe	4.00	4.00	3.98	2.36	Ca-like	0.01
Trumpet Pe				0.01	**total**	**5.25**
Filament				0.63		
Pe/Se or Se/Pe				0.027		
St/Pe				0.10		
total	**4.00**	**4.00**	**3.98**	**3.13**		
Whorl 3:					**Stamen Whorl:**	
St	5.77	5.88	5.94	4.93	St	1.59
Filament			0.01	0.02	Filament	0.041
total	**5.77**	**5.88**	**5.95**	**4.95**	Ca/St	0.027
					total	**1.66**
Whorl 4:					**Inner Whorl:**	
Ca	2.00	2.00	2.00	1.84	Ca and Ca-like	0.49
St/Ca				0.06	St/Ca	0.18
St-like				0.01	Filament	0.36
total	**2.00**	**2.00**	**2.00**	**1.91**	**total**	**1.03**
Total all whorls	**15.77**	**15.88**	**15.94**	**14.06**		**7.94**
% of flowers with subtending filament	0.00	0.00	0.00	69	% of flowers with subtending filament	34.5
% of flowers with subtending bract	0.00	0.00	0.00	0	% of flowers with subtending bract	62.8
% of flowers with organ fusion	0.76	0.00	0.00	22.7	% of flowers with organ fusion	6.8

Abbreviations: Se, sepal; Pe/Se, petaloid sepal; Se/Pe, sepaloid petal; Pe, petal; St/Pe, stamenoid petal; St, stamen; Ca, carpel; St/Ca, stamenoid carpel

Table 2.3 Comparison of *ANT:gAIL6* line 4 first whorl organs in medial (adaxial and abaxial) and lateral positions (flowers 1-10, 11-20 and 21-30 counted).

		whorl 1 ad	whorl 1 ab	whorl 1 lat
ANT:gAIL6 (flowers 1-10)	Se	0.26	0.50	1.82
	Pe/Se	0.56	0.38	0.42
	Se/Pe	0.12	0.06	0.04
	fil			
	Pe	0.04	0.02	0.06
	St/Pe			
ANT:gAIL6 (flowers 11-20)	Se	0.08	0.22	1.70
	Pe/Se	0.16	0.64	0.30
	Se/Pe	0.72	0.14	0.02
	fil		0.02	
	Pe	0.06		
	St/Pe			
ANT:gAIL6 (flowers 21-30)	Se	0.04	0.12	1.08
	Pe/Se	0.12	0.54	0.50
	Se/Pe	0.70	0.20	0.20
	fil		0.02	0.02
	Pe	0.08	0.14	0.08
	St/Pe	0.02		0.02

Abbreviations: ad, adaxial; ab, abaxial; lat, lateral; Se, sepal; Pe/Se, petaloid sepal; Se/Pe, sepaloid petal; fil, filament; Pe, petal; St/Pe, stamenoid petal

Table 2.4 Floral organ counts for L*er* and *ANT:gAIL6* lines 4 and 16 (flowers 1-10, 11-20, 21-30 counted).

	L*er* 1-10	L*er* 11-20	L*er* 21-30	*ANT:gAIL6* #4; 1-10	*ANT:gAIL6* #4; 11-20	*ANT:gAIL6* #4; 21-30		*ANT:gAIL6* #16; 1-10	*ANT:gAIL6* #16; 11-20	*ANT:gAIL6* #16; 21-30
Whorl 1:							**Outer Whorl:**			
Se	4.0	4.0	4.0	2.58	2.0	1.24	Se	0.96	0.10	
Pe/Se				1.36	1.1	1.16	Pe/Se	0.96	0.04	
Se/Pe				0.22	0.88	1.10	Se/Pe	0.94	0.46	0.42
Filament					0.02	0.04	Filament	0.60	2.36	2.52
Pe				0.12	0.06	0.30	Pe	1.40	0.64	0.15
St/Pe						0.04	Pe-St mosaic	0.14	0.48	0.48
total	**4.0**	**4.0**	**4.0**	**4.28**	**4.06**	**3.61**	St/Fil		0.20	0.56
							St	0.20	0.58	1.06
Whorl 2:							Se-Pe-St mosaic		0.06	0.02
Pe	4.0	4.0	4.0	3.20	2.34	1.54	Ca-like			0.02
Trumpet Pe						0.02	**total**	**5.20**	**4.92**	**5.23**
Filament				0.40	0.44	1.04				
Pe/Se or Se/Pe				0.02	0.04	0.02				
St/Pe				0.02	0.18	0.10				
total	**4.0**	**4.0**	**4.0**	**3.64**	**3.00**	**2.72**				
Whorl 3:							**Stamen Whorl:**			
St	5.78	5.86	5.66	5.34	4.92	4.52	St	2.86	1.28	0.60
Filament				0.02		0.04	Filament	0.06	0.06	
total	**5.78**	**5.86**	**5.66**	**5.36**	**4.92**	**4.56**	Ca/St	0.04	0.02	0.02
							total	**2.96**	**1.36**	**0.62**
Whorl 4:							**Inner Whorl:**			
Ca	2.0	2.0	2.0	1.88	1.82	1.82	Ca and Ca-like	0.45	0.59	0.42
St/Ca				0.04	0.06	0.08	St/Ca	0.20	0.08	0.27
St-like						0.02	Filament	0.40	0.40	0.27
total	**2.0**	**2.0**	**2.0**	**1.92**	**1.88**	**1.92**	**total**	**1.05**	**1.07**	**0.96**
% flowers with sub fil	0	0	0	26	92	90	% flowers with sub fil	60.0	26.0	16.7
% flowers with sub bract							% flowers with sub bract	32.0	74.0	83.3
% flowers with Se,Pe,St fusion	0	0	2.6	22	26	20	% flowers with Se,Pe,St fusion	16.0	4.0	0

Table 2.5 Petal area, width and length in *AIL6* misexpression lines.

	Pe area (mm^2)	**Pe length (mm)**	**Pe width (mm)**
L*er*	2.01 ± 0.15	3.19 ± 0.17	1.09 ± 0.06
35S:cAIL6 #31	2.52 ± 0.22	3.45 ± 0.22	1.19 ± 0.08
35S:gAIL6 #6	1.99 ± 0.15	3.14 ± 0.16	1.10 ± 0.07
L*er*	1.79 ± 0.36	2.95 ± 0.29	1.05 ± 0.12
ANT:gAIL6 #16	2.60 ± 0.51	3.67 ± 0.38	1.19 ± 0.16
L*er* mock (8d post)	1.41 ± 0.19	2.64 ± 0.21	0.93 ± 0.07
L*er* ethanol (8d post)	1.38 ± 0.18	2.68 ± 0.22	0.90 ± 0.09
35S:AlcR/AlcA:gAIL6 mock (8d post)	1.58 ± 0.20	2.83 ± 0.23	0.97 ± 0.06
35S:AlcR/AlcA:gAIL6 ethanol (8d post)	2.36 ± 0.34	3.35 ± 0.20	1.23 ± 0.12
L*er* mock	1.54 ± 0.17	2.94 ± 0.16	0.95 ± 0.06
L*er* dex	1.46 ± 0.21	2.86 ± 0.22	0.93 ± 0.09
35S:gAIL6-GR #7 mock	1.57 ± 0.21	3.00 ± 0.20	0.95 ± 0.07
35S:gAIL6-GR #7 dex	2.35 ± 0.19	3.60 ± 0.18	1.10 ± 0.05
L*er* mock	1.79 ± 0.28	2.72 ± 0.25	1.06 ± 0.10
L*er* dex	1.83 ± 0.25	2.87 ± 0.23	1.07 ± 0.08
35S:gAIL6-GR #30 mock	1.90 ± 0.17	2.89 ± 0.16	1.11 ± 0.07
35S:gAIL6-GR #30 dex	2.78 ± 0.31	3.47 ± 0.16	1.30 ± 0.09

Genotypes grouped together were grown and measured at the same time

Table 2.6 Floral organ counts for water and ethanol treated *35S:AlcR/AlcA:gAIL6* from 12-17 days post treatment.

35S:AlcR/AlcA:gAIL6	**EtOH-12d**	**EtOH-13d**	**EtOH-14d**	**EtOH-15d**	**EtOH-16d**	**EtOH-17d**	**H_2O (12-17d)**
1st whorl							
Se	4.00	3.00	2.55	1.00	2.90	3.88	4.00
Pe/Se; Se/Pe		0.09	0.27	0.43	0.18		
Filament		0.27	0.18				
Pe		0.09	0.27	0.43	0.55		
St/Se; Se/St		0.18	0.09	0.29	0.09		
Se-Pe/St			0.09				
St/Pe; Pe/St		0.09	0.45	0.71			
St		0.18	0.18	0.57	0.18		
Total-1st whorl	**4.00**	**3.90**	**4.08**	**3.43**	**3.90**	**3.88**	**4.00**
2nd whorl							
Pe	3.88	2.64	2.27	1.14	2.55	3.75	4.00
Trumpet Pe			0.09				
Se/Pe				0.14			
St/Pe; Pe/St		0.27	0.27	0.14			
Filament	0.125	0.09	0.18	0.43			
St		0.18	0.09	0.14			
Total-2nd whorl	**4.005**	**3.18**	**2.90**	**1.99**	**2.55**	**3.75**	**4.0**
3rd whorl							
St	5.38	4.36	3.09	2.14	3.45	5.38	5.54
St-like		0.09					
Pe		0.09					
Filament		0.18		0.29			
Total-3rd whorl	**5.38**	**4.72**	**3.09**	**2.43**	**3.45**	**5.38**	**5.54**
4th whorl							
Ca	2.00	2.00	2.00	1.70	1.60	2.00	2.00
Total all whorls	**15.38**	**13.8**	**12.1**	**9.55**	**11.5**	**15.0**	**15.54**
% of "reduced" flowers	0%	0%	0%	14.3%	18.2%	0%	0%
% of flowers with organ	0%	9%	0%	14.3%	9%	0%	0%

Abbreviations: Se, sepal; Pe/Se, petaloid sepal; Se/Pe, sepaloid petal; Pe, petal; St/Se, stamenoid sepal; Se/St, sepaloid stamen; Se-Pe/St, sepaloid petaloid stamen; St/Pe, stamenoid petal; Pe/St, petaloid stamen; St, stamen; Ca, carpel; St/Ca, stamenoid carpel

.

Table 2.7 Floral organ counts for water and dex treated *35S:gAIL6-GR* line 30 from 12-20 days post three dex treatments.

35S:gAIL6-GR	**dex-12d**	**dex-13d**	**dex-14d**	**dex-15d**	**dex-16d**	**dex-17d**	**dex-18d**	**dex-19d**	**dex-20d**	**mock (12-15d)**
1st whorl										
Se	4.00	3.91	3.41	3.07	2.92	2.92	3.23	3.44	3.75	4.00
Pe/Se + Se/Pe		0.09	0.59	0.80	1.00	1.08	0.77	0.33	0.25	
Total-1st whorl	**4.00**	**4.00**	**4.00**	**3.87**	**3.92**	**4.00**	**4.00**	**3.77**	**4.00**	**4.00**
2nd whorl										
Pe	4.00	4.00	3.88	4.00	3.61	3.54	3.62	4.00	4.00	4.00
Total-2nd whorl	**4.00**	**4.00**	**3.88**	**4.00**	**3.61**	**3.54**	**3.62**	**4.00**	**4.00**	**4.00**
3rd whorl										
St	5.74	5.82	5.53	5.40	5.31	5.15	5.62	5.33	5.75	5.74
Total-3rd whorl	**5.74**	**5.82**	**5.53**	**5.40**	**5.31**	**5.15**	**5.62**	**5.33**	**5.75**	**5.74**
4th whorl										
Ca	2.00	2.00	2.00	2.00	2.00	2.00	2.00	2.00	2.00	2.00
Total-4th whorl	**2.00**	**2.00**	**2.00**	**2.00**	**2.00**	**2.00**	**2.00**	**2.00**	**2.00**	**2.00**
Total all whorls	**15.74**	**15.82**	**15.41**	**15.27**	**14.84**	**14.69**	**15.24**	**15.10**	**15.75**	**15.74**

Abbreviations: Se, sepal; Pe/Se, petaloid sepal; Se/Pe, sepaloid petal; Pe, petal; St, stamen; Ca, carpel

Table 2.8 Comparison of *AIL6* misexpression lines.

Transgenic line	**mRNA levels (RT-qPCR); mRNA distribution**	**Phenotype**	**Reference**
35S:gAIL6 #6	2.6; wild-type *AIL6* mRNA pattern	wild-type flowers	(Yamaguchi et al., 2016)
35S:cAIL6 #31	30; patchy and absent from stage 1-4 flowers	larger flowers; altered carpel morphology	(Krizek and Eaddy, 2012)
35S:cAIL6 #22	55; patchy and absent from stage 1-4 flowers	altered floral organ morphology; loss of cell differentiation	(Krizek and Eaddy, 2012)
ANT:gAIL6 #16	43; *ANT* mRNA pattern (strong expression in stage 1-4 flowers; lower levels and more restricted expression as flowers mature)	mosaic floral organs, reductions in floral organ number, larger petals	this study
35S:AlcR/AlcA:gAIL6	144 (8 hrs); everywhere except stage 1 and 2 flowers	mosaic floral organs, reductions in floral organ number, larger flowers	this study
35S:gAIL6-GR #30	104; everywhere except stage 1 flowers	larger flowers; mosaic petaloid sepals	this study

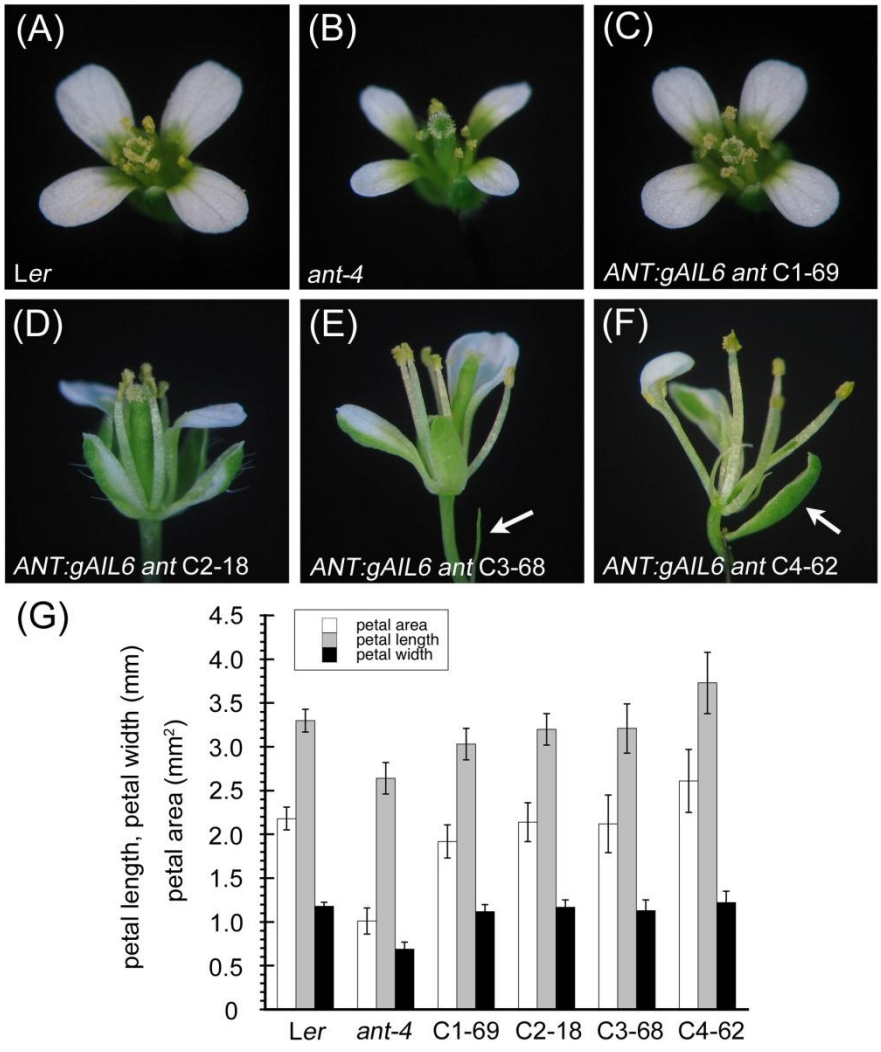

Figure 2.1 *ANT:gAIL6 ant* flowers rescue the petal size defects of *ant*. A L*er* flower. **B** *ant-4* flower. **C** *ANT:gAIL6 ant-4* C1-69 flower. **D** *ANT:gAIL6 ant-4* C2-18 flower. **E** *ANT:gAIL6 ant-4* C3-68 flower. The arrow points to a filament subtending the flower. **F** *ANT:gAIL6 ant-4* C4-62 flower. The arrow points to a bract subtending the flower. **G** Graph of petal area, length and width in L*er*, *ant* and *ANT:gAIL6 ant* lines. The error bars show standard deviation. Petal area, length, and width values of C1-69, C2-18, C3-68 and C4-62 are statistically different from *ant-4* (p value < 0.0001). Petal area, length, and width values of C2-18 and C3-68 are not statistically different from L*er* (p value >0.03). Pictures in **A-F** were taken at the same magnification.

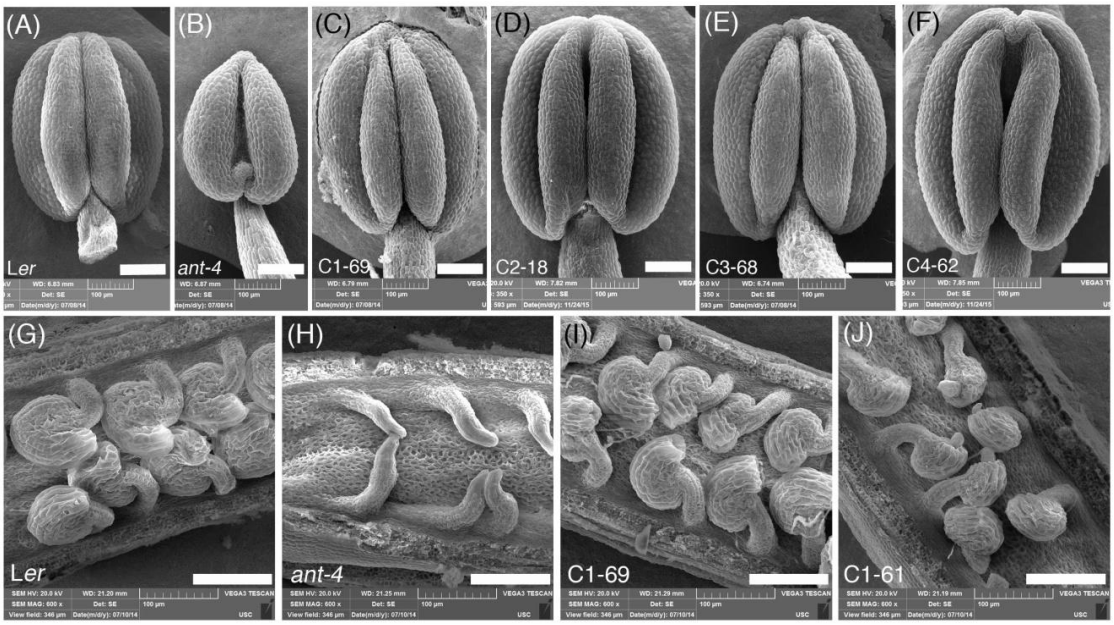

Figure 2.2 SEM of *ANT:gAIL6 ant* anthers and ovules. Stamen anthers from L*er* (**A**), *ant-4* (**B**), *ANT:gAIL6 ant-4* C1-69 (**C**), *ANT:gAIL6 ant-4* C2-18 (**D**), *ANT:gAIL6 ant-4* C3-68 (**E**) and *ANT:gAIL6 ant-4* C4-62 (**F**). Ovules from L*er* (**G**), *ant-4* (**H**), *ANT:gAIL6 ant-4* C1-69 (**I**) and *ANT:gAIL6 ant-4* C1-61 (**J**). Size bars are 100µm.

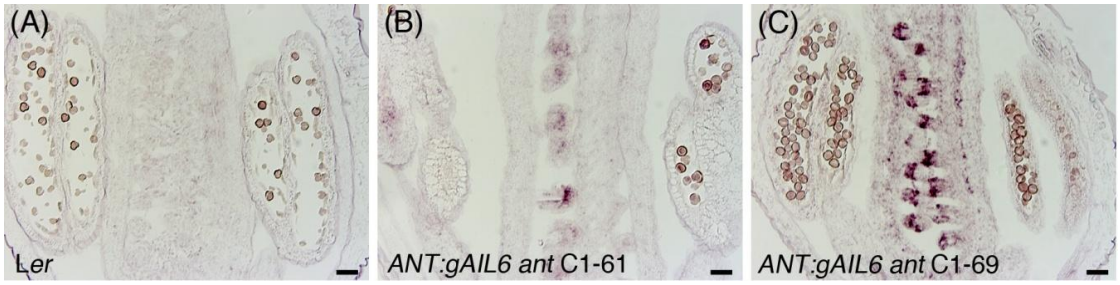

Figure 2.3 *AIL6* expression in *ANT:gAIL6 ant* ovules. A In situ hybridization shows no *AIL6* mRNA in L*er* ovules. **B** *AIL6* mRNA is detected at low levels in *ANT:gAIL6 ant* C1-61 ovules. **C** *AIL6* mRNA is detected at high levels in *ANT:gAIL6 ant* C1-69 ovules. Size bars are 50μm.

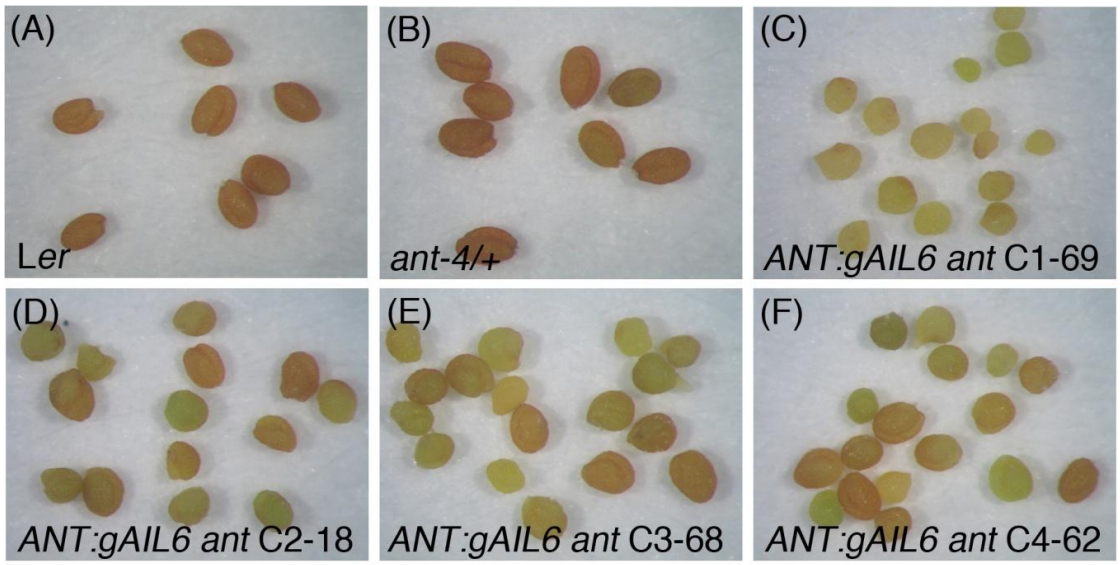

Figure 2.4 *ANT:gAIL6 ant* seeds are altered in color and size. Seeds from L*er* (**A**), *ant-4*/+ (**B**), *ANT:gAIL6 ant-4* C1-69 (**C**), *ANT:gAIL6 ant-4* C2-18 (**D**), *ANT:gAIL6 ant-4* C3-68 (**E**), and *ANT:gAIL6 ant-4* C4-62 (**F**). Pictures in **A-F** were taken at the same magnification.

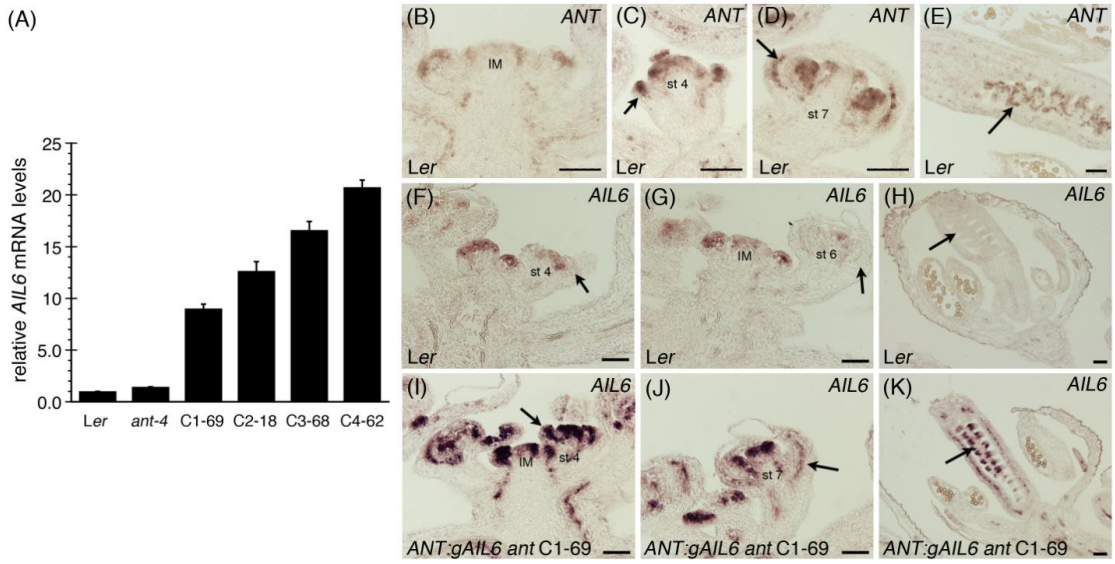

Figure 2.5 *AIL6* expression in *ANT:gAIL6 ant* lines. A Graph of RT-qPCR results showing relative *AIL6* mRNA levels in L*er*, *ant-4* and *ANT:gAIL6 ant* lines C1-69, C2-18, C3-68 and C4-62 inflorescences. The expression level in L*er* is set to one and error bars show standard deviation. **B-E** In situ hybridization of *ANT* mRNA in L*er* inflorescences. **B** *ANT* mRNA accumulates in floral primordia on the periphery of the IM. **c** *ANT* mRNA in a stage 4 flower. Arrow points to a sepal primordia. **D** *ANT* mRNA in a stage 7 flower. Arrow points to a developing sepal. **e** *ANT* mRNA in ovules (arrow). **F-H** In situ hybridization of *AIL6* mRNA in L*er* inflorescences. *AIL6* mRNA accumulates in the inflorescence meristem and young flowers of L*er* inflorescences (**F, G**) but not in the sepals of stage 4 or 7 flowers (**F, G**) (arrows) or in ovules (**H**) (arrow) (**H**). **I-K** In situ hybridization of *AIL6* mRNA in *ANT:gAIL6 ant* C1-69 inflorescences. **I** *AIL6* mRNA accumulates to high levels in the periphery of the inflorescence meristem and in the sepals of stage 4 flowers (arrow) of *ANT:gAIL6 ant* C1-69. **J** *AIL6* mRNA is detected in the sepal (arrow), stamen and carpel primordia of stage 7 *ANT:gAIL6 ant* C1-69 flowers. **K** *AIL6* mRNA is detected in the ovules (arrow) of *ANT:gAIL6 ant* C1-69 carpels. Abbreviations: IM, inflorescence meristem; st 4, stage 4 flower; st 6, stage 6 flower; st 7, stage 7 flower. Size bars are 50µm. Panels **B-E** showing *ANT* mRNA are presented to show the spatial pattern of expression driven by the *ANT* promoter. They are from a separate experiment as compared with panels **F-K** showing *AIL6* mRNA.

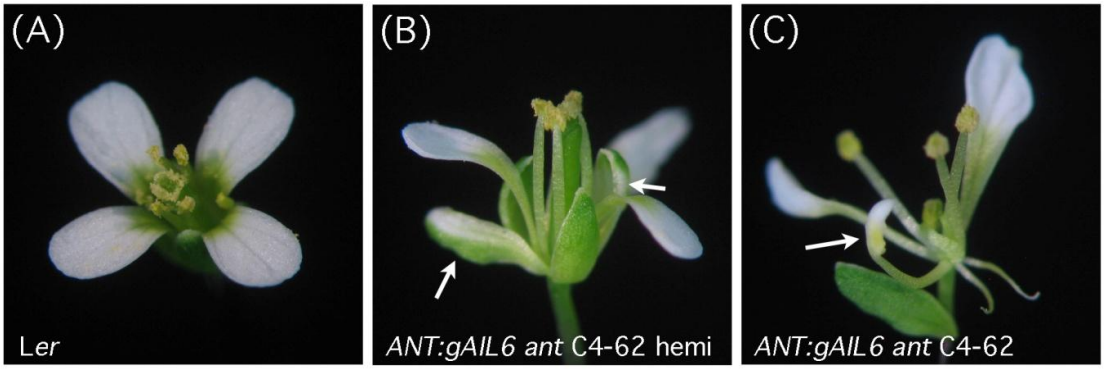

Figure 2.6 Dosage effects of the *ANT:gAIL6* transgene in *ant-4*. A L*er* flower. **B** *ANT:gAIL6 ant* C4-62 flower from a plant hemizygous for the transgene. Flower has reduced numbers of petals and petaloid sepals (arrows). **C** *ANT:gAIL6 ant* C4-62 flower from a plant homozygous for the transgene. Flower has reduced numbers of floral organs, filaments, a stamenoid petal (arrow), and is subtended by a bract. Pictures in **A-C** were taken at the same magnification.

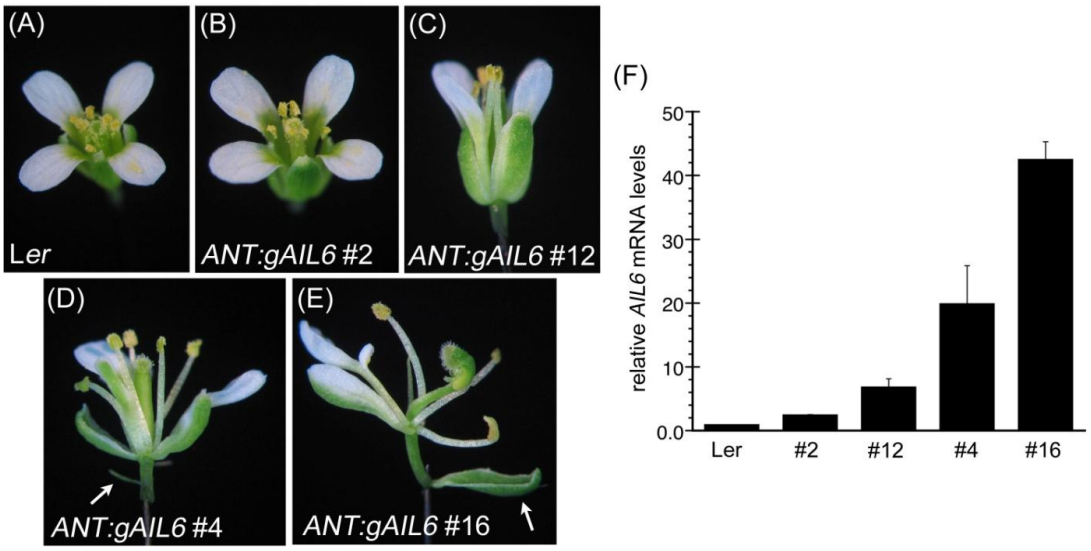

Figure 2.7 *ANT:gAIL6* flower phenotypes and *AIL6* mRNA levels. **A** L*er* flower. **B** *ANT:gAIL6* line 2 flower. **C** *ANT:gAIL6* line 12 flower. **D** *ANT:gAIL6* line 4 flower. The arrow points to a subtending filament. **E** *ANT:gAIL6* line 16 flower. The arrow points to a subtending bract. **F** RT-qPCR of *AIL6* mRNA in L*er* and *ANT:gAIL6* lines 2, 12, 4 and 16. The expression level in L*er* is set to one and error bars show standard deviation. Pictures in **A-E** were taken at the same magnification.

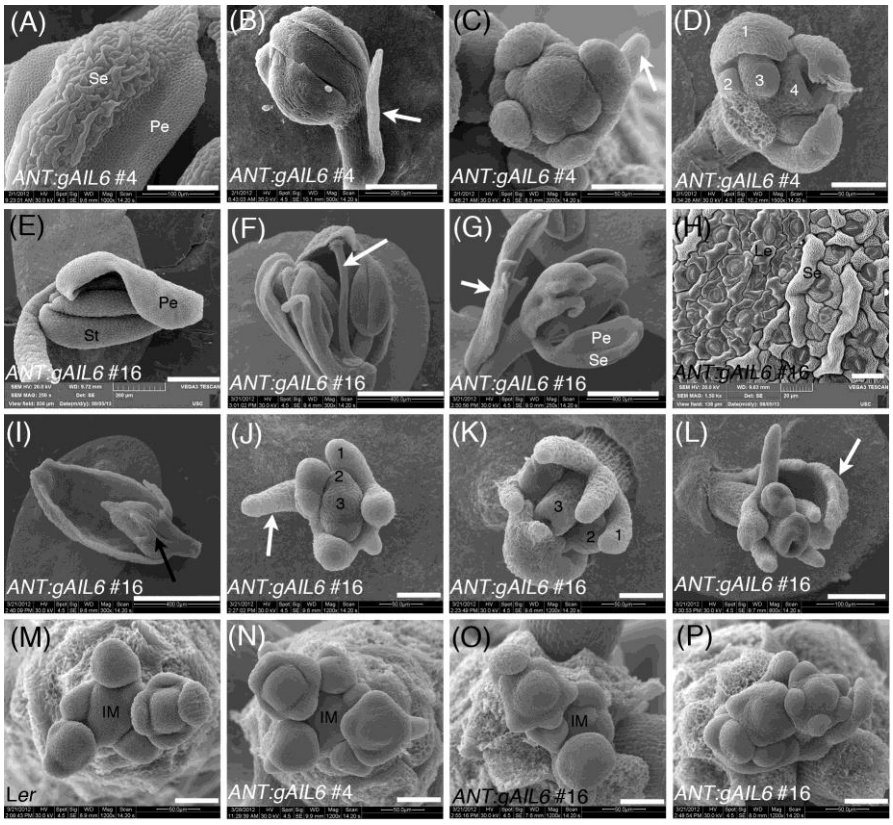

Figure 2.8 SEM of *ANT:gAIL6* flowers. A Mosaic petaloid sepal from *ANT:gAIL6* line 4 with both petal-like (Pe) and sepal-like (Se) cells. **B** Filament (arrow) subtends *ANT:gAIL6* line 4 flower. **C** Young *ANT:gAIL6* line 4 flower with reduced growth of the outer whorl organ primordia, making the inner whorl organ primordia visible. The arrow points to a subtending filament. **D** *ANT:gAIL6* line 4 flower with organs in four whorls (1, 2, 3, 4). **E** Mosaic petaloid stamen from *ANT:gAIL6* line 16 with petal-like (Pe) and stamen-like (St) regions. **F** *ANT:gAIL6* line 16 flower with a thin cylinder topped with stigmatic tissue present in the inner part of the flower. **G** *ANT:gAIL6* line 16 flower with a mosaic petaloid sepal in the outer whorl. Petal-like (Pe) and sepal-like (Se) cells are indicated. The arrow points to a subtending bract. **H** Close-up of a bract subtending an *ANT:gAIL6* line 16 flower showing the presence of both leaf-like (Le) and sepal-like (Se) cells. **I** *ANT:gAIL6* line 16 bract that has additional leaf-like organs (arrow) growing in the leaf axil. **J** Young *ANT:gAIL6* line 16 flower with a subtending filament (arrow) and organs that appear to arise in three whorls (1, 2 and 3). **K** *ANT:gAIL6* line 16 flower with floral organs present in three whorls (1, 2 and 3). Some of the outermost organs are filamentous. **L** *ANT:gAIL6* line 16 flower with a subtending bract (arrow) and organs arising in altered positions. Two organs are fused in the inner part of the flower. **M** L*er* inflorescence meristem. **N** *ANT:gAIL6* line 4 inflorescence meristem showing reduced growth of first whorl organ primordia. Subtending filaments are visible on the flowers. **O** *ANT:gAIL6* line 16 inflorescence meristem showing reduced growth and altered positioning of first whorl organ primordia and the presence of subtending bracts. **P** *ANT:gAIL6* line 16 inflorescence. There is no visible inflorescence meristem; it appears to have been terminated with the initiation of flower primordia. Abbreviations: IM,

inflorescence meristem; Se, sepal-like cells; Pe, petal-like cells; St, stamen-like cells; Le, leaf-like cells; numbers (1, 2, 3, 4) indicate whorls. Size bars are 20µm (**H**), 50µm (**C, D, J, K, M-P**), 100µm (**A, L**), 200 (**B, E**) and 400µm (**F, G, I**).

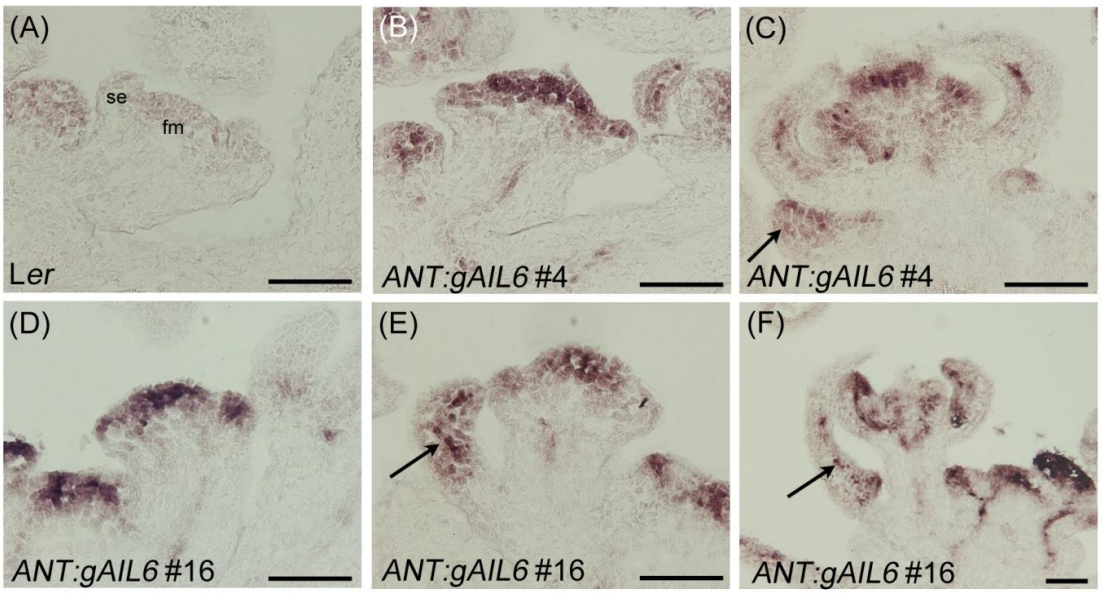

Figure 2.9 *AIL6* is expressed in a broader domain and at higher levels in *ANT:gAIL6* lines 4 and 16 flowers as compared with L*er*. **A** In situ hybridization showing *AIL6* expression in a stage 3 L*er* flower. **B** *AIL6* expression in a stage 3 *ANT:gAIL6* line 4 flower. *AIL6* mRNA accumulates to higher levels in the outer whorl organ primordia and the floral meristem dome of *ANT:gAIL6* line 4 compared to wild type. **C** *AIL6* expression in a stage 6 *ANT:gAIL6* line 4 flower. *AIL6* mRNA is detected in the outer whorl developing organs as well as the stamen and carpel primordia. *AIL6* is also expressed in the subtending filament (arrow). **D, E** *AIL6* expression in stage 3 *ANT:gAIL6* line 16 flowers. Expression is detected in some cells of the outer whorl organ primordia. The arrow points to *AIL6* expression in the subtending filament/bract in **E. F** *AIL6* expression in a stage 6 *ANT:gAIL6* line 16 flower. *AIL6* is expressed in all of the floral organs and the subtending bract (arrow). Size bars are 50μm. Abbreviations: se, sepal; fm, floral meristem dome.

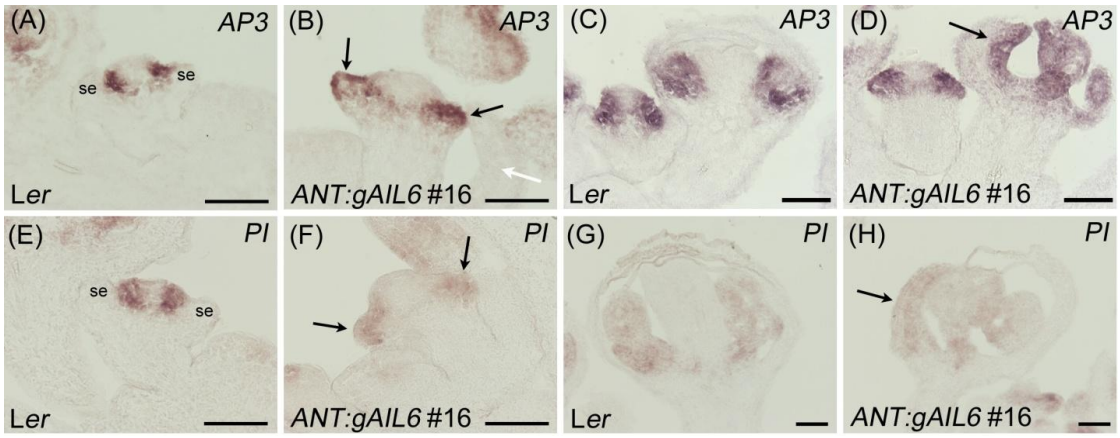

Figure 2.10 *AP3* and *PI* are misexpressed in *ANT:gAIL6* line 16 flowers. A In situ hybridization of *AP3* mRNA in a stage 4 L*er* flower. **B** *AP3* mRNA expression in first whorl organ primordia (black arrows) of a stage 3 *ANT:gAIL6* line 16 flower. No *AP3* mRNA is detected in the subtending bract (white arrow). **C** *AP3* mRNA expression in stage 4 (left) and stage 7 (right) L*er* flowers. **D** *AP3* mRNA is detected in the first whorl organ primordia of the stage 3 *ANT:gAIL6* line 16 flower (left) and in a first whorl organ in an older flower (arrow). **E** In situ hybridization of *PI* mRNA in a stage 4 L*er* flower. **F** *PI* mRNA expression in first whorl organ primordia (arrows) of a stage 3 *ANT:gAIL6* line 16 flower. **G** *PI* mRNA expression in stage 10 L*er* flower. **H** *PI* mRNA is detected in the first whorl organ of an older flower (arrow). Size bars are 50µm.

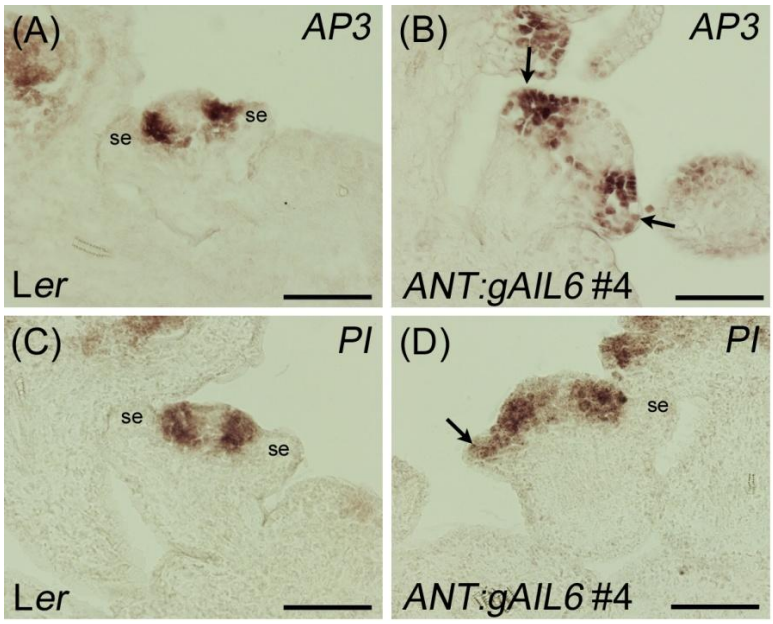

Figure 2.11 *AP3* and *PI* are misexpressed in first whorl organ primordia of *ANT:gAIL6* line 4 flowers. A *AP3* mRNA is not present in sepal primordia of stage 4 L*er* flowers. **B** *AP3* mRNA is present in the first whorl primordia of this *ANT:gAIL6* line 4 stage 3 flower (arrows). **C** *PI* mRNA is not present in sepals of stage 4 L*er* flowers. **D** *PI* mRNA is present in one of the first whorl primordia of this *ANT:gAIL6* line 4 stage 3 flower. Size bars are 50μm. Abbreviations: se, sepal.

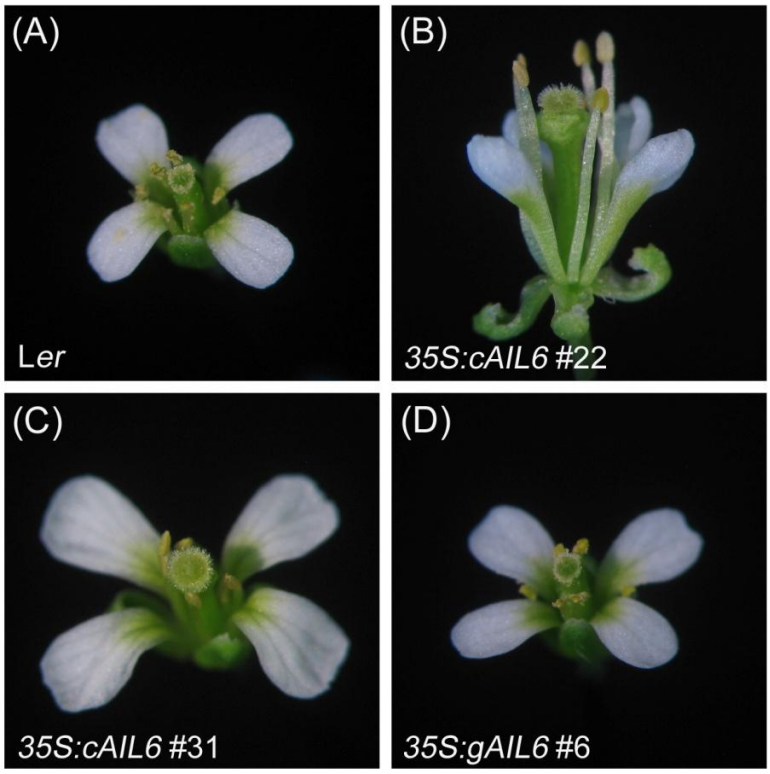

Figure 2.12 Flower phenotypes of previously characterized *AIL6* misexpression lines. A L*er* flower. **B** *35S:cAIL6* line 22 flower. **C** *35S:cAIL6* line 31 flower. **D** *35S:gAIL6* line 6 flower. Pictures in **A-D** were taken at the same magnification and grown at the same time as *ANT:gAIL6* lines.

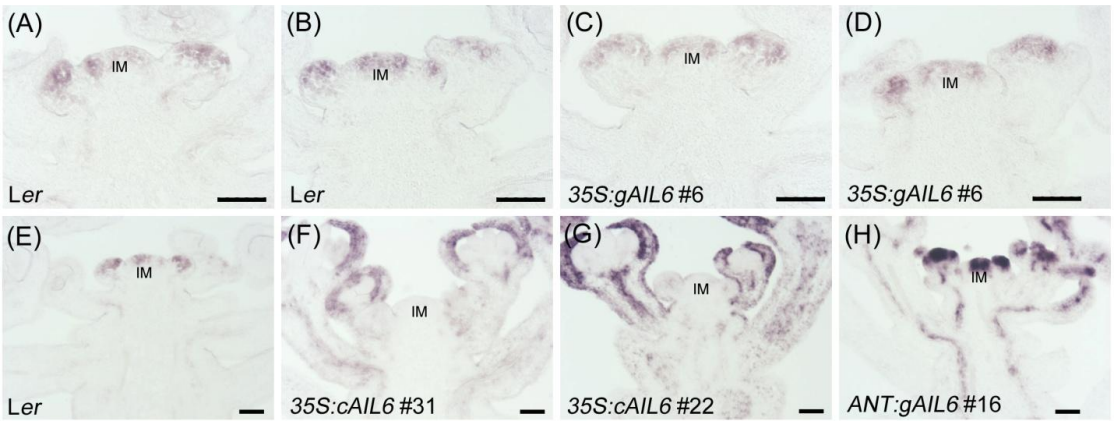

Figure 2.13 *AIL6* mRNA expression patterns in previously characterized *AIL6* misexpression lines and *ANT:gAIL6* line 16. A, B, E In situ hybridization showing *AIL6* mRNA in L*er* inflorescences. *AIL6* mRNA accumulates within the inflorescence meristem and young flowers. **C, D** In situ hybridization shows that *AIL6* mRNA accumulates in a similar pattern in *35S:gAIL6* line 6 inflorescences as compared with L*er*. **F, G** In situ hybridization showing *AIL6* mRNA in *35S:cAIL6* line 31 (**F)** and 22 (**G**) inflorescences. *AIL6* mRNA accumulates unevenly in older flowers and does not accumulate in stage 1-3 flowers. **H** In situ hybridization showing *AIL6* mRNA in *ANT:gAIL6* line 16 inflorescence. *AIL6* mRNA accumulates to high levels in the inflorescence meristem and young flowers. Size bars are 50μm. Abbreviations: IM, inflorescence meristem.

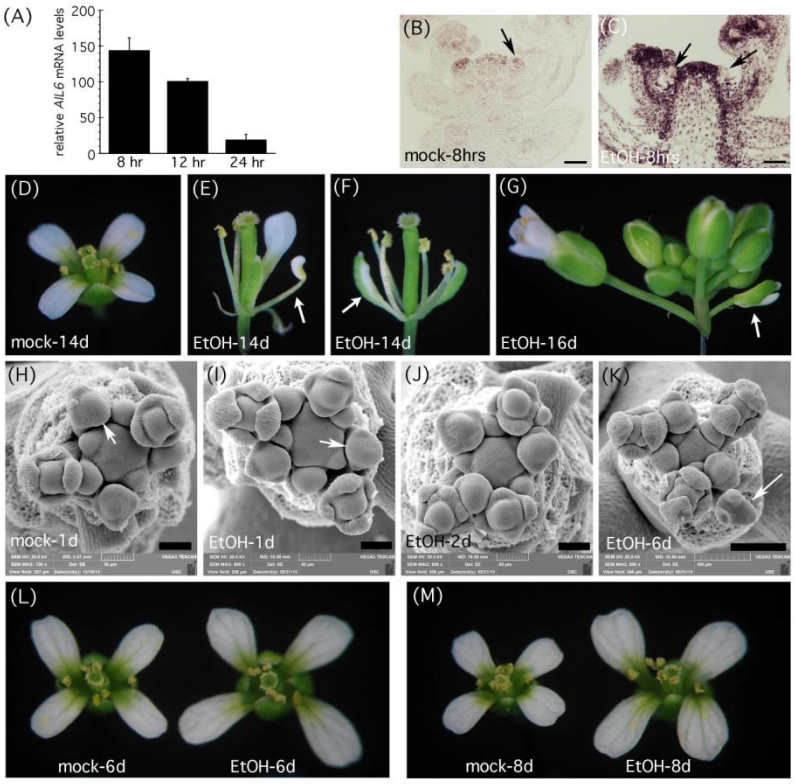

Figure 2.14 *35S:AlcR/AlcA:gAIL6* flowers produce mosaic organs and larger petals and show reductions in floral organ number. In **A-K**, plants were treated with a single 8-hour mock or ethanol exposure. In **L, M**, plants were treated with three 4-hour mock or ethanol exposures. **A** RT-qPCR showing relative *AIL6* mRNA levels in *35S:AlcR/AlcA:gAIL6* inflorescences at 8, 12 and 24 hours after the start of an eight hour ethanol treatment. The expression level is compared to untreated *35S:AlcR/AlcA:gAIL6* inflorescences and error bars show standard deviation. **B** In situ hybridization of *AIL6* mRNA on mock-treated *35S:AlcR/AlcA:gAIL6* collected at the end of the eight-hour mock treatment. Arrow points to stage 1 flower. **C** In situ hybridization of *AIL6* mRNA on ethanol-treated *35S:AlcR/AlcA:gAIL6* at the end of the eight-hour ethanol treatment. Arrows point to stage 1 and 2 flowers. **D** Mock-treated *35S:AlcR/AlcA:gAIL6* flower has a wild-type appearance. **E-F** Ethanol-treated *35S:AlcR/AlcA:gAIL6* flowers have reduced numbers of floral organs and mosaic organs. The arrows point to a petaloid stamen (**e**) and a petaloid sepal (**F**). **G** Inflorescence of an ethanol-treated *35S:AlcR/AlcA:gAIL6* plant with a reduced flower (arrow). **H** SEM of mock-treated *35S:AlcR/AlcA:gAIL6* inflorescence one day after treatment. The arrow points to a stage 3 flower. As in wild type, the abaxial sepal primordium is well defined. **I** SEM of ethanol-treated *35S:AlcR/AlcA:gAIL6* inflorescence one day after treatment. The arrow points to a stage 3 flower in which the lateral sepal primordia are visible while the abaxial sepal is not visible. **J** SEM of ethanol-treated *35S:AlcR/AlcA:gAIL6* inflorescence two days after treatment. The young flower primordia show altered positioning and growth of first whorl organ primordia. **K** SEM of ethanol-treated *35S:AlcR/AlcA:gAIL6* inflorescence six days after treatment. The arrow points to a reduced flower that initiated only two primordia in the outer whorl. **L** Mock and ethanol-treated *35S:AlcR/AlcA:gAIL6* flower 6

days after the first of three four-hour mock (left) or ethanol (right) treatments. **M** Mock and ethanol-treated *35S:AlcR/AlcA:gAIL6* flower 8 days after the first of three four-hour mock (left) or ethanol (right) treatments. Size bars are 50µm (**B, C, H-K**).

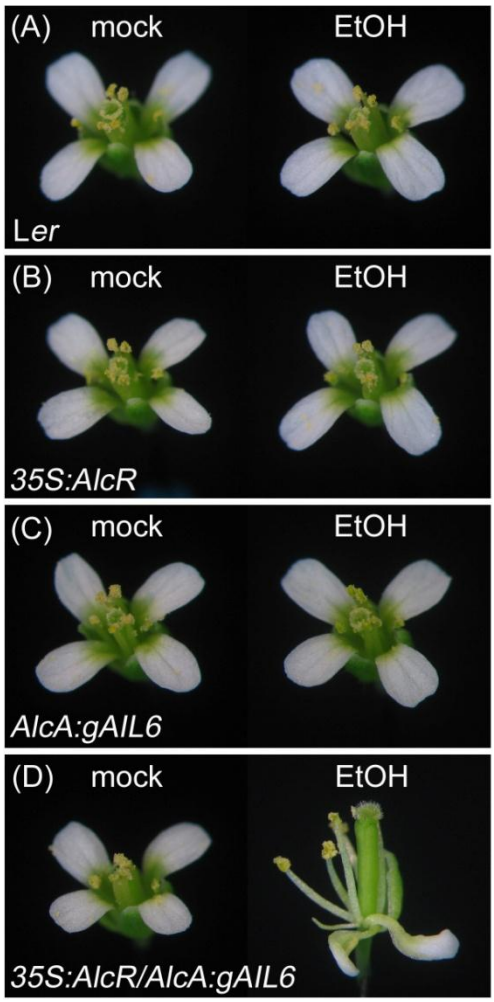

Figure 2.15 Flower phenotypes of mock and ethanol treated L*er* (**A**), *35S:AlcR* (**B**), *AlcA:gAIL6* (**C**) and *35S:AlcR/AlcA:gAIL6* (**D**). Only plants carrying both the *35S:AlcR* transgene and the *AlcA:gAIL6* transgene show a phenotype after ethanol treatment. Pictures in **A-D** were taken at the same magnification.

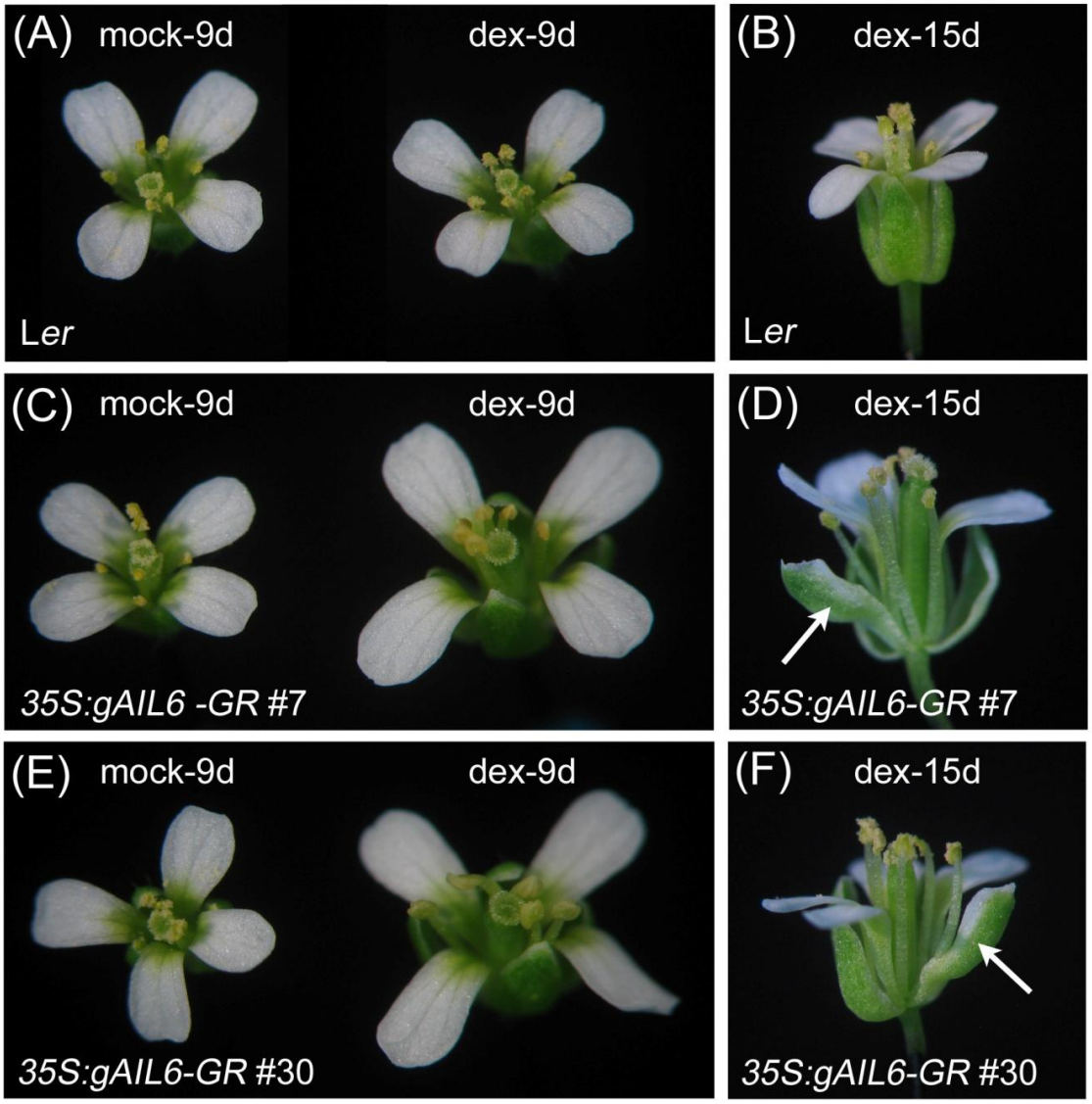

Figure 2.16 Dex treatment of *35S:gAIL6-GR* inflorescences results in larger flowers and the production of first whorl petaloid sepals. **A** L*er* flowers nine days after mock (left) or dex (right) treatments. **B** L*er* flower 15 days after dex treatment. **C** *35S:gAIL6-GR* line 7 flowers nine days after mock (left) or dex (right) treatments. **D** *35S:gAIL6-GR* line 7 flower 15 days after dex treatment. Arrow points to first whorl petaloid sepal. **E** *35S:gAIL6-GR* line 30 flowers nine days after mock (left) or dex (right) treatments. **F** *35S:gAIL6-GR* line 30 flower 15 days after dex treatment. Arrow points to first whorl petaloid sepal. Pictures in **A-F** were taken at the same magnification.

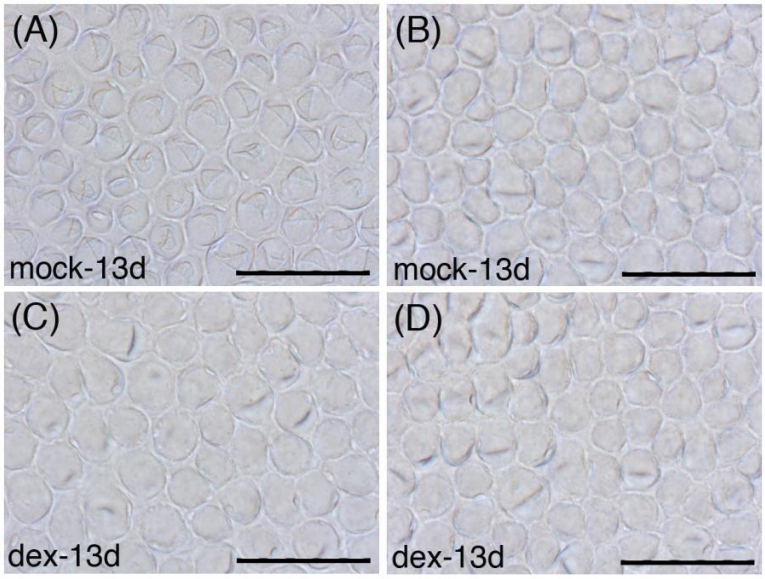

Figure 2.17 Petal cell size comparison in mock and dex-treated *35S:gAIL6-GR* line 30. Adaxial petal epidermal cells of *35S:gAIL6-GR* line 30 flowers from mock (**A, B**) and dex-treated (**C, D**) plants 13 days after the first treatment. Size bars are 50μm.

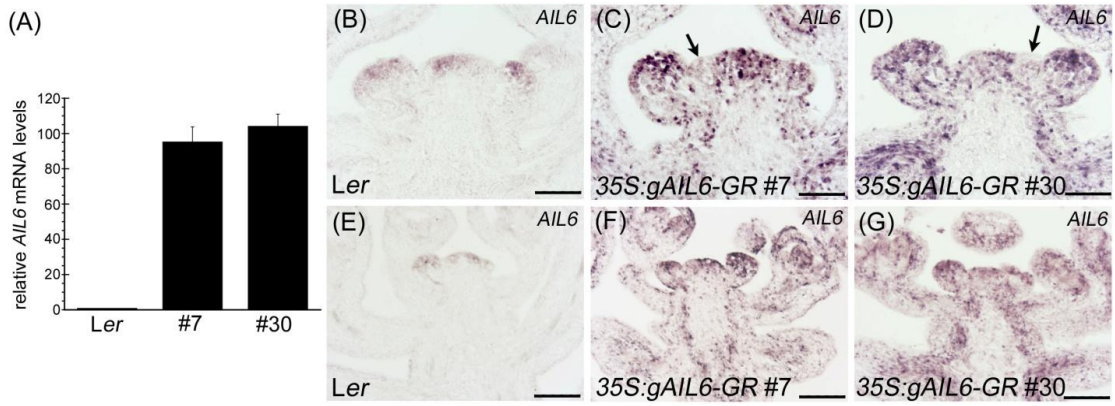

Figure 2.18 *AIL6* mRNA expression in *35S:gAIL6-GR* lines 7 and 30. A Graph of RT-qPCR results showing relative *AIL6* mRNA levels in L*er*, *35S:gAIL6-GR* lines 7 and 30. The expression level in L*er* is set to one and error bars show standard deviation. **B** In situ hybridization of *AIL6* mRNA in L*er* inflorescence. *AIL6* mRNA accumulates in the inflorescence meristem and young flowers of L*er* inflorescences. **C, D** In situ hybridization of *AIL6* mRNA in *35S:gAIL6-GR* line 7 (**C**) and line 30 (**D**) inflorescences. *AIL6* mRNA accumulates throughout the inflorescence meristem and flowers of stage 2 and older. Arrows point to stage 1 flowers. **E** In situ hybridization of *AIL6* mRNA in L*er* inflorescence. *AIL6* mRNA is restricted to the inflorescence meristem and young flowers. **F, G** In situ hybridization of *AIL6* mRNA in *35S:gAIL6-GR* line 7 (**f**) and line 30 (**G**) inflorescences. *AIL6* mRNA accumulates in inflorescence stem tissue and older *35S:gAIL6-GR* flowers. Size bars are 50µm (**B-D**) and 100µm (**E-G**).

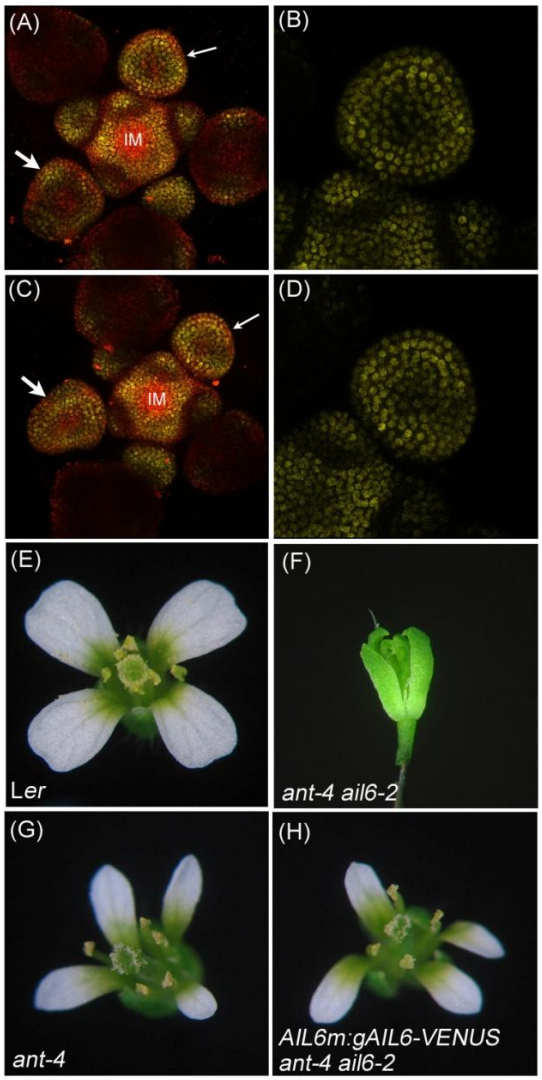

Figure 2.19 AIL6 protein distribution in *AIL6m:gAIL6-VENUS ail6-2* inflorescences and complementation of *AIL6* function by *AIL6m:gAIL6-VENUS*. (**A, C**) Top view confocal images of *AIL6m:gAIL6-VENUS ail6-2* inflorescences with the VENUS signal shown in yellow and chlorophyll signal shown in red. The thin arrow points to a stage three flower primordium and the thick arrow points to a stage four flower primodium. The VENUS signal is higher around the periphery of stage three and four flower primordia. (**B, D**) Top view confocal images showing the VENUS signal in the stage three flowers indicated in (**A**, **C**) respectively. **E** L*er* flower. **F** *ant-4 ail6-2* flower. **g** *ant-4* flower. **H** *AIL6m:gAIL6-VENUS ant-4 ail6-2* flower. AIL6-VENUS complements *ail6-2*. Pictures in **E-H** were taken at the same magnification

CHAPTER 3
CHARACTERIZATION OF AIL6 PROTEIN AND IDENTIFICATION OF POTENTIAL TARGETS OF AIL6 REGULATION

INTRODUCTION

Previously, ANT was shown to bind *in vitro* to the DNA consensus site 5'-gCAC(A/G)N(A/T)TcCC(a/g)ANG(c/t)-3', where the uppercase letters indicate the most highly conserved positions, lowercase letters indicate less conserved positions, and N indicates positions for which no particular base appeared to be preferred (Nole-Wilson and Krizek, 2000). The DNA-binding activity of ANT has been extensively characterized using the sequence 5'-ttgGTGCACATATCCCGATGCTTaca-3' (also known as binding site 15 or BS 15). The BS 15 binds to the ANT protein fragment containing two AP2 repeats and an intervening linker (i.e. ANT-AP2R1R2) at a dissociation constant of 1.3×10^{-8} M. Although ANT and AIL6 share high sequence similarity between their two tandem AP2 repeats and intervening linker (Nole-Wilson et al., 2005), little is known about AIL6 protein. AIL6 presumably functions as a transcription factor, but there are no reports on whether AIL6 can bind DNA and activate transcription. In chapter 2, we showed that AIL6 can act like ANT when *AIL6* is expressed in the same domain and level as *ANT*. We hypothesize that AIL6 can bind to the ANT consensus binding site *in vitro* and activate transcription through the ANT BS 15 *in vivo*. Such data would provide

biochemical support for AIL6 function as a transcriptional activator with a similar DNA binding activity as ANT.

Moreover, very few downstream targets of AIL proteins have been identified. To better understand the biological roles of AIL6 during flower development, we would like to identify targets of AIL6 regulation. Previous data showed that *AP3* and *AG* expression is reduced in *ant ail6* mutants indicating that ANT and AIL6 are necessary for expression of the floral homeotic genes *AP3* and *AG* (Krizek, 2009). Furthermore, in Chapter 2, we showed that *AP3* and *PI* expression is shifted into the first whorl in *ANT:gAIL6*, suggesting that high AIL6 activity is sufficient to activate these genes in an ectopic location. It is not known whether floral homeotic genes are direct targets of AIL6 regulation in wild-type flowers.

METHODS AND MATERIALS

β-galactosidase liquid assay

The yeast reporter strain BK1 containing the lacZ reporter gene under the control of a trimerized BS 15 and the TATA portion of the CYC1 gene was described previously (Krizek, 2003). The coding region of *AIL5*, *AIL6* and *AIL7* were cloned into pGAD424 in which the GAL4 activation domain has been removed (Clontech). These constructs were transformed into BK1 yeast strain. Transformed yeast strains were grown and harvested as previously described (Krizek, 2003). β-galactosidase liquid assays were performed using the Galacto Light Plus kit following the manufacturer's protocol (Applied Biosystems). 5 µl of crude yeast extract was added to 200 µl of a 1:100 dilution of the

Galacton-Plus substrate. After incubation for 40min at room temperature, the enzyme activity was terminated and light emission was initiated by the addition of 300µl of accelerator. Luminescence was measured with a luminometer. The assays were performed in triplicate and repeated at least three times. The amount of protein present in each sample was determined by a Bradford assay.

Plasmid construction and plant transformation

Epitope tagged *AIL6-VENUS* (i.e. *AIL6m:gAIL6-VENUS*) was constructed by first cloning a 919bp fragment of *AIL6* 3' sequence into the *Xba*I site of *9Ala-VENUS/BJ36*. This *AIL6* 3' sequence was PCR amplified with AIL6-46 (5'-AATATCTAGAAACCAATCATATAAGTTGATTGAG-3') and AIL6-47 (5'-AAGATCTAGACCTCGGCTAGGAAATATGTTT-3'). A genomic copy of *AIL6* was created in pGEM3Z and subcloned into the *Sma*I/*Bam*HI sites of *9Ala-VENUS-3'/BJ36*. 591 bp of *AIL6* 5' sequence was subcloned into the *Sma*I site of *gAIL6-VENUS-3'/BJ36* to create *AIL6m:gAIL6-VENUS-3'/BJ36*. *AIL6m:gAIL6-VENUS-3'* was subcloned into the *Not*I site of pART27 and transformed into the *Agrobacterium* strain ASE by electroporation. *35S:AP1-GR ap1 cal* plants were transformed with this Agrobacterium strain and *AIL6-VENUS 35S:AP1-GR ap1 cal* transformants were selected for kanamycin resistance.

For the *AIL6m:gAIL6-GR* construct, 919bp fragment of *AIL6* 3' sequence was first subcloned into the *Xba*I site of BJ36. A genomic copy of *AIL6* lacking the stop codon was subcloned into *Sma*I/*Bam*HI sites of *AIL6 3'/BJ36*. The ligand binding domain of the glucocorticoid receptor (GR) was added to the *Bam*HI site of *gAIL6-3'/BJ36*. 591

bp of AIL6 5’ sequence previously made in pCRScript (Krizek, 2015b) was subcloned into the *Not*I (by partial digestion) and *Sma*I sites of *gAIL6-GR-3’/BJ36*. The *AIL6m:gAIL6-GR-3’/BJ36* was cloned into the *Not*I site of pART27 and transformed into the *Agrobacterium* strain ASE by electroporation. *ant-4 ail6* plants were transformed with this Agrobacterium strain by vacuum infiltration (Bechtold et al., 1993). *AIL6m:gAIL6-GR-3’/BJ36* transformants were selected for kanamycin resistance.

For *35S:AlcR/AlcA:AIL6-amiRNA2* construct, AIL6-amiRNA2 DNA contains two 21mer DNAs within a 404-bp *MIR319a* stem loop fragment. These two 21mer DNAs are self-complementary and will be processed into an artificial microRNA (amiRNA) designed to target *AIL6*. These two 21mer DNA sequences were designed using an online amiRNA designing tool (http://wmd.weigelword.org) (Schwab et al., 2006). AIL6-amiRNA2 DNA (IDT) is

ttacgtatgaattccaaacacacgctcggacgcatattacacatgttcatacacttaatactcgctgttttgaattgatgttttaggaat
atatatgtagaCGATGTTACTCGAGATAGATTtcacaggtcgtgatatgattcaattagcttccgactcattcatc
caaataccgagtcgccaaaattcaaactagactcgttaaatgaatgaatgatgcggtagacaaattggatcattgattctctttgaT
ATCTATGTCGAGTAACACCGtctctctttttgtattccaattttcttgattaatctttcctgcacaaaaacatgcttgat
ccactaagtgacatatatgctgccttcgtatatatagttctggtaaaattaacattttgggtttatctttatttaaggcatcgccatgggat
cctgacgtta, where the underlined sequences correspond to restriction sites and the capitalized sequences are the two 21mers. This AIL6-amiRNA2 was cloned into the *Eco*RI and *BamH*I sites of AlcA/BJ36 (Leibfried et al., 2005). AlcA:AIL6-amiRNA2 was subcloned into the *Not*I site of AlcR/pMLBart and transformed into the *Agrobacterium* strain ASE by electroporation. *ant-4/+* plants were transformed with this Agrobacterium

strain. *35S:AlcR/AlcA:AIL6-amiRNA2 ant-4/+* transformants were selected for basta resistance.

Plasmid construction and protein expression

AIL6-AP2R1R2 containing amino acid 246-426 was PCR amplified from cDNA using primers AIL6-29-1 (5'-CATTGGATCCACGTTTGGTCAAAGGACTTCG-3') and AIL6-30-1 (5'-GAATGGATCCTGCACTCTTCATGATGGCTTC-3'). Both primers contain the underlined *Bam*HI restriction sites. The purified PCR fragment was inserted into the *Bam*HI site of pET32a (Novagen). The plasmid was sequenced and confirmed. AIL6-AP2R1R2 was expressed as a fusion protein. The N-terminus of AIL6-AP2R1R2 was fused with Trx-His-S-enterokinase and the C-terminus of AIL6-AP2R1R2 was fused with a His tag. Proteins were expressed by induction with 1mM IPTG in BL21(DE3)plysS cells. The cells were harvested after growth at 30°C for 2.5 hours. Cells were lysed using four freeze/thaw cycles followed by sonication. Proteins were purified using Ni-NTA (Thermo Fisher Scientific) according to the manufacturer's instructions. ANT-AP2R1R2 were purified as previously described (Nole-Wilson and Krizek, 2000), except Ni-NTA was purchased from Thermo Fisher Scientific.

fEMSA

5' Cy5 labeled oligodeoxynucleotides (5'-CCTGTAAGCATCGGGATATGTGCACCAAGT-3') and non-labeled complementary oligodeoxynucleotides (5'-ACTTGGTGCACATATCCCGATGCTTACAGG-3') were ordered from Fisher Scientific. Oligodeoxynucleotides were annealed in 10mM Tris

pH7.5, 150mM NaCl and 1mM EDTA. Purified AIL6-AP2R1R2 was incubated with 20ng florescent Cy5 labeled DNA probe in 20mM Tris pH8, 100mM KCl, 1mM EDTA, 12% glycerol, 1 mM DTT, 20 ng/µl dI-dc, 20 ng/ µl calf thymus DNA and 0.3 mg/ml BSA overnight at 4 °C. The protein-DNA complexes were separated on 5% acrylamide (29:1 polyacrylamide:bisacrylamide) gels in 1 x TBE at 4 °C. Images were scanned using Typhoon FLA-7000.

Chromatin immuniprecipitation (ChIP)

35S:AP1-GR ap1 cal inflorescences and *AIL6m*:*AIL6-VENUS-3' 35S:AP1-GR ap1 cal* inflorescences were treated with 10µM dexamethasone (DEX) in 0.015% Silwet L-77 and collected for ChIP two days after DEX treatment. ChIP was carried out similar to a previously described procedure (Kwon et al., 2005) and one posted online (https://www.plant-epigenome.org/protocols/wagner-lab-simplified-chromatin-immunoprecipitation-chip) with the following changes: the inflorescence tissue was collected into cold PBS and kept on ice for 2-3 hours and in some experiments a Biorupter (Diagenode) was used for shearing DNA. GFP antibodies (Abcam ab290) coupled to Dynabeads Protein A were used for the immunoprecipitation. Primers used for ChIP are in Table 3.2. The negative control (NC) gene is *Ta3* (At1g37110) (Han et al., 2012). At least three biological replicates were performed for each gene. Each biological replicate was examined in triplicate.

GUS staining

The GUS assays were performed as described in (Mudunkothge and Krizek, 2014). The tissue was incubated in 2mM 5-bromo-4-chloro-3-indolyl-β-glucuronic acid for approximately 15 hours. The tissue was embedded in paraplast, sectioned, mounted on slides and observed under dark-field and bright-field illumination.

RNA extraction and real-time RT-PCR

Buds younger than stage 6 or 8 were identified by the diameter of buds (Smyth et al., 1990) and collected under dissecting microscope. RNA was extracted from inflorescences using TRIzol (Life Technologies) and further purified on an RNeasy column (Qiagen) and DNased while on the column. First-strand cDNA synthesis was performed using qScript cDNA Supermix (Quanta BioSciences). PCR reactions were performed on a BioRad CFX96 using PerfeCTa SYBR Green FastMix for iQ (Quanta BioSciences). The AP3 and AG primers used were AG-F (5'-GTTCTTTGTGATGCGTAAGTCG-3'), AG-R (5'-TGTACCTCTCAATAGTCCCTTTTAC-3'), AP3-F (5'-CGAATGCAAGAAACCAAGAGG-3') and AP3-R (5'-GAATGTCAAGCTCGTCCAAAC-3'). Data analyses were carried out as described previously (Krizek and Eaddy, 2012). Two biological replicates were two sets of plants that were grown, chemical treated and collected at the same time but in separate trays. Data were averaged from four biological replicates that carried out in two independent experiments. Each biological replicate was examined in triplicate.

RESULTS

AIL6 activates transcription in yeast through BS 15

To investigate whether AIL6 can bind to the BS 15 *in vitro*, we performed a fEMSA with E. coli expressed AIL6-AP2R1R2 protein and a fluorescently tagged BS 15. Similar to ANT-AP2R1R2, AIL6-AP2R1R2 bound to BS 15 in a protein concentration dependent manner (Figure 3.1).

To determine whether AIL6 can activate transcription in yeast through BS 15 , we transformed the yeast reporter strain BK1, which contains three copies of BS 15, with AIL6 (Krizek, 2003). Yeast expressing AIL6 produces high levels of β-galactosidase activity, indicating that AIL6 can activate transcription through BS 15 (Figure 3.2). To compare the transcriptional activation activities of different AILs, ANT, AIL5 and AIL7 were transformed into BK1. Slightly higher levels of β-galactosidase activity were seen in yeast cells expressing ANT as compared with those expressing AIL6. Only a small amount of β-galactosidase activity was detected in yeast cells expressing AIL5 and AIL7. These results show that ANT and AIL6 but not AIL5 or AIL7 can activate transcription through BS 15 in yeast at high levels.

The floral homeotic gene *AG* is misexpressed in *ANT:gAIL6* flowers

In chapter 2, we showed that expression of the class B floral homeotic genes *AP3* and *PI* genes are shifted to the first whorl of *ANT:gAIL6* flowers, which correlate with the petal cells present in the first whorl organ. Because stamens and stamenoid organs are present in the outer whorl of *ANT:gAIL6* line 16 flowers, we also examined expression of

the class C gene *AG* in these inflorescences. *ANT:gAIL6* line 16 flowers were crossed to *AG:GUS* (pMD200) (Deyholos and Sieburth, 2000), which contains ~6 kb of *AG* upstream sequences plus 3.8 kb of *AG* genomic sequence (corresponding to exons 1-2 and introns 1-2) which were sufficient for *AG* normal expression (Deyholos and Sieburth, 2000; Sieburth and Meyerowitz, 1997). GUS expression is stronger and broader in *ANT:gAIL6 AG:GUS* stage 4 and stage 6 flowers as compared with the parental *AG:GUS* line (Figure 3.3A, D). GUS is detected in the third and fourth whorls of stage 4 *AG:GUS* flowers and in developing stamen and carpel primordia in older flowers (Figure 3.3A-C). In *ANT:gAIL6 AG:GUS* flowers, GUS is expressed throughout stage 4 flowers, indicating that *AG* is misexpressed in the outer whorls of these flowers (Figure 3.3D). In older *ANT:gAIL6 AG:GUS* flowers, GUS expression was detected in some outer whorl organs, which have morphologies suggestive of organs with some stamenoid identity (Figure 3.3E, F). *AG* was not detected in the bracts subtending *ANT:gAIL6* line 16 flowers (Figure 3.3E). Interestingly, strong GUS expression was observed in the innermost arising organs in *ANT:gAIL6 AG:GUS* flowers even though normal gynoecium are not formed in *ANT:gAIL6* line 16 flowers (Figure 3.3D, E). Thus, the absence of normal carpels does not appear to result from reductions in *AG* mRNA expression in these organs. These results indicate that high AIL6 activity is sufficient to promote *AG* misexpression in the outer whorl of *ANT:gAIL6* line 16 flowers.

AIL6 is bound to regulatory sequences of floral homeotic genes

Our results indicate that misexpression of *AIL6* in first whorl organs, as conferred by the *ANT* promoter can activate *AP3*, *PI*, and *AG* expression in the outermost whorl of

the flower. Previous work has shown that expression of *AP3* and *AG* is decreased in *ant ail6* double mutants (Krizek, 2009). Also, a sequence with similarity to the ANT consensus binding site is present in the second intron of *AG* which is essential for the normal expression of *AG* (Nole-Wilson and Krizek, 2000; Sieburth and Meyerowitz, 1997). To investigate whether this might be a consequence of direct regulation of these genes by AIL6, we performed chromatin immunoprecipitation (ChIP) using a VENUS tagged AIL6 line (AIL6-VENUS) in the *35S:AP1-GR ap1cal* floral induction system in which flower development can be synchronized (Wellmer et al., 2006). This floral induction system allowed us to investigate binding of AIL6 to these promoters at stage 3 of flower development, which is the time at which *AP3* and *AG* are first expressed (Drews et al., 1991; Jack et al., 1992). The stage 3 flowers correspond to two days after DEX treatment in the *35S:AP1-GR ap1cal* floral induction system.

In Chapter 2, we showed that high levels of *AIL6* mRNA result in severe flower defects. Hence, high levels of AIL6 may regulate genes that are not regulated by AIL6 in physiological conditions. Our epitope tagged AIL6-VENUS line contains all regulatory elements necessary for normal *AIL6* expression (Krizek, 2015b). We also confirmed that AIL6 is expressed at approximately normal levels in this line. *AIL6* mRNA levels are 2.45 $\pm$ 0.22 fold higher in *AIL6-VENUS; 35S:AP1-GR ap1 cal* inflorescences as compared with *35S:AP1-GR ap1cal* (Table 3.1). Previous work has shown that plants expressing 2.3 fold higher *AIL6* mRNA in *ant ail6* mutants complement but don't overcomplement the loss of *AIL6* function in *ant ail6* double mutants (Krizek, 2015b). This suggests that the *AIL6-VENUS; 35S:AP1-GR ap1 cal* line provides a reasonable level of AIL6 activity. *AIL6-VENUS 35S:AP1-GR ap1 cal* inflorescences have a slightly

higher amount of *AIL6* mRNAs (3.39±0.11 fold higher than *35S:AP1-GR ap1cal*) two days after DEX treatment, suggesting that AP1 activation induces *AIL6* expression. This is consistent with previous work showing that AP1 positively regulates *AIL6* expression (Kaufmann et al., 2010).

The ChIP experiments showed that AIL6 bound to two characterized elements of the *AP3* promoter that are required for *AP3* expression in early stages of flower development: the distal early element (DEE) and the proximal early element (PEE) (Hill et al., 1998; Lamb et al., 2002) but not to sequences further upstream or a negative control gene (Figure 3.4A, B). ChIP with the control *35S:AP1-GR ap1 cal* did not show such enrichment to any of these genomic regions (Figure 3.4B). We also detected binding of AIL6 to the large second intron of *AG*, which is known to be required for proper *AG* expression (Sieburth and Meyerowitz, 1997). AIL6 bound to several regions within the second intron of *AG* with region 2 showing very strong enrichment (Figure 3.4C, D). Interestingly, the region 2 contains an ANT consensus binding site. No binding of AIL6 was detected to a region at the 3' end of *AG* or to a negative control gene (Figure 3.4D). ChIP with the control *35S:AP1-GR ap1 cal* did not show enrichment to any of these regions (Figure 3.4D).

Floral homeotic gene expression in response to changes in AIL6 activity

The ChIP results suggest that *AP3* and *AG* may be direct targets of AIL6 regulation. However, binding to a genomic region is not sufficient to claim this. To further investigate the direct regulation of *AP3* and *AG* by AIL6, we used the previously described *35S:AlcR/AlcA:gAIL6* line and made two additional transgenic tools in which

we could induce (i.e. *AIL6m:AIL6-GR ant ail6*) or downregulate (i.e. *35S:AlcR/AlcA:AIL6-amiRNA2 ant*) AIL6 activity. These transgenic lines allow us to examine the expression of potential AIL6 target genes at time points soon after induction or downregulation of AIL6 activity. *AIL6m:gAIL6-GR ant ail6* expressed the AIL6-GR fusion protein in the endogenous *AIL6* expression domain in the *ant ail6* mutant background. Of 30 lines generated, line 14 was the most promising. DEX treated *AIL6m:gAIL6-GR* line 14 shows partial rescue of *AIL6* activity (Figure 3.5A). *35S:AlcR/AlcA:AIL6-amiRNA2 ant* generates an artificial microRNA (amiRNA) that specifically targets *AIL6* after ethanol induction. Of seven lines generated, lines 1 and 2 were the most promising. Ethanol treated *35S:AlcR/AlcA:AIL6-amiRNA2 ant* line 1 displays a partial loss of AIL6 activity (Figure 3.5B).

We investigated *AG* and *AP3* expression in both *AIL6m:AIL6-GR ant ail6* and *35S:AIL6-GR* (Chapter 2) lines by RT-qPCR. Because of the severe flower defects in *ant ail6,* it is hard to identify stage specific flower buds. Based on experience, I tried collecting *AIL6m:AIL6-GR ant ail6* inflorescences consisting of unopen buds (floral stages 1-12) at 4hr, 8hr and/or 24hr post Mock/DEX treatment. *AP3* mRNA levels were slightly higher (1.38 ± 0.29) 8 hr after DEX treatment in comparison to the Mock treatment in one experiment consisting of two biological replicates. However, a second experiment also consisting of two biological replicates showed no change of *AP3* mRNA levels between Mock and DEX treatment in any time points. These experiments show that there is no dramatic change in *AP3* mRNA levels after AIL6 induction.

Because *AP3* and *AG* are primarily expressed in young flowers, I collected buds younger than stage 6 in *35S:AIL6-GR* inflorescences. Unexpectedly, *AG* and *AP3* mRNA

levels were lower 4hr after DEX treatment compared to Mock in *35S:AIL6-GR* line 30 (*AG*: 0.69±0.69; *AP3:* 0.69±0.71). In a second experiment, *AG* and *AP3* mRNA levels were unchanged. All together, these data also indicate that there is no dramatic chance in expression of *AG* and *AP3* after AIL6 induction.

I next performed a time course experiment examining *AP3* and *AG* expression in stage 8 and younger *35S:AlcR/AlcA:gAIL6* flowers. *AP3* mRNAs levels were lower at 2, 4 and 8 hours after the start of an ethanol treatment and steadily decreased during the eight hour treatment in *35S:AlcR/AlcA:gAIL6* (Figure 3.6A). *AG* mRNA levels were lower at 2, 4, and slightly increased from 4hr to 8hr (Figure 3.6B). *AP3* and *AG* mRNA levels were not changed in the H_2O treated plants suggesting that similarly staged flowers were collected in all of the samples. The lower levels of *AP3* and *AG* mRNA in *35S:AlcR/AlcA:gAIL6* lines may be a consequence of fewer petals, stamens and carpels in these flowers.

DISCUSSION

AIL6 has similar DNA binding properties as ANT

Here, we showed that AIL6 can bind to BS 15 *in vitro* and activate transcription in yeast through this site. This suggests that AIL6, like ANT, can function as a transcription factor and can bind to similar DNA sequences. Future experiments could be done to determine the disassociation constant of AIL6 binding to BS 15. By comparing the affinities of ANT and AIL6 to BS 15, and with knowledge of the relative concentrations of these two proteins, we could better understand which protein would

primarily bind to target genes if both proteins are present in cells. Also, we could determine whether ANT and AIL6 might form a complex when they bind to BS 15.

The floral homeotic class B and C genes are potential direct targets of AIL6

The class B genes *AP3* and *PI* are potential direct targets of AIL6. *AP3* and *PI* are expressed in the second and third whorls in wild-type floral primordia. *AP3* expression is reduced in *ant ail6* double mutants (Krizek, 2009). This indicates that both ANT and AIL6 are required for normal *AP3* expression; however loss of both *ANT* and *AIL6* does not abolish *AP3* expression indicating the presence of additional pathways regulating *AP3* expression. In *ANT:gAIL6, AP3* and *PI* mRNA are expanded to the outer whorl floral organs, suggesting AIL6 is sufficient for inducing *AP3* and *PI* expression in the first whorl organs. However, the lower *AP3* and *PI* expression in whorls 2 and 3 of *ANT:gAIL6* (in situ data shown in Chapter 2) and overall lower expression measured by RT-qPCR (Figure 3.6) conflicts with the hypothesis that AIL6 is a positive regulator of *AP3* based on the reduced expression of these genes in *ant ail6*.

The downregulation of *AP3* mRNA levels after induction of AIL6 in *35S:AlcR/AlcA:gAIL6* inflorescences consisting of flowers younger than stage 8 may be a consequence of reduced numbers of second and third whorl organs in these flowers (Chapter 2). In this case, the downregulation of *AP3* in these flowers might not be due to direct repression by AIL6 but an indirect effect of changes in cell proliferation patterns. Alternatively, the regulation of *AP3* by AIL6 may be complex with tissue and flower stage dependent contexts. For example, perhaps high AIL6 activity can induce *AP3* in the

first whorl, but repress AP3 in the second and third whorls. AIL6 might play a role in establishing the outer boundary of *AP3* and *PI* expression.

The class C gene *AG* is another potential target of AIL6 regulation. In stage 3 wild-type flowers, *AG* is expressed in cells of the floral meristem that will develop into the third and fourth whorls of the flower. In *ant ail6* flowers, *AG* mRNA is reduced and/or absent in the centermost cells of the floral meristem indicating that ANT and AIL6 activities are required for *AG* expression in the center of a flower (Krizek, 2009). *AG* mRNA is also expanded outward to the second whorl of *ant ail6*, which is consistent with the fact that ANT functions redundantly with AP2 to restrict *AG* expression in the second whorl (Krizek et al., 2000). In contrast, *AG* expression is expanded to outer whorl organs in *ANT:gAIL6*, suggesting that ectopic AIL6 can induce *AG* in the outer whorl organs.

The downregulation of *AG* mRNA levels after induction of AIL6 in *35S:AlcR/AlcA:gAIL6* inflorescences consisting of flowers younger than stage 8 conflicts with the hypothesis that AIL6 is a positive regulator of *AG* based on the reduced expression of these genes in *ant ail6*. This result is not easily explainable as *AG:GUS* flowers showed a broad pattern of *AG* expression in *ANT:gAIL6* (Figure 3.3). These results suggest that AIL6 overexpression lines are not a relevant system for examining the potential regulation of floral homeotic genes.

While ChIP assays showed that AIL6 is bound to the regulatory sequences of *AG* and *AP3* in stage 3 flowers, further evidence is needed to determine confirm direct regulation of AIL6 on *AG* and *AP3* in physiological conditions. To examine possible tissue and/or flower stage dependent regulation of AIL6 on *AP3* and *AG*, we could use

laser capture microdissection to capture second and third whorl cells of stage 3-6 flowers in DEX induced *AIL6m:gAIL6-GR ant ail6* and ethanol treated *35S:AlcR/AlcA:AIL6-amiRNA2 ant* for gene expression analysis.

Table 3.1 Relative *AIL6* mRNA levels in *AIL6-VENUS; 35S:AP1-GR ap1 cal* compared to *35S:AP1-GR ap1 cal* in both untreated and 2 day post Dex treatment.

Relative *AIL6* mRNA levels	*35S:AP1-GR ap1 cal*	*AIL6-VENUS; 35S:AP1-GR ap1 cal*
For untreated plants	1	2.45±0.22
For Dex 2day plants	1	3.39±0.11

Standard deviations are calculated from two biological replicates.

Table 3.2 Primers used for ChIP

AP3-1-F	CGATCATACGGCTGGGTGAT
AP3-1-R	AAGGCATTCCCCGTATCTGC
AP3-2-F	TGATTTGATGGACTGTTTGGAG
AP3-2-R	TTTGGATTAATCGTCACTTCCA
AP3-3-F	CATCGATGTCCGTTGATTTA
AP3-3-R	TTTGGTGGAGAGGACAAGAGA
Ta3-F	CTGCGTGGAAGTCTGTCAAA
Ta3-R	CTATGCCACAGGGCAGTTTT
AG-1-F	AGAGAGTCCCACGTGATTACTT
AG-1-R	AATCTTGCGCTCAATTCCAACC
AG-2-F	TGGGTACTGAGAGGAAAGTGAG
AG-2-R	TGGTCTGAACATGTCTAGGGTT
AG-3-F	ACCCTAGACATGTTCAGACCAA
AG-3-R	TCTCAATAGTCCCTTTTACACTGCA
AG-4-F	AGACCAAACCGCTCTCCAGT
AG-4-R	TTGCTTGCTCAACCCAATTC

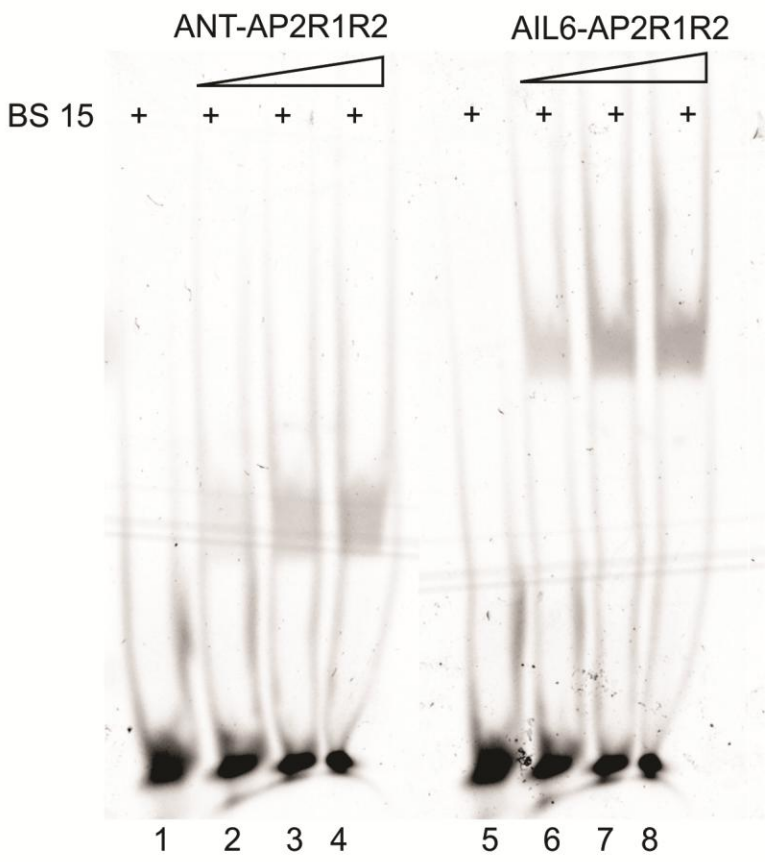

Figure 3.1 ANT-AP2R1R2 and AIL6-AP2R1R2 bind to binding site 15 (BS 15). Equal amount of probes were used in each lane. Free probes (lanes 1 and 5); increasing concentration of ANT-AP2R1R2 protein with probes (lanes 2-4); increasing concentration of AIL6-AP2R1R2 protein with probes (lanes 6-8).

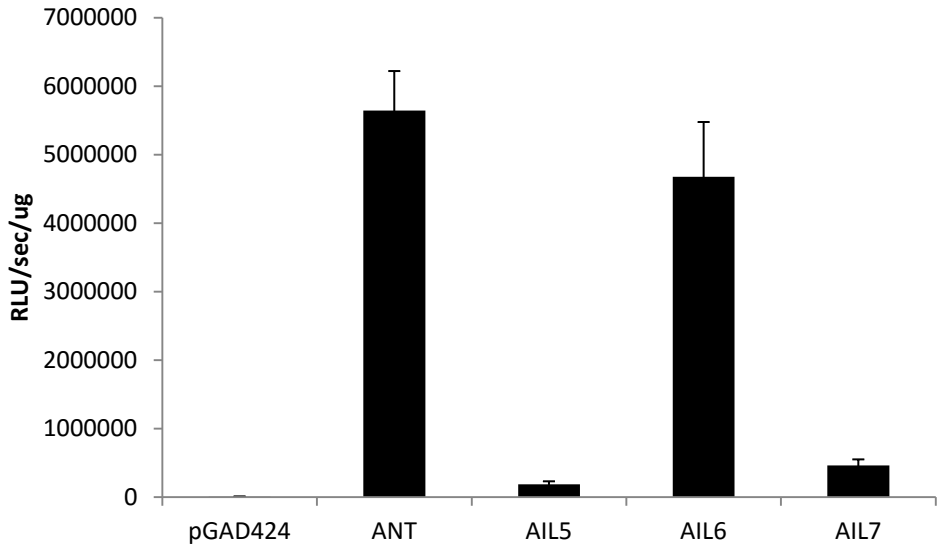

Figure 3.2 Transcriptional activation by ANT, AIL5, AIL6 and AIL7 through BS 15 in yeast. Each effector plasmid was tested for its ability to activate expression of the reporter plasmid. The reporter plasmid contained *lacZ* under the control of three copies of BS 15 and the TATA region of the CYC1 promoter. Error bars show standard deviations calculated from three technical replicates.

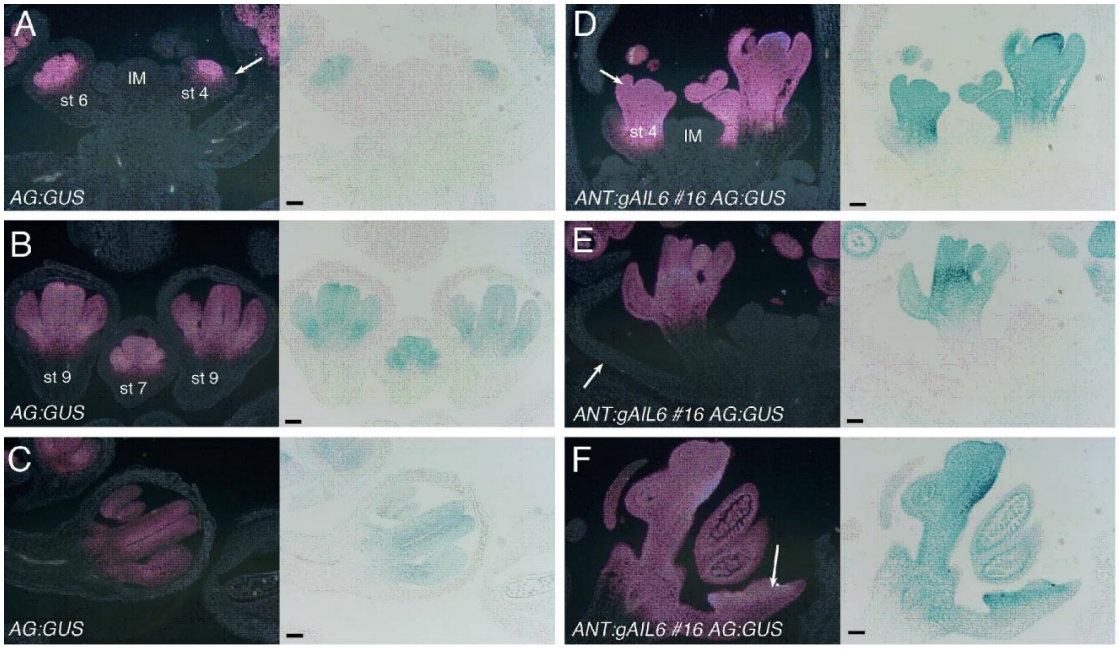

Figure 3.3 *AG* is misexpressed in *ANT:gAIL6* flowers. (A)(B)(C) Dark-field (left) and bright field (right) images of *AG:GUS* inflorescence. (A) GUS expression is detected in the third and fourth whorls of the stage 3 *AG:GUS* flower but not in the sepal primordia (arrow). GUS expression is also detected in the developing stamen and carpel in the stage 6 flower. (B) GUS expression is detected in the stamens and carpels of stage 7 and 9 flowers. (C) GUS expression is detected in the stamens and carpels of stage 11 flower. (D)(E)(F) Dark-field (left) and bright-field (right) images of *ANT:gAIL6* line 16 *AG:GUS* inflorescence. (D) GUS expression is detected in throughout the stage 4 flower including the sepal primordia (arrow). GUS expression is also detected throughout the older flower on the right. (E) *ANT:gAIL6* line 16 *AG:GUS* flower showing GUS expression throughout the flower but not in the subtending bract (arrow). (F) GUS is detected in all of the organs including a first whorl organ that looks to have stamenoid identity (arrow) in a *ANT:gAIL6* line 16 *AG:GUS* flower. Scale bars are 50μm.

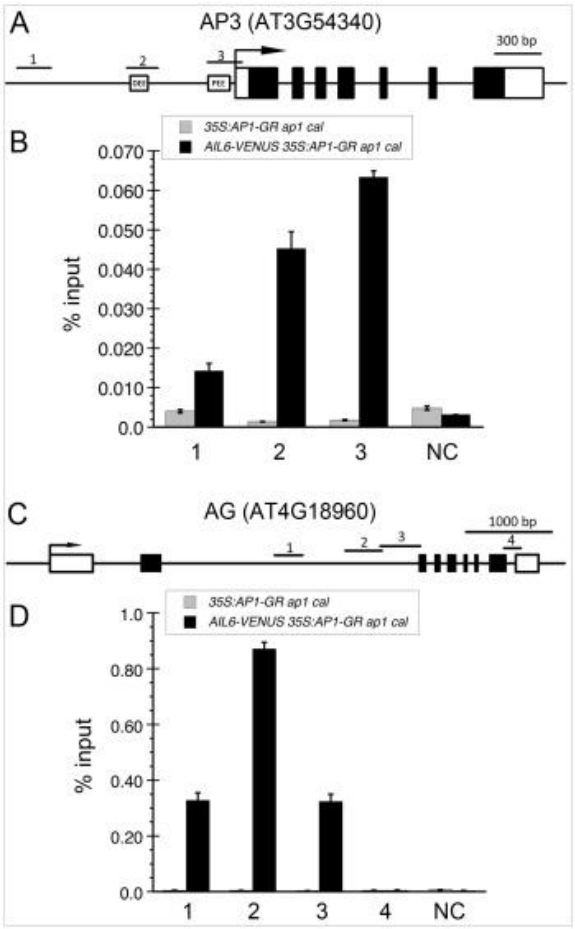

Figure 3.4 AIL6 binds to *AP3* and *AG* regulatory regions. (A) Genomic structure of *AP3* gene (top) with the positions of regions (1, 2, 3) examined with ChIP. Black boxes represent exons and the white boxes represent untranslated regions. Region 2 includes the characterized distal enhancer element (DEE) and region 3 includes the characterized proximal enhancer element (PEE). (B) Graph of a representative *AP3* real time PCR ChIP experiment. The negative control (NC) gene is *Ta3* (At1g37110). Error bars show standard deviation of three technical replicates. (C) Genomic structure of *AG* gene (top) with the positions of regions (1, 2, 3, 4) examined with ChIP. Black boxes represent exons and the white boxes represent untranslated regions. (B) Graph of a representative *AG* real time PCR ChIP experiment. Error bars show standard deviation of three technical replicates.

Figure 3.5 Additional genetic tools to induce or downregulate AIL6 activity. (A) *AIL6m:gAIL6-GR ant-4 ail6-2* line 14 mock (left) and dex (right). Images were taken two weeks after a single mock and dex treatment. (B) *35S:AlcR/AlcA:AIL6-amiRNA2 ant-4* line 1 H_2O (left) and EtOH (right). Images were taken two weeks after a single eight-hour H_2O or EtOH treatment. Images in (A) and (B) were taken under the same magnification.

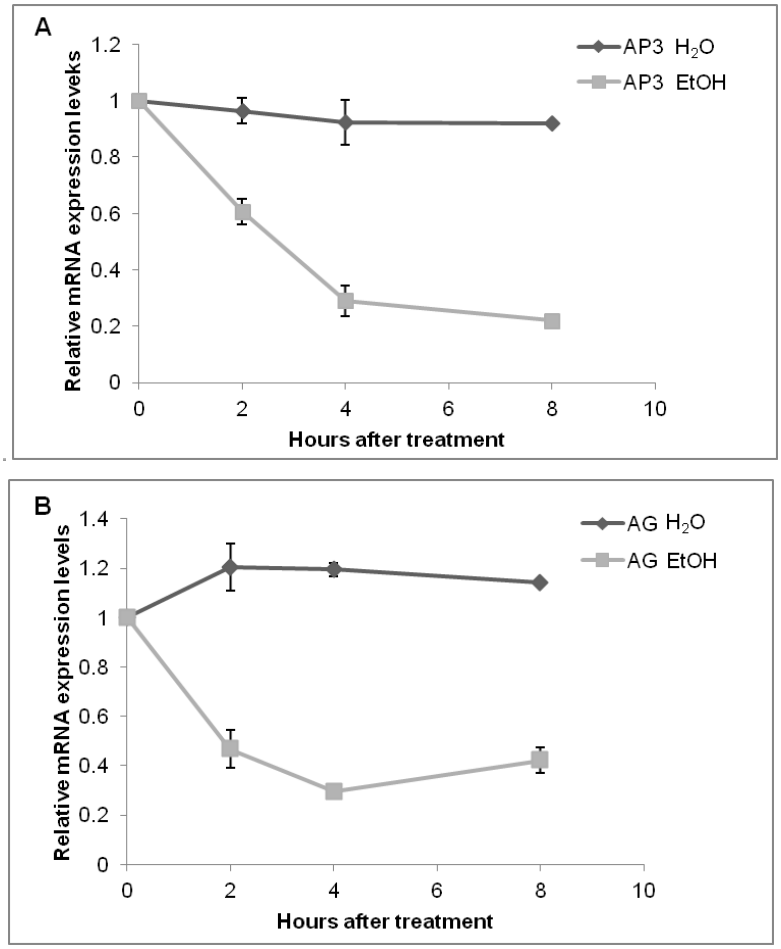

Figure 3.6 *AP3* and *AG* mRNA levels decrease after ethanol (EtOH) treatment of *35S:AlcR/AlcA:gAIL6* plants. Inflorescences consisting of flowers younger than stage 8 were collected from 22 day old *35S:AlcR/AlcA:gAIL6* plants at 0hr, 2hr, 4hr and 8hr after the start of an eight hour mock/ethanol treatment for RT-qPCR analysis. *AP3* (A) *AG* (B) mRNA levels decreased in EtOH treated plants but not in H_2O treated plants. Expression levels for all samples were compared to the 0hr time point.

REFERENCES

Aida, M., Ishida, T., Fukaki, H., Fujisawa, H., and Tasaka, M. (1997). Genes involved in organ separation in Arabidopsis: an analysis of the cup-shaped cotyledon mutant. The Plant Cell *9*, 841-857.

An, H., Roussot, C., Suárez-López, P., Corbesier, L., Vincent, C., Piñeiro, M., Hepworth, S., Mouradov, A., Justin, S., and Turnbull, C. (2004). CONSTANS acts in the phloem to regulate a systemic signal that induces photoperiodic flowering of Arabidopsis. Development *131*, 3615-3626.

Baker, S.C., Robinson-Beers, K., Villanueva, J.M., Gaiser, J.C., and Gasser, C.S. (1997). Interactions among genes regulating ovule development in Arabidopsis thaliana. Genetics *145*, 1109.

Bechtold, N., Ellis, J., and Pelletier, G. (1993). In planta Agrobacterium mediated gene transfer by infiltration of adult Arabidopsis thaliana plants. Comptes rendus de l'Académie des sciences Série 3, Sciences de la vie *316*, 1194-1199.

Benková, E., Michniewicz, M., Sauer, M., Teichmann, T., Seifertová, D., Jürgens, G., and Friml, J. (2003). Local, efflux-dependent auxin gradients as a common module for plant organ formation. Cell *115*, 591-602.

Brand, U., Fletcher, J.C., Hobe, M., Meyerowitz, E.M., and Simon, R. (2000). Dependence of stem cell fate in Arabidopsis on a feedback loop regulated by CLV3 activity. Science *289*, 617-619.

Brewer, P.B., Howles, P.A., Dorian, K., Griffith, M.E., Ishida, T., Kaplan-Levy, R.N., Kilinc, A., and Smyth, D.R. (2004). PETAL LOSS, a trihelix transcription factor gene, regulates perianth architecture in the Arabidopsis flower. Development *131*, 4035-4045.

Cho, H.-T., and Cosgrove, D.J. (2000). Altered expression of expansin modulates leaf growth and pedicel abscission in Arabidopsis thaliana. Proceedings of the National Academy of Sciences *97*, 9783-9788.

Chuang, C.-F., Running, M.P., Williams, R.W., and Meyerowitz, E.M. (1999). The PERIANTHIA gene encodes a bZIP protein involved in the determination of floral organ number in Arabidopsis thaliana. Genes & development *13*, 334-344.

Clark, S.E., Williams, R.W., and Meyerowitz, E.M. (1997). The CLAVATA1gene encodes a putative receptor kinase that controls shoot and floral meristem size in Arabidopsis. Cell *89*, 575-585.

Corbesier, L., Vincent, C., Jang, S., Fornara, F., Fan, Q., Searle, I., Giakountis, A., Farrona, S., Gissot, L., and Turnbull, C. (2007). FT protein movement contributes to long-distance signaling in floral induction of Arabidopsis. science *316*, 1030-1033.

Crickmore, M.A., and Mann, R.S. (2008). The control of size in animals: insights from selector genes. BioEssays : news and reviews in molecular, cellular and developmental biology *30*, 843-853.

Das, P., Ito, T., Wellmer, F., Vernoux, T., Dedieu, A., Traas, J., and Meyerowitz, E.M. (2009). Floral stem cell termination involves the direct regulation of AGAMOUS by PERIANTHIA. Development *136*, 1605-1611.

Deyholos, M.K., and Sieburth, L.E. (2000). Separable whorl-specific expression and negative regulation by enhancer elements within the AGAMOUS second intron. The Plant Cell *12*, 1799-1810.

Dinneny, J.R., Yadegari, R., Fischer, R.L., Yanofsky, M.F., and Weigel, D. (2004). The role of JAGGED in shaping lateral organs. Development *131*, 1101-1110.

Disch, S., Anastasiou, E., Sharma, V.K., Laux, T., Fletcher, J.C., and Lenhard, M. (2006). The E3 ubiquitin ligase BIG BROTHER controls Arabidopsis organ size in a dosage-dependent manner. Current Biology *16*, 272-279.

Drews, G.N., Bowman, J.L., and Meyerowitz, E.M. (1991). Negative regulation of the Arabidopsis homeotic gene AGAMOUS by the APETALA2 product. Cell *65*, 991-1002.

Elliott, R.C., Betzner, A.S., Huttner, E., Oakes, M.P., Tucker, W., Gerentes, D., Perez, P., and Smyth, D.R. (1996). AINTEGUMENTA, an APETALA2-like gene of Arabidopsis with pleiotropic roles in ovule development and floral organ growth. The Plant Cell *8*, 155-168.

Endrizzi, K., Moussian, B., Haecker, A., Levin, J.Z., and Laux, T. (1996). The SHOOT MERISTEMLESS gene is required for maintenance of undifferentiated cells in Arabidopsis shoot and floral meristems and acts at a different regulatory level than the meristem genes WUSCHEL and ZWILLE. The Plant Journal *10*, 967-979.

Fletcher, J.C., Brand, U., Running, M.P., Simon, R., and Meyerowitz, E.M. (1999). Signaling of cell fate decisions by CLAVATA3 in Arabidopsis shoot meristems. Science *283*, 1911-1914.

Floyd, S.K., and Bowman, J.L. (2007). The ancestral developmental tool kit of land plants. International journal of plant sciences *168*, 1-35.

Galinha, C., Hofhuis, H., Luijten, M., Willemsen, V., Blilou, I., Heidstra, R., and Scheres, B. (2007). PLETHORA proteins as dose-dependent master regulators of Arabidopsis root development. Nature *449*, 1053-1057.

Gälweiler, L., Guan, C., Müller, A., Wisman, E., Mendgen, K., Yephremov, A., and Palme, K. (1998). Regulation of polar auxin transport by AtPIN1 in Arabidopsis vascular tissue. Science *282*, 2226-2230.

Han, S.K., Sang, Y., Rodrigues, A., Wu, M.F., Rodriguez, P.L., and Wagner, D. (2012). The SWI2/SNF2 chromatin remodeling ATPase BRAHMA represses abscisic acid responses in the absence of the stress stimulus in Arabidopsis. Plant Cell *24*, 4892-4906.

Heisler, M.G., Ohno, C., Das, P., Sieber, P., Reddy, G.V., Long, J.A., and Meyerowitz, E.M. (2005). Patterns of auxin transport and gene expression during primordium development revealed by live imaging of the Arabidopsis inflorescence meristem. Current biology *15*, 1899-1911.

Hibara, K.-i., Karim, M.R., Takada, S., Taoka, K.-i., Furutani, M., Aida, M., and Tasaka, M. (2006). Arabidopsis CUP-SHAPED COTYLEDON3 regulates postembryonic shoot meristem and organ boundary formation. The Plant Cell *18*, 2946-2957.

Hofhuis, H., Laskowski, M., Du, Y., Prasad, K., Grigg, S., Pinon, V., and Scheres, B. (2013). Phyllotaxis and rhizotaxis in Arabidopsis are modified by three PLETHORA transcription factors. Current Biology *23*, 956-962.

Honma, T., and Goto, K. (2001). Complexes of MADS-box proteins are sufficient to convert leaves into floral organs. Nature *409*, 525-529.

Hu, Y., Xie, Q., and Chua, N.-H. (2003). The Arabidopsis auxin-inducible gene ARGOS controls lateral organ size. The Plant Cell *15*, 1951-1961.

Huang, T., and Irish, V.F. (2015). Temporal control of plant organ growth by TCP transcription factors. Current Biology *25*, 1765-1770.

Huang, T., López-Giráldez, F., Townsend, J.P., and Irish, V.F. (2012). RBE controls microRNA164 expression to effect floral organogenesis. Development *139*, 2161-2169.

Hwang, M., Perez, C.A., Moretti, L., and Lu, B. (2008). The mTOR signaling network: insights from its role during embryonic development. Current medicinal chemistry *15*, 1192-1208.

Irish, V.F., and Sussex, I.M. (1990). Function of the apetala-1 gene during Arabidopsis floral development. The plant cell *2*, 741-753.

Ito, T., Ng, K.-H., Lim, T.-S., Yu, H., and Meyerowitz, E.M. (2007). The homeotic protein AGAMOUS controls late stamen development by regulating a jasmonate biosynthetic gene in Arabidopsis. The Plant Cell *19*, 3516-3529.

Jack, T., Brockman, L.L., and Meyerowitz, E.M. (1992). The homeotic gene APETALA3 of Arabidopsis thaliana encodes a MADS box and is expressed in petals and stamens. Cell *68*, 683-697.

Jaeger, K.E., and Wigge, P.A. (2007). FT protein acts as a long-range signal in Arabidopsis. Current Biology *17*, 1050-1054.

Jofuku, K.D., Den Boer, B., Van Montagu, M., and Okamuro, J.K. (1994). Control of Arabidopsis flower and seed development by the homeotic gene APETALA2. The Plant Cell *6*, 1211-1225.

Kareem, A., Durgaprasad, K., Sugimoto, K., Du, Y., Pulianmackal, A.J., Trivedi, Z.B., Abhayadev, P.V., Pinon, V., Meyerowitz, E.M., and Scheres, B. (2015). PLETHORA Genes Control Regeneration by a Two-Step Mechanism. Current Biology *25*, 1017-1030.

Kaufmann, K., Wellmer, F., Muiño, J.M., Ferrier, T., Wuest, S.E., Kumar, V., Serrano-Mislata, A., Madueno, F., Krajewski, P., and Meyerowitz, E.M. (2010). Orchestration of floral initiation by APETALA1. science *328*, 85-89.

Kim, G.-T., Tsukaya, H., Saito, Y., and Uchimiya, H. (1999). Changes in the shapes of leaves and flowers upon overexpression of cytochrome P450 in Arabidopsis. Proceedings of the National Academy of Sciences *96*, 9433-9437.

Kim, G.-T., Tsukaya, H., and Uchimiya, H. (1998). The ROTUNDIFOLIA3 gene of Arabidopsis thalianaencodes a new member of the cytochrome P-450 family that is required for the regulated polar elongation of leaf cells. Genes & development *12*, 2381-2391.

Kim, S., Soltis, P.S., Wall, K., and Soltis, D.E. (2006). Phylogeny and domain evolution in the APETALA2-like gene family. Molecular Biology and Evolution *23*, 107-120.

Klucher, K.M., Chow, H., Reiser, L., and Fischer, R.L. (1996). The AINTEGUMENTA gene of Arabidopsis required for ovule and female gametophyte development is related to the floral homeotic gene APETALA2. The Plant Cell *8*, 137-153.

Kondo, T., Sawa, S., Kinoshita, A., Mizuno, S., Kakimoto, T., Fukuda, H., and Sakagami, Y. (2006). A plant peptide encoded by CLV3 identified by in situ MALDI-TOF MS analysis. Science *313*, 845-848.

Krizek, B.A. (1999). Ectopic expression of AINTEGUMENTA in Arabidopsis plants results in increased growth of floral organs. Developmental Genetics *25*, 224-236.

Krizek, B.A. (2003). AINTEGUMENTA utilizes a mode of DNA recognition distinct from that used by proteins containing a single AP2 domain. Nucleic acids research *31*, 1859-1868.

Krizek, B.A. (2009). AINTEGUMENTA and AINTEGUMENTA-LIKE6 act redundantly to regulate Arabidopsis floral growth and patterning. Plant physiology *150*, 1916-1929.

Krizek, B.A. (2011). Aintegumenta and Aintegumenta-Like6 regulate auxin-mediated flower development in Arabidopsis. BMC research notes *4*, 1.

Krizek, B.A. (2015a). AINTEGUMENTA-LIKE genes have partly overlapping functions with AINTEGUMENTA but make distinct contributions to Arabidopsis thaliana flower development. Journal of experimental botany *66*, 4537-4549.

Krizek, B.A. (2015b). Intronic sequences are required for AINTEGUMENTA-LIKE6 expression in Arabidopsis flowers. BMC research notes *8*, 1.

Krizek, B.A., and Eaddy, M. (2012). AINTEGUMENTA-LIKE6 regulates cellular differentiation in flowers. Plant Molecular Biology *78*, 199-209.

Krizek, B.A., and Fletcher, J.C. (2005). Molecular mechanisms of flower development: an armchair guide. Nature Reviews Genetics *6*, 688-698.

Krizek, B.A., Lewis, M.W., and Fletcher, J.C. (2006). RABBIT EARS is a second-whorl repressor of AGAMOUS that maintains spatial boundaries in Arabidopsis flowers. The Plant Journal *45*, 369-383.

Krizek, B.A., and Meyerowitz, E.M. (1996). The Arabidopsis homeotic genes APETALA3 and PISTILLATA are sufficient to provide the B class organ identity function. Development *122*, 11-22.

Krizek, B.A., Prost, V., and Macias, A. (2000). AINTEGUMENTA promotes petal identity and acts as a negative regulator of AGAMOUS. The Plant Cell *12*, 1357-1366.

Lampugnani, E.R., Kilinc, A., and Smyth, D.R. (2013). Auxin controls petal initiation in Arabidopsis. Development *140*, 185-194.

Leibfried, A., To, J.P., Busch, W., Stehling, S., Kehle, A., Demar, M., Kieber, J.J., and Lohmann, J.U. (2005). WUSCHEL controls meristem function by direct regulation of cytokinin-inducible response regulators. Nature *438*, 1172-1175.

Lenhard, M., Bohnert, A., Jürgens, G., and Laux, T. (2001). Termination of stem cell maintenance in Arabidopsis floral meristems by interactions between WUSCHEL and AGAMOUS. Cell *105*, 805-814.

Lenhard, M., Jürgens, G., and Laux, T. (2002). The WUSCHEL and SHOOTMERISTEMLESS genes fulfil complementary roles in Arabidopsis shoot meristem regulation. Development *129*, 3195-3206.

Li, Y., Zheng, L., Corke, F., Smith, C., and Bevan, M.W. (2008). Control of final seed and organ size by the DA1 gene family in Arabidopsis thaliana. Genes & development *22*, 1331-1336.

Liu, L.-J., Zhang, Y.-C., Li, Q.-H., Sang, Y., Mao, J., Lian, H.-L., Wang, L., and Yang, H.-Q. (2008). COP1-mediated ubiquitination of CONSTANS is implicated in cryptochrome regulation of flowering in Arabidopsis. The Plant Cell *20*, 292-306.

Lohmann, D., Stacey, N., Breuninger, H., Jikumaru, Y., Muller, D., Sicard, A., Leyser, O., Yamaguchi, S., and Lenhard, M. (2010). SLOW MOTION is required for within-plant auxin homeostasis and normal timing of lateral organ initiation at the shoot meristem in Arabidopsis. Plant Cell *22*, 335-348.

Lohmann, J.U., Hong, R.L., Hobe, M., Busch, M.A., Parcy, F., Simon, R., and Weigel, D. (2001). A molecular link between stem cell regulation and floral patterning in Arabidopsis. Cell *105*, 793-803.

Long, J., and Barton, M.K. (2000). Initiation of axillary and floral meristems in Arabidopsis. Developmental biology *218*, 341-353.

Maier, A.T., Stehling-Sun, S., Wollmann, H., Demar, M., Hong, R.L., Haubeiß, S., Weigel, D., and Lohmann, J.U. (2009). Dual roles of the bZIP transcription factor PERIANTHIA in the control of floral architecture and homeotic gene expression. Development *136*, 1613-1620.

Mathieu, J., Warthmann, N., Küttner, F., and Schmid, M. (2007). Export of FT protein from phloem companion cells is sufficient for floral induction in Arabidopsis. Current Biology *17*, 1055-1060.

Mayer, K.F., Schoof, H., Haecker, A., Lenhard, M., Jürgens, G., and Laux, T. (1998). Role of WUSCHEL in regulating stem cell fate in the Arabidopsis shoot meristem. Cell *95*, 805-815.

Mizukami, Y., and Fischer, R.L. (2000). Plant organ size control: AINTEGUMENTA regulates growth and cell numbers during organogenesis. Proceedings of the National Academy of Sciences *97*, 942-947.

Mudunkothge, J.S., and Krizek, B.A. (2012). Three Arabidopsis AIL/PLT genes act in combination to regulate shoot apical meristem function. The Plant Journal *71*, 108-121.

Mudunkothge, J.S., and Krizek, B.A. (2014). The GUS reporter system in flower development studies. Methods in molecular biology (Clifton, NJ) *1110*, 295-304.

Nole-Wilson, S., and Krizek, B.A. (2000). DNA binding properties of the Arabidopsis floral development protein AINTEGUMENTA. Nucleic Acids Research *28*, 4076-4082.

Nole-Wilson, S., Tranby, T.L., and Krizek, B.A. (2005). AINTEGUMENTA-like (AIL) genes are expressed in young tissues and may specify meristematic or division-competent states. Plant Molecular Biology *57*, 613-628.

Ogawa, M., Shinohara, H., Sakagami, Y., and Matsubayashi, Y. (2008). Arabidopsis CLV3 peptide directly binds CLV1 ectodomain. Science *319*, 294-294.

Ohno, C.K., Reddy, G.V., Heisler, M.G., and Meyerowitz, E.M. (2004). The Arabidopsis JAGGED gene encodes a zinc finger protein that promotes leaf tissue development. Development *131*, 1111-1122.

Pinon, V., Prasad, K., Grigg, S.P., Sanchez-Perez, G.F., and Scheres, B. (2013). Local auxin biosynthesis regulation by PLETHORA transcription factors controls phyllotaxis in Arabidopsis. Proceedings of the National Academy of Sciences *110*, 1107-1112.

Prasad, K., Grigg, S.P., Barkoulas, M., Yadav, R.K., Sanchez-Perez, G.F., Pinon, V., Blilou, I., Hofhuis, H., Dhonukshe, P., and Galinha, C. (2011). Arabidopsis PLETHORA transcription factors control phyllotaxis. Current Biology *21*, 1123-1128.

Przemeck, G.K., Mattsson, J., Hardtke, C.S., Sung, Z.R., and Berleth, T. (1996). Studies on the role of the Arabidopsis gene MONOPTEROS in vascular development and plant cell axialization. Planta *200*, 229-237.

Ptashne, M. (1988). How eukaryotic transcriptional activators work. Nature *335*, 683-689.

Reinhardt, D., Mandel, T., and Kuhlemeier, C. (2000). Auxin regulates the initiation and radial position of plant lateral organs. The Plant Cell *12*, 507-518.

Reinhardt, D., Pesce, E.-R., Stieger, P., Mandel, T., Baltensperger, K., Bennett, M., Traas, J., Friml, J., and Kuhlemeier, C. (2003). Regulation of phyllotaxis by polar auxin transport. Nature *426*, 255-260.

Riechmann, J.L., Krizek, B.A., and Meyerowitz, E.M. (1996). Dimerization specificity of Arabidopsis MADS domain homeotic proteins APETALA1, APETALA3, PISTILLATA, and AGAMOUS. Proceedings of the National Academy of Sciences *93*, 4793-4798.

Riechmann, J.L., and Meyerowitz, E.M. (1998). The AP2/EREBP family of plant transcription factors. Biological chemistry *379*, 633-646.

Roslan, H.A., Salter, M.G., Wood, C.D., White, M.R., Croft, K.P., Robson, F., Coupland, G., Doonan, J., Laufs, P., and Tomsett, A.B. (2001). Characterization of the ethanol‐inducible alc gene‐expression system in Arabidopsis thaliana. The Plant Journal *28*, 225-235.

Schultz, E.A., and Haughn, G.W. (1993). Genetic analysis of the floral initiation process (FLIP) in Arabidopsis. Development *119*, 745-765.

Schwab, R., Ossowski, S., Riester, M., Warthmann, N., and Weigel, D. (2006). Highly specific gene silencing by artificial microRNAs in Arabidopsis. The Plant Cell *18*, 1121-1133.

Sieburth, L.E., and Meyerowitz, E.M. (1997). Molecular dissection of the AGAMOUS control region shows that cis elements for spatial regulation are located intragenically. The Plant Cell *9*, 355-365.

Smaczniak, C., Immink, R.G., Muiño, J.M., Blanvillain, R., Busscher, M., Busscher-Lange, J., Dinh, Q.P., Liu, S., Westphal, A.H., and Boeren, S. (2012). Characterization of MADS-domain transcription factor complexes in Arabidopsis flower development. Proceedings of the National Academy of Sciences *109*, 1560-1565.

Smyth, D.R., Bowman, J.L., and Meyerowitz, E.M. (1990). Early flower development in Arabidopsis. The Plant Cell *2*, 755-767.

Sonoda, Y., Sako, K., Maki, Y., Yamazaki, N., Yamamoto, H., Ikeda, A., and Yamaguchi, J. (2009). Regulation of leaf organ size by the Arabidopsis RPT2a 19S proteasome subunit. The Plant Journal *60*, 68-78.

Suárez-López, P., Wheatley, K., Robson, F., Onouchi, H., Valverde, F., and Coupland, G. (2001). CONSTANS mediates between the circadian clock and the control of flowering in Arabidopsis. Nature *410*, 1116-1120.

Szécsi, J., Joly, C., Bordji, K., Varaud, E., Cock, J.M., Dumas, C., and Bendahmane, M. (2006). BIGPETALp, a bHLH transcription factor is involved in the control of Arabidopsis petal size. The EMBO Journal *25*, 3912-3920.

Takeda, S., Matsumoto, N., and Okada, K. (2004). RABBIT EARS, encoding a SUPERMAN-like zinc finger protein, regulates petal development in Arabidopsis thaliana. Development *131*, 425-434.

Theissen, G., and Saedler, H. (2001). Plant biology: floral quartets. Nature *409*, 469-471.

Trost, G., Vi, S.L., Czesnick, H., Lange, P., Holton, N., Giavalisco, P., Zipfel, C., Kappel, C., and Lenhard, M. (2014). Arabidopsis poly (A) polymerase PAPS1 limits founder‐cell recruitment to organ primordia and suppresses the salicylic acid‐independent immune response downstream of EDS1/PAD4. The Plant Journal *77*, 688-699.

Tsuge, T., Tsukaya, H., and Uchimiya, H. (1996). Two independent and polarized processes of cell elongation regulate leaf blade expansion in Arabidopsis thaliana (L.) Heynh. Development *122*, 1589-1600.

Vernoux, T., Besnard, F., and Traas, J. (2010). Auxin at the shoot apical meristem. Cold Spring Harbor Perspectives in Biology *2*, a001487.

Wang, J.W., Schwab, R., Czech, B., Mica, E., and Weigel, D. (2008). Dual effects of miR156-targeted SPL genes and CYP78A5/KLUH on plastochron length and organ size in Arabidopsis thaliana. Plant Cell *20*, 1231-1243.

Weigel, D., Alvarez, J., Smyth, D.R., Yanofsky, M.F., and Meyerowitz, E.M. (1992). LEAFY controls floral meristem identity in Arabidopsis. Cell *69*, 843-859.

Weigel, D., and Nilsson, O. (1995). A developmental switch sufficient for flower initiation in diverse plants. Nature *377*, 495-500.

Wellmer, F., Alves-Ferreira, M., Dubois, A., Riechmann, J.L., and Meyerowitz, E.M. (2006). Genome-wide analysis of gene expression during early Arabidopsis flower development. PLoS Genet *2*, e117.

Wilson, R.N., Heckman, J.W., and Somerville, C.R. (1992). Gibberellin is required for flowering in Arabidopsis thaliana under short days. Plant Physiology *100*, 403-408.

Wiśniewska, J., Xu, J., Seifertová, D., Brewer, P.B., Růžička, K., Blilou, I., Rouquié, D., Benková, E., Scheres, B., and Friml, J. (2006). Polar PIN Localization Directs Auxin Flow in Plants. Science *312*, 883-883.

Wu, G., Park, M.Y., Conway, S.R., Wang, J.-W., Weigel, D., and Poethig, R.S. (2009). The sequential action of miR156 and miR172 regulates developmental timing in Arabidopsis. Cell *138*, 750-759.

Wu, G., and Poethig, R.S. (2006). Temporal regulation of shoot development in Arabidopsis thaliana by miR156 and its target SPL3. Development *133*, 3539-3547.

Yadav, R.K., Perales, M., Gruel, J., Girke, T., Jönsson, H., and Reddy, G.V. (2011). WUSCHEL protein movement mediates stem cell homeostasis in the Arabidopsis shoot apex. Genes & development *25*, 2025-2030.

Yamaguchi, N., Jeong, C.W., Nole-Wilson, S., Krizek, B.A., and Wagner, D. (2016). AINTEGUMENTA and AINTEGUMENTA-LIKE6/PLETHORA3 Induce LEAFY Expression in Response to Auxin to Promote the Onset of Flower Formation in Arabidopsis. Plant physiology *170*, 283-293.

Yamaguchi, N., Wu, M.-F., Winter, C.M., Berns, M.C., Nole-Wilson, S., Yamaguchi, A., Coupland, G., Krizek, B.A., and Wagner, D. (2013). A molecular framework for auxin-mediated initiation of flower primordia. Developmental Cell *24*, 271-282.

Yanofsky, M.F., Ma, H., Bowman, J.L., Drews, G.N., Feldmann, K.A., and Meyerowitz, E.M. (1990). The protein encoded by the Arabidopsis homeotic gene agamous resembles transcription factors. Nature *346*, 35-39.

Yoo, S.K., Chung, K.S., Kim, J., Lee, J.H., Hong, S.M., Yoo, S.J., Yoo, S.Y., Lee, J.S., and Ahn, J.H. (2005). Constans activates suppressor of overexpression of constans 1

through Flowering Locus T to promote flowering in Arabidopsis. Plant Physiology *139*, 770-778.

Zadnikova, P., and Simon, R. (2014). How boundaries control plant development. Curr Opin Plant Biol *17*, 116-125.

APPENDIX A

ECTOPIC EXPRESSION OF *AIL6* ALTERS LEAF INITIATION RATES AND THE SWITCH TO FLOWER FORMATION

INTRODUCTION

In Arabidopsis, the juvenile-to-adult phase transition is regulated by a decrease in the level of microRNA156s (miR156s). miR156s are present at high levels after germination and decline during shoot development, leading to an increase in its targets, transcripts encoding SQUAMOSA PROMOTER BINDING (SBP/SPL) transcription factors (Wu et al., 2009; Wu and Poethig, 2006). At the end of the vegetative phase, plants undergo the vegetative-reproductive phase transition.

The vegetative-to-reproductive phase transition is also termed the reproductive phase transition or flowering. Flowering time refers to the time to the vegetative-to-reproductive phase transition. Temporal control of the vegetative-reproductive phase transition determines the time invested in vegetative growth and hence the vegetative resources available during reproduction. In Arabidopsis, long-day photoperiods promote flowering while short-day photoperiods delay it. The activity of the circadian oscillator CONSTANS (CO) in leaves fluctuates over a 24 hour period, and is regulated at both transcriptional and post-transcriptional levels in concert with the length of photoperiod (Liu et al., 2008; Suárez-López et al., 2001). In long days, CO promotes flowering by

activating expression of the small protein FT, which acts as a long distance signal moving from leaves to the shoot apex (An et al., 2004; Corbesier et al., 2007; Jaeger and Wigge, 2007; Mathieu et al., 2007). FT integrates signals from several other positively and negatively acting pathways and triggers the expression of another floral integrator *SOC1* (Yoo et al., 2005). In response, shoot apical meristem identity switches from a vegetative meristem into an inflorescence meristem.

There are two subphases of the reproductive phase: an early inflorescence phase and a flower formation phase. The shoot branching pattern of plants is crucial for light interception efficiency and adaptation to resource availability. After making two to three cauline leaves and axillary meristems, the inflorescence meristem (IM) transits to the flower formation phase. In Arabidopsis, flowers are not subtended by any leaf-like structures while secondary inflorescences are subtended by cauline leaves. The transition from branching to floral fate in the lateral primordia of the IM in Arabidopsis requires the transcription factor LFY and its direct target gene *AP1*.

ANT and AIL6 and the auxin response factor MP act in parallel pathways to directly upregulate the expression of *LFY* to promote the switch to flower formation (Yamaguchi et al., 2016). Because AIL6 is known to play a role in promoting the switch to flower formation, I decided to investigate developmental phase transitions in *ANT:gAIL6* which showed differences in vegetative development and the time to flower formation.

METHODS AND MATERIALS

Plant growth conditions

Plants were sown on half MS plates and transplanted at 7 days to a soil mixture of Metro-Mix 360: perlite: vermiculite (5:1:1) and grown in 16 hour days (100-150μmol/m^2/s) at 22^{o}C for long day condition and in 8 hour days at 20^{o}C for short day condition. The plants used for these studies were the transgenic *ANT:gAIL6* line 16 in the L*er* background described in Chapter 2.

Measurement of phase length

Leaves longer than 1mm were counted every day under a dissecting microscope. Juvenile leaf number was scored as the number of rosette leaves lacking abaxial trichomes (excluding coyledons) while adult leaf number was scored as the number of rosette leaves with abaxial trichomes. A minimum of 14 plants of each genotype were used in each study.

Tissue sectioning

Shoot apices were fixed, embedded and sectioned similarly to tissue prepared for in situ hybridization (Krizek, 1999).

RESULTS

ANT:gAIL6 plants are delayed in the switch to flower formation

ANT:gAIL6 line 16 plants take longer to form the first flower as compared with L*er*. The opening of the first *ANT:gAIL6* line 16 flower occurs at 29.28 dap (days post planting) $\pm$ 1.34 while the opening of the first L*er* flower occurs at 23.28 dap $\pm$ 0.75 (Table A.1). To determine the age of the plant when the first flower was initiated by the inflorescence meristem, we sectioned L*er* and *ANT:gAIL6* line 16 seedlings. Flower meristems are easily distinguished from leaf primordia by their round shape. The generation of the first floral meristem of *ANT:gAIL6* line 16 occurs at 14-16 dap which is later than L*er* at 10-12 dap.

ANT:gAIL6 delayed flowering time and have a prolonged early inflorescence phase

To determine whether the delay in flower formation is due to a delay in the vegetative-to-reproductive transition or due to a prolonged early inflorescence phase, I measured the time to the formation of the first cauline leaf (i.e. flowering time) and counted the number of secondary inflorescences. The initiation of the first cauline leaf of *ANT:gAIL6* line 16 occurs at 15.09 dap $\pm$ 1.06 which is slightly but significantly later than that of L*er* at 13.44 dap $\pm$ 0.78. Thus, the vegetative-to-reproductive transition appears to be delayed in *ANT:gAIL6* line 16. Next, we measured the number of cauline leaves produced in the early inflorescence phase. *ANT:gAIL6* line 16 makes significantly more cauline leaves and secondary inflorescences (2.64 $\pm$ 0.57) compared with L*er* (1.94 $\pm$ 0.54) (Table A.1). In addition, 16% of the first flower of *ANT:gAIL6* line 16 plants are

subtended by a cauline leaf, which suggests that these flowers has some inflorescence identity (Figure A.1). These data indicate a longer early inflorescence phase in *ANT:gAIL6* line 16. Thus the delay in first flower formation appears to be due to both a delay in the vegetative-to-reproductive transition and a prolonged early inflorescence phase.

ANT:gAIL6 plants show altered leaf development and produce fewer juvenile leaves

In addition to changes in flower development (Chapter 2), *ANT:gAIL6* line 16 plants show alterations in leaf development. They produce fewer rosette leaves than wild type: 4.88 $\pm$ 0.78 rosette leaves compared with 5.63 $\pm$ 1.42 for L*er* (Table A.1). These rosette leaves are narrower and serrated (Figure A.2A-C). In addition, the cauline leaves margins are curled upward (Figure A.2D,E). Using the presence of trichomes on the abaxial surface of rosette leaves as a marker, the number of juvenile leaves in *ANT:gAIL6* line 16 and L*er* was counted. *ANT:gAIL6* line 16 produces significantly fewer (3.28 $\pm$ 0.68) juvenile leaves compared with wild type (4.33 $\pm$ 0.49). The number of adult leaves in *ANT:gAIL6* line 16 is unchanged compare to L*er*.

ANT:gAIL6 generate leaves at a slower rate

ANT:gAIL6 line 16 plants were delayed in the switch from vegetative to reproductive development indicating that they spent more time in the vegetative phase although they produce fewer rosette leaves. This suggested that they might produce leaves at a slower rate than wild type. The time interval between the initiations of two successive leaves is referred to as plastochron. To determine plastochron length in

ANT:gAIL6 line 16, the production of leaf primordia were counted every day in both long-day and short-day conditions (Figures A.3, A.4). *ANT:gAIL6* line 16 initiates leaves at a slower rate than L*er* in both long day and short day photoperiods, indicating that *ANT:gAIL6* has a lengthened plastochron during both vegetative and early inflorescences phases (Figures A.3, A.4 and Table A.2).

DISCUSSION

ANT:gAIL6 plants exhibit a longer plastochron and delayed flowering

ANT:gAIL6 have a longer plastochron than wild type. The leaf initiation rate could be affected either by the size of the meristem or by the rate of cell division in the meristem (Wang et al., 2008). *AIL6* overexpression might limit cell number in the meristem periphery. This could be examined by scanning electron microscopy. *ANT:gAIL6* plants are also delayed in the switch from vegetative to reproductive development (i.e. flowering time). Plastochron length and flowering time are regulated by separate mechanisms. Genes can affect plastochron length without affecting flowering time and vice versa. *slow motion* mutants exhibit a longer plastochron but flowered at the same time as WT (Lohmann et al., 2010). Similarly, genes can accelerate or delay flowering time with either a longer or shorter plastochron. Mutants in gibberellin synthesis (*ga1*) and gibberellin sensitivity (*gai*) have delayed flowering time with a slightly longer plastochron (Wilson et al., 1992). *spl9 spl15* double mutants show a delayed flowering time with a shorter plastochron while overexpressing SPLs lengthened plastochron and accelerated flowering (Wang et al., 2008). *CYP78A5* loss-of-function

mutants flowered early and exhibited a shortened plastochron (Wang et al., 2008). The molecular mechanism of how *AIL6* might regulate plastochron length is not clear and requires further work.

ANT:gAIL6 and *ant ail6* double mutants exhibit a prolonged early inflorescence phase

ANT:gAIL6 line 16 makes more branches than L*er* and the first flower is often subtended by a big cauline leaf (Figure A.1). This later phenotype suggests that the first flower of *ANT:gAIL6* line 16 has some inflorescence-like properties. These results suggest that *AIL6* overexpression promotes the early inflorescence phase and/or represses flower formation. This was not expected since previous work has show that *ant ail6* double mutants also have a prolonged early inflorescence phase (Yamaguchi et al., 2013). Thus, it appears that either too little or too much *AIL6* activity can interfere with the timing of flower formation.

Table A.1 Number of leaves and length of phases in L*er* and *ANT:gAIL6* line 16 in long day photoperiods.

	L*er* (n=18)	*ANT:gAIL6* line 16 (n=24)
Days to first flower opening	23.28 ± 0.75	29.28 ± 1.34 *
Days to first CL visible (>1mm)	13.44 ± 0.78	15.09 ± 1.06 *
Number of Juvenile RL	4.33 ± 0.49	3.28 ± 0.68 *
Number of Adult RL	1.61 ± 0.51	1.6 ± 1.00
Number of CL (subtending infl.)	1.94 ± 0.54	2.64 ± 0.57*
Number of CL (subtending flowers)	0 ± 0	0.16 ± 0.37
Total RL number	5.63 ± 1.42	4.88 ± 0.78 *
Total CL number	1.94 ± 0.54	2.8 ± 0.65 *
Total number of RL and CL	**7.47 ± 1.93**	**7.68 ± 0.69**

- * Statistically different from L*er* (99% confidence level; p-value <0.01)
- n is the number of plants used
- Abbreviations: RL, rosette leaves; CL, cauline leaves; infl, inflorescences

Table A.2 The leaf initiation rate of L*er* and *ANT:gAIL6* line 16 grown in short day photoperiods.

	Rosette leaf number
L*er* (n=19)	0.69 ± 0.05
ANT:gAIL6 line 16 (n=17)	0.39 ± 0.03 *

- * Statistically different from L*er* (99% confidence level; p-value <0.01)
- n is the number of plants used

Figure A.1 The first flower produced on *ANT:gAIL6* line 16 inflorescence is sometimes subtended by a cauline leaf (arrow). A cauline leaf subtends secondary inflorescence (left); a flower subtends by a bract (right).

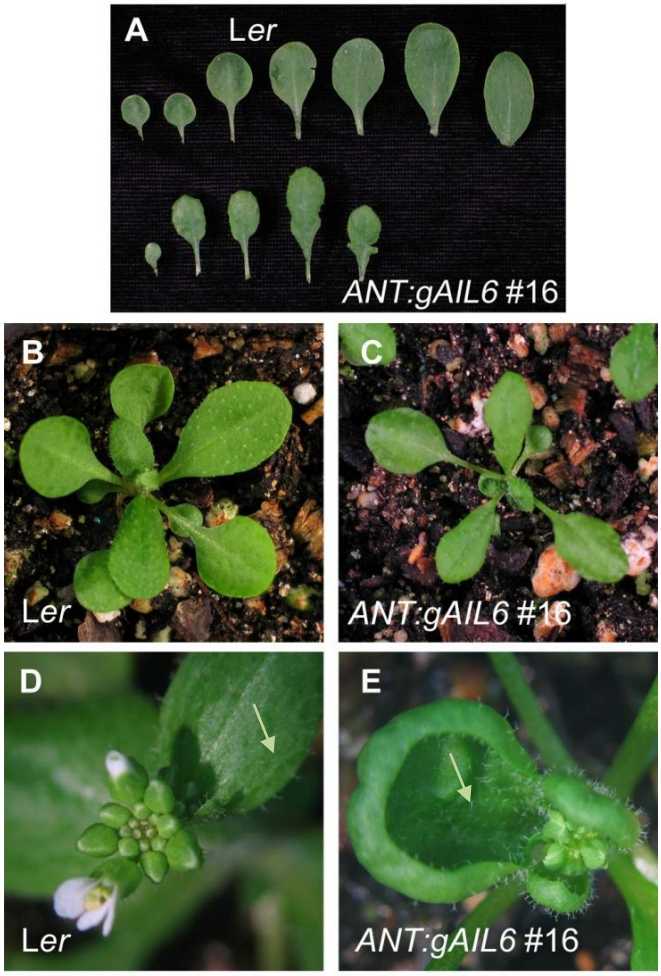

Figure A.2 *ANT:gAIL6* leaf phenotypes. (A) Rosette leaves removed from L*er* and *ANT:gAIL6* line 16 plants. *ANT:gAIL6* plants produce fewer rosette leaves, some of which show lobing along their margins. (B) 20 day old L*er* plant. (C) 20 day old *ANT:gAIL6* line 16 plant (D) L*er* inflorescence. The cauline leaf (arrow) is relatively flat. (E) ANT:gAIL6 line 16 inflorescence. The edges of the cauline leaf (arrow) are curled upward. Image B-C and D-E are taken under the same magnification, respectively.

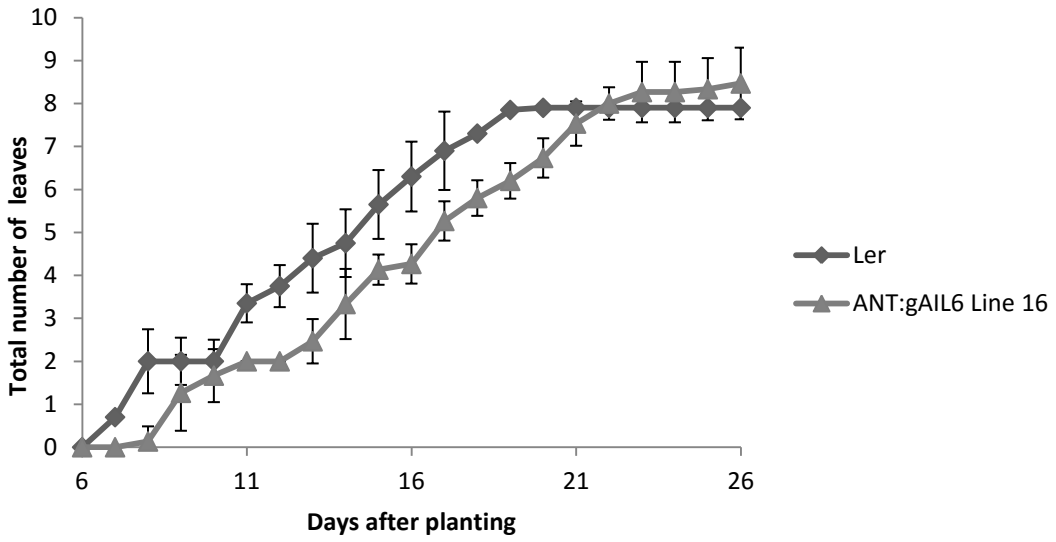

Figure A.3 Number of leaves in L*er* and *ANT:gAIL6* line 16 plants grown in long-day photoperiods. Average and standard deviation were calculated from 20 L*er* plants, and 14 *ANT:gAIL6* line 16 plants.

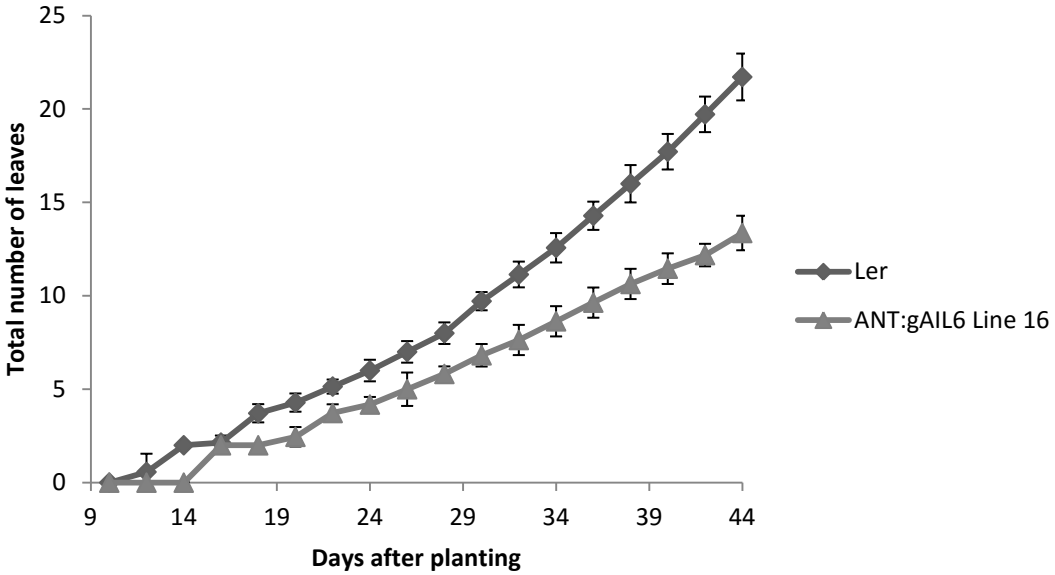

Figure A.4 Number of leaves in L*er* and *ANT:gAIL6* line 16 plants grown in short-day photoperiods. Average and standard deviation were calculated from seven L*er* plants and 11 *ANT:gAIL6* line 16 plants.